Inaugural dissertation

for

obtaining the doctoral degree

of the

Combined Faculty of Mathematics, Engineering and Natural Sciences

of the

Ruprecht - Karls - University

Heidelberg

Presented by

M.Sc. Dennis Alexander Agardy

Born in: Bielefeld, Germany

Oral examination: 05.12.2024

Immune cell dynamics in irradiated gliomas

Referees: Prof. Dr. Michael Platten

Prof. Dr. Dr. Ralf Bartenschlager

GESAMTFAKULTÄT FÜR MATHEMATIK, INGENIEUR- UND NATURWISSENSCHAFTEN

Eidesstattliche Versicherung gemäß § 8 der Promotionsordnung der Gesamtfakultät für Mathematik, Ingenieur- und Naturwissenschaften der Universität Heidelberg

1. Bei der eingereichten Dissertation mit dem Titel

   “Immune cell dynamics in irradiated gliomas”

   handelt es sich um meine eigenständig erbrachte Leistung.

2. Ich habe nur die angegebenen Quellen und Hilfsmittel benutzt und mich keiner unzulässigen Hilfe Dritter bedient. Insbesondere habe ich wörtlich oder sinngemäß aus anderen Werken übernommene Inhalte als solche kenntlich gemacht.

3. Die Arbeit oder Teile davon habe ich bislang nicht an einer Hochschule des In- oder Auslands als Bestandteil einer Prüfungs- oder Qualifikationsleistung vorgelegt.

4. Die Richtigkeit der vorstehenden Erklärungen bestätige ich.

5. Die Bedeutung der eidesstattlichen Versicherung und die strafrechtlichen Folgen einer unrichtigen oder unvollständigen eidesstattlichen Versicherung sind mir bekannt.

Ich versichere an Eides statt, dass ich nach bestem Wissen die reine Wahrheit erklärt und nichts verschwiegen habe.

Heidelberg,

…….. ……..……

Ort und Datum Unterschrift

I Acknowledgments

First of all, I would like to thank Prof. Dr. Michael Platten for giving me the opportunity to pursue my doctorate in his lab and for the continuous support.

Next, I would like to thank Prof. Dr. Dr. Ralf Bartenschlager, Prof. Dr. Walter Mier and Dr. Tim Waterboer for being part of my examination committee and refereeing this dissertation. Furthermore, I would like to thank my thesis advisory committee members Prof. Dr. Jessica Hassel, Prof. Dr. Frank Winkler and Dr. Guoliang Cui for the great discussions and valuable feedback during our meetings.

Furthermore, I would like to thank the SFB1389 “UNITE Glioblastoma” and the RTG2099 “Hallmarks of Skin Cancer” for funding my PhD. Especially the RTG2099 for funding my research stay at the Dana-Farber Cancer Institute and Harvard Medical School. In line with this, I would like to thank Prof. Dr. Stephanie Dougan and her entire lab for hosting me.

A special thanks goes to my team leaders and supervisors Dr. Theresa Bunse and Dr. Dr. Lukas Bunse. Thank you for all the great discussions, your feedback and help throughout the years.

I would like to thank all collaborators throughout the years that participated in these projects and beyond: Alexandros Kourtesakis, Dr. Matthia Karreman, Calvin Thommek, Berin Boztepe, Prof. Dr. Michael Breckwoldt, Manuel Fischer, PD Dr. David Reuss and Jana Reuss.

Next, I would like to thank all the supporting staff in the core facilities of the DKFZ. Especially the animal caretakers of the ATV101 and Barriere B, Jens Lang of the radiation safety department, the staff of the flow cytometry core facility and the staff of the light microscopy core facility. Thank you all for the kind help and support.

I would also like to thank Alex, Dirk and Rajiv from the Wick lab. Especially during COVID-times you made the late evenings in the lab a lot of fun and I was glad that we shared so many dinners together. Special thanks go to Alex for being an exceptionally supportive colleague and good friend!

I would like to thank all past and present members of the Platten lab. Especially Frederik and his husband Markus. Thank you for many joyful brunches and cocktail evenings! I would also like to thank the “Pentagon 19” members Ankita, Katharina, Kyle and Alice and the “extended” member Jessica for always being supportive colleagues and friends along the PhD journey.

Next, I would like to thank my office mates and friends David, Tamara and Yu-Chan. Thank you for all the fun times, gossip and mental and experimental support! <3

Special thanks go also to my past and present students Julia, Teresa and Zeren. I also learned a lot from you and I hope that I was able to teach you some things about science. Positive and negative.

I would also like to thank Clara for all the hard work she put into the bioinformatic analyses. Thank you for your support and I am looking forward to collaborating with you on various other projects.

Thank you to our technical assistants Kristine, Vicky, Claudia, Steffi and Chris. Thank you for your support and keeping things running. Special thanks to Kristine and her husband Paul for taking good care of my garden and house plants while I was away and being good friends outside the lab.

Next, I would like to thank all my past classmates, colleagues and supervisors that accompanied me along my journey to become a scientist. Especially Dr. Tatjana Wallmann, Dr. Marco Carretta and Prof. Dr. Daniel H. Madsen made a huge impact on my personal and/or professional growth, for which I am very grateful.

I would also like to thank all my friends around the globe, and especially my hometown, for their continuous friendship, support and fun moments! I am sorry for missing a lot of parties, birthdays and other events. I am very grateful that after every long period of not seeing each other, it is always like we have seen each other yesterday!

Finally, I would like to thank my whole family for all the support during my studies and my whole life. Without you, I would have not come this far!

II Abstract

Surgical resection followed by adjuvant radio-chemotherapy remains the mainstay of glioma management. However, the clinical benefit is highly limited. Therefore, there is an urgent clinical need to develop and improve novel therapeutic options. Various types of immunotherapies are emerging as promising new options for the treatment of gliomas, but their efficacy, when applied as monotherapy or in combination with standard-of-care treatment, remains low due to the highly immunosuppressive tumor microenvironment (TME) of gliomas. Thus, it is crucial to combine immunotherapies with other therapies, such as radiotherapy, that can favorably modulate the TME. However, in clinical trials, standard-of-care radiotherapy regimens have failed to show a benefit in combination with immunotherapies. To determine the optimal dosage and schedule that induces a potent immune response and modulates the TME, this study aimed to investigate the effect of different dosages and fractionations on the tumor immune microenvironment in a preclinical glioma model. In this study, I demonstrate that a single application of a medium-high dosage of 5 Gy induced the strongest T cell, NK cell, and type I IFN response, the highest expression of *Cxcl10* and genes related to antigen presentation, and the lowest levels of inhibitory immune checkpoints among all tested dosages and fractionation schemes. Additionally, I identified *Lgals1* expression as a marker of activated CD8+ T cells, though the functional role of *Lgals1* in CD8+ T cells and its potential implications for cellular immunotherapies are currently being further investigated in ongoing research. Lastly, I identified a novel perivascular T cell niche (PVTN), in which brain-infiltrating T cells and macrophages accumulate in the brains of tumor-bearing mice and glioma patients. Preliminary data on the migration behavior of T cells suggests that these cells are detained in the niche. Understanding the cellular composition, cellular crosstalk, migration behavior, and underlying mechanisms of T cell entrapment could lead to the development of novel therapeutic strategies that release T cells from the niche, allowing them to migrate to the tumor and exert their anti-tumoral functions.

III Zusammenfassung

Die chirurgische Resektion in Kombination mit adjuvanter Strahlen- und Chemotherapie gilt nach wie vor als Standardtherapie zur Behandlung von Gliomen. Allerdings sind die klinischen Erfolge sehr begrenzt, weshalb es einer dringenden Entwicklung neuer Therapieansätze bedarf. Immuntherapien bringen neue Hoffnung für die Behandlung von Gliompatienten. Im Gegensatz zu anderen soliden Tumorerkrankungen sind die bisherigen klinischen Erfolge jedoch auch hier leider begrenzt. Es wird vermutet, dass das immunsuppressive Tumormikromilieu im Gehirn die durch Immuntherapien ausgelösten Immunantworten unterdrückt. Daher ist die Kombination mit weiteren Therapien, die das Tumormikromilieu positiv beeinflussen können, essentiell für den Erfolg von Immuntherapien gegen Hirntumoren. Strahlentherapie hat theoretisch das Potenzial, das Tumormikromilieu positiv zu beeinflussen, doch in klinischen Studien mit dem Standardbehandlungsschema blieben die therapeutischen Erfolge aus. Deshalb ist es notwendig, die optimale Dosis und zeitliche Abfolge der Strahlentherapie zu ermitteln, um die Kombination mit Immuntherapien zu verbessern. Im Rahmen dieser Dissertation wurden daher mehrere Strahlungsdosen und Fraktionierungen sowie deren Einfluss auf Immunzellen im Tumormikromilieu in einem präklinischen Gliommodell untersucht. Dabei konnte ich zeigen, dass die einmalige Gabe einer mittelhohen Dosis von 5 Gy die beste T- und NK-Zell-Immunantwort unter allen getesteten Gruppen ausgelöst hat. Zudem konnte ich zeitlich aufzeigen, dass die durch 5 Gy ausgelöste Antwort noch mindestens sieben Tage nach der Behandlung anhielt. Zusätzlich konnte ich die Expression von *Lgals1* als Marker für aktivierte CD8+ T Zellen identifizieren. Die funktionelle Rolle von *Lgals1* und der potenzielle therapeutische Nutzen eines Knockouts werden jedoch in laufenden Experimenten weiter untersucht. Darüber hinaus konnte ich eine zuvor unbeschriebene perivaskuläre T-Zell-Nische im Gehirn von tumortragenden Mäusen und Gliompatienten identifizieren. Der Ursprung der T Zellen in dieser Nische ist zwar noch ungeklärt, aber die ersten Ergebnisse deuten darauf hin, dass die T Zellen in der Nische gefangen sind und nicht in der Lage sind, zum Tumor zu migrieren. Weitere Untersuchungen sollen die zugrundeliegenden Mechanismen entschlüsseln, um neue therapeutische Ansätze zu entwickeln, die es den T-Zellen ermöglichen, die Nische zu verlassen. Dies wird ein entscheidender Schritt zur Verbesserung von Immuntherapien zur Behandlung von Hirntumoren sein.

IV List of Publications

Publications related to this thesis:

-

Publications not related to this thesis:

- Banerjee, K., Kerzel, T., Bekkhus, T., de Souza Ferreira, S., Wallmann, T., Wallerius, M., Landwehr, L.S., **Agardy, D. A.**, Schauer, N., Malmerfeldt, A., Bergh, J., Bartish, M., Hartman, J., Östman, A., Squadrito, M.L. & Rolny, C. (2023). VEGF-C-expressing TAMs rewire the metastatic fate of breast cancer cells. *Cell Reports*, 42(12). doi.org/10.1016/j.celrep.2023.113507

- Carretta, M., Thorseth, M. L., Schina, A., **Agardy, D. A.**, Johansen, A. Z., Baker, K. J., [...] & Madsen, D. H. (2023). Dissecting tumor microenvironment heterogeneity in syngeneic mouse models: insights on cancer-associated fibroblast phenotypes shaped by infiltrating T cells. *Frontiers in Immunology*, 14. doi.org/10.3389/fimmu.2023.1320614

- Gellert, J., **Agardy, D. A.**, Kumar, S., Kourtesakis, A., Boschert, T., Jähne, K., Breckwoldt, M.O., Bunse, L., Wick, W., Davies, M.A., Platten, M. & Bunse, T. (2024). Tumoral Interferon Beta Induces an Immune-Stimulatory Phenotype in Tumor-Associated Macrophages in Melanoma Brain Metastases. *Cancer Research Communications*, 4(8), 2189-2202. doi.org/10.1158/2767-9764.CRC-24-0024

- Hunger, J., Schregel, K., Boztepe, B., **Agardy, D. A.**, Turco, V., Karimian-Jazi, K., [...] & Breckwoldt, M. O. (2023). In vivo nanoparticle-based T cell imaging can predict therapy response towards adoptive T cell therapy in experimental glioma. *Theranostics*, 13(15), 5170. doi.org/10.7150/thno.87248

- Schregel, K., Heinz, L., Hunger, J., Pan, C., Bode, J., Fischer, M., Sturm, V., Venkataramani, V., Karimian-Jazi, K., **Agardy, D.A.**, Streibel, Y. […] & Breckwoldt, M. O. (2023). A Cellular Ground Truth to Develop MRI Signatures in Glioma Models by Correlative Light Sheet Microscopy and Atlas-Based Coregistration. *Journal of Neuroscience*, 43(30), 5574-5587. doi.org/10.1523/JNEUROSCI.1470-22.2023

- Streibel, Y., Breckwoldt, M. O., Hunger, J., Pan, C., Fischer, M., Turco, V., Boztepe, B., Fels-Palesandro, H., Scheck, J.G., Sturm, V., Karimian-Jazi, K., **Agardy, D. A.**, [...] & Schregel, K. (2024). Tumor biomechanics as a novel imaging biomarker to assess response to immunotherapy in a murine glioma model. *Scientific Reports*, 14(1), 15613. doi.org/10.1038/s41598-024-66519-7

- Turco, V., Pfleiderer, K., Hunger, J., Horvat, N. K., Karimian-Jazi, K., Schregel, K., Fischer, M., Brugnara, G., Jähne, K., Sturm, V., Streibel, Y., Nguyen, D., Altamura, S., **Agardy, D. A.**, Soni, S. S., Alsasa, A., Bunse, T., Schlesner, M., Muckenthaler, M. U., Weissleder, R., […] & Platten, M. (2023). T cell-independent eradication of experimental glioma by intravenous TLR7/8-agonist-loaded nanoparticles. *Nature Communications*, 14(1), 771. doi.org/10.1038/s41467-023-36321-6

V List of Abbreviations

3D	Three dimensional
ACT	Adoptive cell therapy
APC	Antigen presenting cell
Arg1	Arginase 1
ATP	Adenosine triphosphate
BABB	Benzyl alcohol, benzyl benzoate
BBB	Blood-brain-barrier
B-CSF	Blood-cerebrospinal fluid barrier
CAR	Chimeric antigen receptor
Ccl	CC-chemokine ligand
CD	Cluster of differentiation
cGAS	Cyclic GMP-AMP synthase
CIC	Capicua transcriptional repressor
CNS	Central nervous system
CRT	Calreticulin
CSF	Cerebrospinal fluid
CTLA-4	Cytotoxic T-lymphocyte associated protein 4
Cxcl	Chemokine (C-X-C motif) ligand
DAMP	Damage-associated molecular pattern
DARC	Duffy antigen receptor for chemokines
DC	Dendritic cell
DKFZ	Deutsches Krebsforschungszentrum
DMEM	Dulbecco's Modified Eagle Medium
DNA	Deoxyribonucleic acid
DSB	Double-strand break
EAE	Experimental autoimmune encephalomyelitis
EBRT	External Beam Radiation Therapy
EC	Endothelial cell
EGFRvIII	Epidermal growth factor receptor variant III
FACS	Fluorescent activated cell sorting
FBS	Fetal bovine serum
FFPE	Formalin-Fixed Paraffin-Embedded
FLASH-RT	Fast Low Angle Shot Hypofractionation Radiotherapy
Gal-1	Galectin 1
Gd T cell	Gamma delta T cell
GD2	Disialoganglioside GD2
GFP	Green fluorescent protein
Gy	Gray (unit)
H3	Histone 3
HBSS	Hanks' Balanced Salt Solution
HEV	High endothelial venules
HMGB1	High mobility group box 1
HSP	Heat shock protein
Iba1	Ionized calcium-binding adaptor molecule 1
IDH1	Isocitrate dehydrogenase 1
IDO	Indoleamine 2,3-dioxygenase

IFN	Interferon
IFNAR1	Interferon alpha receptor 1
IL	Interleukin
Irf	Interferon regulatory factor
ISG	Interferon-stimulated gene
KO	Knockout
KPS	Karnofsky Performance Scale
LN	Lymph node
MACS	Magnetic activated cell sorting
MAIT T cell	Mucosal-associated invariant T cell
MHC	Major histocompatibility complex
MRI	Magnetic resonance imaging
mRNA	Messenger ribonucleic acid
NK cell	Natural killer cells
NKG2D	Natural killer group 2D
NKG2DL	NKG2D ligand
NKT cell	Natural killer T cell
NLGN4X	Neuroligin 4, X-Linked
OVA	Ovalbumin
PBS	Phosphate buffer saline
PD1	Programmed cell death protein 1
PD-L1	Programmed death-ligand 1
PFA	Paraformaldehyde
PRR	Pattern recognition receptor
PVTN	Perivascular T cell niches
RNA	Ribonucleic acid
ROS	Reactive oxygen species
RT	Radiotherapy
Stat	Signal transducer and activator of transcription
STING	Stimulator of interferon response cGAMP interactor 1
TAA	Tumor-associated antigen
Tap1	Transporter associated with antigen processing
TCR	T cell receptor
TGF-β	Transforming growth factor beta
TIME	Tumor immune microenvironment
TLR	Toll-like receptor
TLS	Tertiary lymphoid structure
TME	Tumor microenvironment
TMZ	Temozolomide
Treg	Regulatory T cell
TRITC	Tetramethylrhodamine-isothiocyanate
UMAP	Uniform Manifold Approximation and Projection
UT	Untreated
WHO	World Health Organization

VI List of Figures

VII List of Tables

Table of Contents

1 Introduction

1.1 Gliomas

Primary brain tumors are tumors which originate in the brain, while secondary brain tumors arise from metastases outside of the brain (Weller et al., 2024). Gliomas account for approximately 26% of all primary brain tumors and are responsible for the most deaths (Ostrom et al., 2023). They are a heterogenous group of brain tumors which develop from glial cells such as astrocytes, oligodendrocytes and ependymal cells (Lehman, 2008; Liu et al., 2011). Glial cells are supportive cells in the central nervous system (CNS) and play an essential role in CNS development, maintaining homeostasis, as well as protecting and supporting neurons in the brain (Allen & Lyons, 2018). Gliomas can occur in different parts of the CNS and are further classified by the 2021 WHO classifications based on the cell type they originate from as well as histological and genetic features. The 2021 WHO classifications separate gliomas into two categories: adult-type diffuse gliomas and pediatric-type diffuse gliomas (Louis et al., 2021). An overview and the criteria for the diagnosis of adult-type diffuse gliomas can be found in Figure 1 (Byun & Park, 2022).

With approximately 55% of all gliomas, glioblastomas are the most common type of glioma (G.-M. Wang et al., 2022). The incidence rate of gliomas varies according to various factors such as glioma subtype, sex, age and even ethnicity. But overall, the incidence rate per 100,000 population is 3.23 for glioblastoma, ranges from 0.42 to 0.46 for astrocytoma, and ranges from 0.11 to 0.22 for oligodendroglioma. (Pellerino et al., 2022). The distribution of incidence between male and female varies with age and glioma subtype, but overall, males have a 30-50% higher incidence for gliomas over females (G.-M. Wang et al., 2022). Gliomas can occur at any age, but the age group with the highest incidence with 20% of all cases is 60-69 years old, while with 5.1% the age group with the lowest incidence is 10-19 years (G.-M. Wang et al., 2022). The factors causing the development of gliomas are still largely unknown, but a combination of genetic predisposition and environmental and lifestyle factors is believed to play a role (Ostrom et al., 2019). The only validated environmental factor identified to increase the risk of brain tumors is the exposure to ionizing irradiation, especially during childhood (Braganza et al., 2012; Ostrom et al., 2019).

Gliomas are usually only diagnosed after patients present themselves with neurological symptoms such as seizures, headaches, cognitive problems, change in personality or motor impairments (Peeters et al., 2020; Snyder et al., 1993). The diagnosis is then

performed by magnetic resonance imaging (MRI). However, the final diagnosis of the glioma subtype can only be confirmed by pathological tissue analysis if a biopsy was taken or surgical resection was performed (Weller et al., 2020). After surgical resection, standard-of-care continues with an adjuvant radio-chemotherapy (Weller et al., 2020). The success of the current standard-of-care is highly limited and results in an overall survival of only 9.2 months among glioblastoma patients (Brown et al., 2022). However, emerging immunotherapeutic approaches, which include immune checkpoint inhibitors, therapeutic vaccinations, nanoparticle-mediated delivery of immune modulators, and cellular therapies such as T cell receptor (TCR) or chimeric antigen receptor (CAR) transgenic T cells, have shown encouraging advancements as potential future treatments (Aslan et al., 2020; Cloughesy et al., 2019; Kilian et al., 2022; Krämer et al., 2024; Platten et al., 2021; Schumacher et al., 2014; Turco et al., 2023).

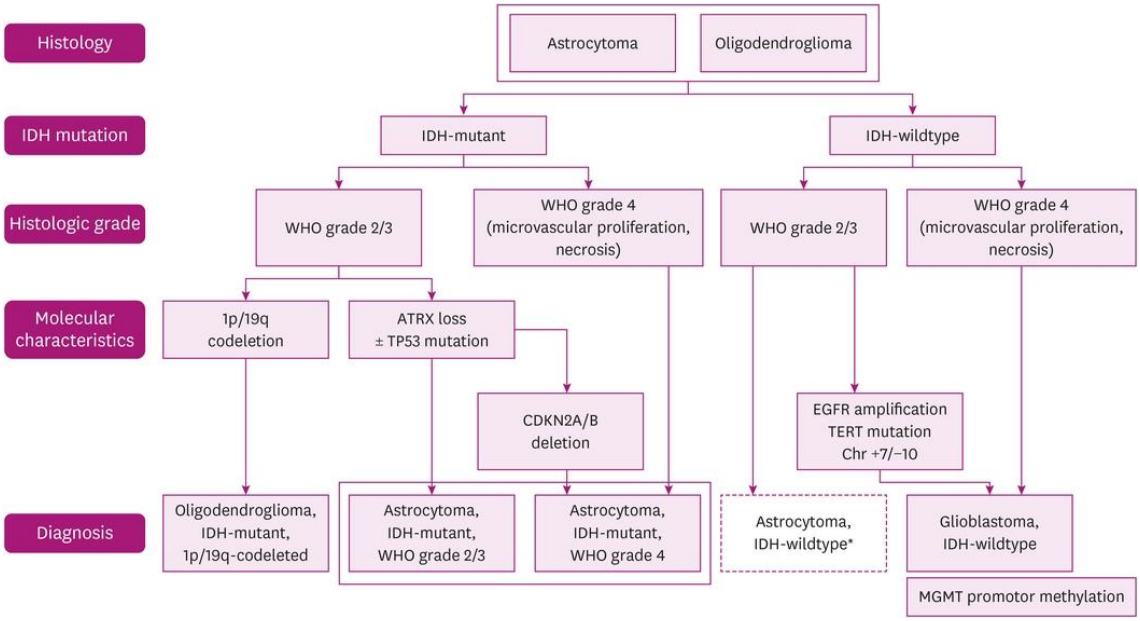

Figure 1: Overview of the 2021 WHO classification of adult-type diffuse gliomas.

H3-altered (midline) gliomas are not displayed. With permission adapted from Byun & Park (Byun & Park, 2022).

1.2 The immune landscape of the brain and gliomas

For the longest time, the brain has been thought to be a fully immune-privileged organ in order to protect itself from inflammation or other peripheral threats. However, the advancements in neuroimmunology research in the recent decades have shed light on

the interactions between the (peripheral) immune system and the brain (Engelhardt et al., 2017). In healthy humans and mice, the brain is indeed partially immune-privileged. The brain protects itself from peripheral immune cells and other potential threats through several physical barriers such as the blood-brain barrier (BBB) (Engelhardt et al., 2017). The BBB is formed by tight junctions between brain endothelial cells, pericytes and astrocytes, and controls the migration of cells and influx of other factors to the brain (Kadry et al., 2020). At the same time, during neuroinflammation, traumatic brain injury, autoimmune diseases and cancer, the BBB is often compromised and thereby allows peripheral immune cells to enter the brain (Kadry et al., 2020). Classically, immune cells transmigrate from the blood stream into the brain by passing through the BBB (Marchetti & Engelhardt, 2020). However, recent studies have proposed alternative routes for immune cell migration to the brain via direct connections between the dura and the brain (Smyth et al., 2024). It also has recently been shown that the skull holds a reservoir of tumor-reactive T cells that are able to infiltrate the brain (Dobersalske et al., 2024).

Another physical barrier is the blood-cerebrospinal fluid (B-CSF) barrier. This barrier is composed of the choroid plexus epithelium in the ventricles and the arachnoid barrier in the meninges (Solar et al., 2020). The arachnoid barrier forms between the dura mater and the subarachnoid space. The epithelium in the ventricles produces the majority of cerebrospinal fluid (CSF), but also the intracellular and interstitial fluid of the brain parenchyma drains into the CSF (Wichmann et al., 2022). The drainage of these fluids happens through the glymphatic system, which is crucial for the transport of debris and antigens out of the brain and drains into the lymphatic system (Iliff et al., 2012; Johnston et al., 2004).

Although, the mechanisms of priming an immune response to the brain are still incompletely understood, it has been shown that when injecting tracers into the brain or the CSF, they will drain to cervical lymph nodes (Eide et al., 2018). In preclinical glioma models it has also been shown that dendritic cells can prime immune responses against brain tumors by trafficking antigens from the tumor to cervical lymph nodes (Bowman-Kirigin et al., 2023). Thereby, these studies suggest that adaptive immune responses in the brain are primed in the periphery at cervical lymph nodes. Still, cervical lymph nodes might not be the exclusive location of priming adaptive immune responses in the CNS. In a study by Rustenhoven et al., antigen presenting cells at the dural sinuses have been shown to capture CNS-derived antigens from the CSF and to present them to patrolling T cells in the dural meninges (Rustenhoven et al., 2021). Furthermore, the presence of tertiary lymphoid structures (TLS) in human and murine gliomas has been reported and suggested as additional location of T cell priming (van de Walle et al., 2021; Luuk van

Hooren et al., 2021). Nevertheless, further studies are needed to comprehensively understand the complex dynamics of priming immune responses against tumors in the brain.

In the healthy brain, microglia are the main immune cell in the brain and provide CNS immune surveillance (Li & Barres, 2018), but in the choroid plexus, meninges and CSF also T cells, natural killer (NK) cells, B cells, neutrophils, dendritic cells (DCs) and various other immune cells are patrolling and surveilling the environment (Croese et al., 2021). Depending on the anatomical region, microglia constitute up to 16.6% of all cells in the human brain and up to 12% of all cells in the mouse brain (Bachiller et al., 2018). They derive from yolk-sac derived progenitor cells during embryonic development and their population is not replenished by peripheral hematopoietic stem cells (Ginhoux et al., 2010; Gomez Perdiguero et al., 2014). Like their peripheral counterparts, microglia are highly plastic cells and have the ability to change their functional capacities depending on the external or internal threats such as inflammation, infection or tumors (Li & Barres, 2018; Yabo et al., 2024). In the healthy brain, they rather maintain an immunosuppressive phenotype to support tissue maintenance and repair (Gomez-Nicola & Perry, 2015). But, they can alter their secretion of cytokines and chemokines, morphology, phagocytic capacity, antigen presentation machinery and even proliferation in order to react to the possible threats (Bachiller et al., 2018).

The tumor microenvironment (TME) of gliomas is predominantly populated by myeloid cells. Studies have shown that more than 50% of the cells in gliomas can be of the myeloid lineage (Hambardzumyan et al., 2015; Morantz et al., 1979; Rossi et al., 1987). But during tumor development, also peripheral monocytes, macrophages, neutrophils, basophils, and dendritic cells infiltrate the CNS, yet many of the myeloid cell infiltrating the brain are adapting an immunosuppressive phenotype (Friedrich et al., 2023). Immunosuppressive regulatory T cells (Tregs) are also recruited to the tumor microenvironment (Sayour et al., 2015). Altogether, these cells generate an immunosuppressive milieu by secreting anti-inflammatory cytokines such as transforming growth factor beta (TGF-β), interleukin 10 (IL-10), expressing other factors such as Arginase1 (Arg1), indoleamine 2,3 dioxygenase (IDO), or immune checkpoints such as CTLA-4 and PD-L1 (Lin et al., 2024; Zhai et al., 2021; Zhang et al., 2016). That's why the treatment-naïve TME of gliomas is considered "immunologically cold" and highly immunosuppressive (Lin et al., 2024). At the same time, also effector CD4+ and CD8+ T cells, as well as NK and B cells infiltrate the tumor microenvironment. However, the effectiveness of the mounted responses is overshadowed by the immunosuppressive environment and results in tumor immune evasion (Gangoso et al., 2021; Lin et al.,

2024). Another factor that makes it difficult to mount adaptive immune responses against the tumor, is the relatively low mutational burden and the resulting low amount of neoantigens in the majority of gliomas (Sha et al., 2020). Overall, it is therefore crucial for the success of immunotherapy to modulate the tumor and its microenvironment to a more immunogenic and a less immunosuppressive state.

1.3 Immunotherapies for brain tumors

Emerging immunotherapeutic approaches bring new hope for improving the survival of glioma patients. They can be categorized into three main categories: therapeutic vaccines, antibodies such as immune checkpoint inhibitors, and cellular therapies such as TCR- or CAR-transgenic T or NK cells (Montoya et al., 2020). All three aim to stimulate or provide a potent immune response that is specific to the tumor. In solid tumors outside the brain they have already shown substantial success and some have been implemented as first-line treatment in the standard-of-care (Boydell et al., 2023). However, for gliomas no immunotherapeutic modality has been so far approved, due to the early stage some of the therapies are still in, or due to limited success in clinical trials (Lim et al., 2022; Omuro et al., 2023). Here I aim to give a short overview of the current immunotherapeutic approaches that are in development for the treatment of gliomas.

Several therapeutic vaccines against gliomas have been in preclinical and clinical development and show promising results. Vaccine platforms in development include mRNA vaccines, peptide vaccines, and DC vaccines, that utilize the adoptive transfer of mRNA or peptide loaded DCs (Xiong et al., 2024). Some approaches aim at fully personalizing the vaccine based on the patient's specific transcriptomic profile, while other approaches rather target mutations that are common in certain subtypes of gliomas such as isocitrate dehydrogenase 1 (IDH1) (R132H) or histone H3(K27M) (Grassl et al., 2023; Latzer et al., 2024; Platten et al., 2021; Schumacher et al., 2014). In many clinical trials, the vaccination is combined with checkpoint inhibitors to overcome the immunosuppressive tumor microenvironment. Checkpoint inhibitors are not personalized and have systemic effects on immune cells. They are antibodies that block inhibitory immune checkpoints such as PD-1, PD-L1 and CTLA-4 on immune cells and/or tumor cells. They have also been tested as single modality against gliomas with promising preclinical results (Aslan et al., 2020; Reardon et al., 2016), but failed to demonstrate success in clinical trials (Reardon et al., 2020; Reardon et al., 2017). Only one study, which applied checkpoint inhibitors as a neoadjuvant therapy in glioblastoma, showed a significantly better survival compared to patients that received the therapy in an adjuvant

fashion (Cloughesy et al., 2019). CAR receptors are artificial receptors that are able to specifically target single epitopes that are expressed on the surface of tumor cells. Classically, T cells are genetically equipped with these receptors, but also studies utilizing NK cells and even macrophages have been proposed and are under clinical development (Ehrend et al., 2024; Lei et al., 2024; Murakami et al., 2018). CAR receptors bring the problem that targets need to be identified that are uniquely expressed or overexpressed on the surface of tumor cells alone and not on healthy cells to limit off-tumor toxicity (Hou et al., 2021). Still, several potential targets have been identified for gliomas, such as GD2, IL13Ra2, or EGFRvIII, and are currently undergoing clinical trials and demonstrated first promising results (Brown et al., 2016; Brown et al., 2015; Kilian et al., 2021; Majzner et al., 2022; Sampson et al., 2014). However, only targeting one target on the surface of tumor cells can lead to immunoediting and subsequent immune evasion of heterogenous tumors and is a major limitation of CAR T cell therapy for solid tumors in general (Luksik et al., 2023). TCR-transgenic cellular products have the advantage that they can also target intracellular targets, as the peptide antigens that are targeted by TCR-transgenic T cells, are processed inside the tumor cell and presented on MHC molecules (Kilian et al., 2021). The antigens targeted by TCR-transgenic T cells are usually mutation-derived neoantigens and are therefore specific to the tumor cells which lowers the risk for off-target toxicity (Boschert et al., 2024; Kilian et al., 2021; Kilian et al., 2022). As these TCRs are highly personalized, identification of reactive TCRs and their targets in patients can be very difficult, as well as time and cost-intensive. Novel advancements in machine-learning algorithms can help to predict and identify neoantigens and reactive TCRs and speed up and simplify the process of development (Cai et al., 2022; Tan et al., 2024). A few glioma-specific TCRs have been identified against mutations like IDH1(R132H), H3(K27M), capicua transcriptional repressor (CIC) CIC(R215W/Q) or the tumor-associated antigen neuroligin 4 X-linked (NLGN4X) and some might soon undergo clinical trials (Boschert et al., 2024; Kilian et al., 2022; Krämer et al., 2024; Platten et al., 2021).

Overall, immunotherapies are providing a promising future for the treatment of glioma patients, but more research is needed to improve their overall efficacy. The limited access to the brain, tumor heterogeneity and the immunosuppressive environment seem to be the main challenges (Akhavan et al., 2019). Therefore, immunotherapies could highly benefit from combinatorial therapies, that modulate the TME and access to the brain. Radiotherapy holds such potential for combination with immunotherapies (Akhavan et al., 2019). The combination of radiotherapy with immunotherapies and the

effects on the immune system will therefore be further described in the following two chapters.

1.4 Radiotherapy and its effect on the tumor microenvironment

Radiotherapy for the treatment of gliomas and other types of brain tumors has been long implemented into the management of patients. Radiotherapy is usually given as adjuvant therapy together with the chemotherapeutic Temozolomide (TMZ) after surgery (Stupp et al., 2005). If a tumor is inoperable, radiotherapy and chemotherapy might be used as primary care. The primary goal is the control of tumor growth without causing neurotoxicity (Weller et al., 2020). The dosage and fractionation of irradiation is determined based on multiple factors including glioma subtype, age of the patient, prognosis, the assessment of functional impairment of the patient by Karnofsky Performance Scale (KPS) and the tumor volume left after surgery (Weller et al., 2020). The common total dosage patients receive is between 50 and 60 Gy administered in daily fractions of 1.8-2 Gy (Stupp et al., 2005; Weller et al., 2020). Early clinical trials comparing total dosages of 45 Gy and 59.4 Gy in low grade gliomas saw no significant differences in patient outcome (Karim et al., 1996). Dose-escalation trials using total dosages of up to 80 Gy and hypofractionated dosages of up to 8.5 Gy per fraction showed enhanced patient benefit only when used alone, but not in combination with TMZ (Singh et al., 2021). At the same time, a study using preclinical glioma models GL261 and CT-2A showed that the timing between fractionations did made significant differences (McKelvey et al., 2022). In this study, McKelvey et al. compared two groups of mice both treated with 20 Gy. One group received 10 fractions with 2 Gy daily for ten days with only a two-day break after five fractions and the other group received 4 fractions with 5 Gy every third day. The mice treated with the 4 fractions of 5 Gy every third day, not only showed an increase in survival by ~125% compared to the other group, but also showed decreased tumor cell proliferation, increased DNA damage and a higher immune infiltration, while showing no signs of increased radiotoxicity (McKelvey et al., 2022). Concluding these clinical and preclinical studies, the overall dosage does not seem to matter, but the timing between fractionations might be an important factor in increasing therapeutic efficacy and in inducing potent immune responses. Yet, no study so far has investigated the influence of different dosages of radiotherapy on the entire tumor immune microenvironment (TIME) in gliomas.

Radiotherapy can directly influence tumor cells by inducing various processes and can modulate the entire tumor microenvironment (Awada et al., 2023). Ionizing radiation

energy causes DNA damage by inducing single-strand and double-strand breaks in DNA strands and alterations in DNA bases (Lomax et al., 2013). Another rather indirect mechanism of DNA damage can occur by irradiation-induced free radicals inside cells. Radiation reacts with water molecules inside cells, which results in the production of reactive oxygen species (ROS). These ROS can cause oxidative damage to bases and the sugar-phosphate backbone which can lead to strand breaks and base modifications (Dizdaroglu & Jaruga, 2012). Especially when such strand breaks and base damage occur within a short distance, often referred to as clustered DNA damage, they are difficult to be repaired by DNA repair mechanisms and often leads to cell death (Goodhead, 1994; Sutherland et al., 2000; Sutherland et al., 2002). Radiation-induced cell death is often referred to as immunogenic cell death due to the release of tumor-associated antigens (TAA) and damage-associate molecular patterns (DAMPs) (Gameiro et al., 2014; Liu et al., 2023). DAMPs can include cellular compartments such as calreticulin (CRT), free nucleic acids, adenosine triphosphate (ATP), heat shock proteins (HSP) and high mobility group box 1 (HMGB1) (See Figure 2) (Awada et al., 2023; Panaretakis et al., 2009). These signals are sensed by pattern recognition receptors (PRRs) on antigen presenting cells such as macrophages, microglia and dendritic cells in the tumor microenvironment and initiate the clearance of dying tumor cells (Lauber et al., 2012; Yamazaki et al., 2014). These cells then trigger an adaptive immune response by lymphocytes through the presentation of antigens and co-stimulation in lymphoid organs such as the cervical lymph nodes or at other suggested sites of potential immune cell priming of the brain as described above (see 1.2). In addition, the genomic instability caused by irradiation-induced DNA damage and mislocation of nucleic acids into the cytosol of cells can trigger type I IFN responses through activation of nucleic acid sensing PRRs pathways such as the retinoic acid inducible gene I (RIG-I), toll-like receptors (TLR) or the cGAS-STING pathway. These pathways can be triggered within tumor cells themselves or in immune cells such as macrophages or dendritic cells through uptake of tumor cell debris or during phagocytosis of tumor cells (Deng et al., 2014; Goubau et al., 2014; Haroun et al., 2023). The whole cascade that results in type I IFN expression usually takes several hours and peaks usually at 48-72h after irradiation (Burnette et al., 2011; Feng et al., 2020). Type I IFN responses are known to induce many interferon-stimulated genes (ISGs) and many other immune stimulatory pathways, such as the upregulation of MHC molecules or the expression of the major T cell chemoattractant CXCL10 in tumor, stromal and immune cells (Buttmann et al., 2007; Ignarro et al., 2022; Makuch et al., 2022; Yu et al., 2022). In experiments with a systemic knockout of the type I IFN receptor 1 (IFNAR1) in mice, it has been shown that the immune-dependent efficacy of radiotherapy relies on the

induction of type I IFN (Burnette et al., 2011). STING activation and type I IFN induction have been shown to be essential for dendritic cell-mediated initiation of T cell-mediated tumor rejections by promoting their ability to cross-prime CD8+ T cells (Burnette et al., 2011; Deng et al., 2014; Diamond et al., 2011). Regulation of the type I IFN response after radiotherapy can occur through the expression of the DNA exonuclease Trex1, which degrades DNA in the cytosol and dampens thereby STING-mediated expression of type I IFNs (Vanpouille-Box et al., 2017). Although, it has also been shown that radiation-induced oxidative DNA damage can induce resistance to Trex1-mediated DNA degradation (Gehrke et al., 2013). Depending on timing, duration and strength, type I IFN responses might not always be beneficial for anti-tumor immunity. Other reports also suggest mechanism of immune suppression and resistance induced by type I IFN (J. Chen et al., 2019; Jacquelot et al., 2019). Overall, irradiation and the following downstream events of immunogenic cell death, release and presentation of tumor antigens and T cell priming, initiate the classical immunity cycle as described by Mellman et al. and leads to an increased infiltration of antigen-specific T cells and anti-tumoral responses (see Figure 2) (Mellman et al., 2023). Natural Killer (NK) cells are another major immune cell which are capable of direct killing of tumor cells through antigen-independent mechanisms. Radiotherapy has been shown to induce NK cell responses with increased infiltration into, and cytotoxicity against, solid tumors (Canter et al., 2017; Walle et al., 2022). One study demonstrated that natural-killer group 2 member D ligands (NKG2DL), a group of ligands initiating NK cell killing through the receptor NKG2D, were upregulated on murine and human glioma cells following radiotherapy and led to NK cell driven anti-tumor responses *in vivo* (Weiss, Schneider, et al., 2018). However, the majority of studies investigating direct and indirect effects on NK cells have not been performed in the context of brain tumors and thereby the effects of radiotherapy on NK cells and their response in the brain remain largely unclear. Radiotherapy also induces the recruitment of macrophages to the tumor through the induction of expression of cytokines and chemokines such as IL-6 and CCL2 (Morganti et al., 2014). Unfortunately, the TME of gliomas favors the polarization towards a rather immunosuppressive anti-inflammatory phenotype. At the same time, M2-like anti-inflammatory macrophages are also more radioresistant compared to pro-inflammatory macrophages in glioblastomas (Leblond et al., 2017). However, we have recently shown that type I IFN secreted by melanoma brain metastases reprograms macrophages towards a beneficial pro-inflammatory phenotype that correlated with improved survival (Gellert et al., 2024). Microglia on the other hand have been shown to become more activated and potent in priming immune responses following radiation (Monje et al., 2002; Voshart, Klaver, et al., 2024; Voshart, Oshima, et al., 2024). However, an overshooting of microglia activation

has been shown to be responsible for the long-term cognitive decline observed in patients and mice treated with radiotherapy (Acharya et al., 2016; Feng et al., 2016; Voshart, Oshima, et al., 2024). Overall, the direct and indirect effects of radiotherapy on myeloid cells in the brain are highly complex, incompletely understood and may vary based on location of the tumor, dosage and timing of radiation, and the heterogeneity of the tumor microenvironment (Beach et al., 2022; Betlazar et al., 2016; Hohsfield et al., 2020).

Irradiation also causes the increased expression of adhesion molecules on endothelial cells, which supports the recruitment of immune cells to the tumor (Hallahan et al., 1996; Himburg et al., 2016). Irradiation-induced modulations in endothelial cells may also lead to alterations in the integrity of the vasculature, making it more permeable for cells to pass through endothelial barriers (Guipaud et al., 2018; Sharma et al., 2013). At the same time, too high dosages of radiotherapy can also lead to the apoptosis of endothelial cells, which may lead the breakdown of the BBB or even the complete loss of vasculature (Li et al., 2003; Wijerathne et al., 2021).

Despite all positive effects, radiotherapy can also induce further immunosuppressive mechanisms. Immune cells, especially lymphocytes, can be highly sensitive to radiation and can be depleted (Venkatesulu et al., 2018; Yovino & Grossman, 2012). At the same time, regulatory T cells (T_{regs}) are less radiosensitive compared to other lymphocytes and might escape radiation-induced depletion at lower dosages (Persa et al., 2015; Qu et al., 2010). Through the expression of the immune-checkpoint CTLA-4 or through secretion of immunosuppressive cytokines and factors such as IL-10, TGF-β and IDO, T_{regs} can facilitate an immunosuppressive TME and dampen cytotoxic T and NK cell responses (Awada et al., 2023; Schmidt et al., 2012). Another immunosuppressive mechanism triggered by radiotherapy is the recruitment of myeloid-derived suppressor cells and tumor-associated macrophages to the TME (Beach et al., 2022; Liang et al., 2017). Together with the brain-resident microglia, these anti-inflammatory myeloid cells also secrete immunosuppressive cytokines as well as IDO and arginase 1 (Arg1), which can interfere with T cell-mediated anti-tumor responses and can drive radiation resistance (Kang et al., 2020; Liang et al., 2017). Hypoxia, which is a common feature of glioblastomas, also drives the polarization of myeloid cells towards an immunosuppressive and anti-inflammatory phenotype. Radiotherapy can also induce hypoxic regions in gliomas through the destruction of blood vessels as mentioned above (Li et al., 2003; Wijerathne et al., 2021). Through the expression of type I and II interferon in the post-irradiated TME, the expression of the immune-checkpoint programmed death-ligand 1 (PD-L1) on antigen presenting cells, but also on tumor cells, can be significantly

enhanced (Sato et al., 2019; N. H. Wang et al., 2022). This highlights that radiotherapy can benefit from the combination with immune checkpoint inhibitors.

To summarize, radiotherapy is able to modulate the tumor microenvironment and triggers potent anti-tumor immune responses. Evidence provides a strong rationale for combinatorial regimens with immunotherapies. However, further studies are needed to evaluate the best dosage and timing for optimal combinatorial efficacy. Nevertheless, many of these studies have not been performed in glioma models, but in subcutaneous models or orthotopic models of other organs. Due to the unique environment of the brain, immune cells in brain tumors might behave differently compared to peripheral solid tumors. Therefore, there is an unmet need to comprehensively characterize the immune response to different dosages of radiotherapy in the brain.

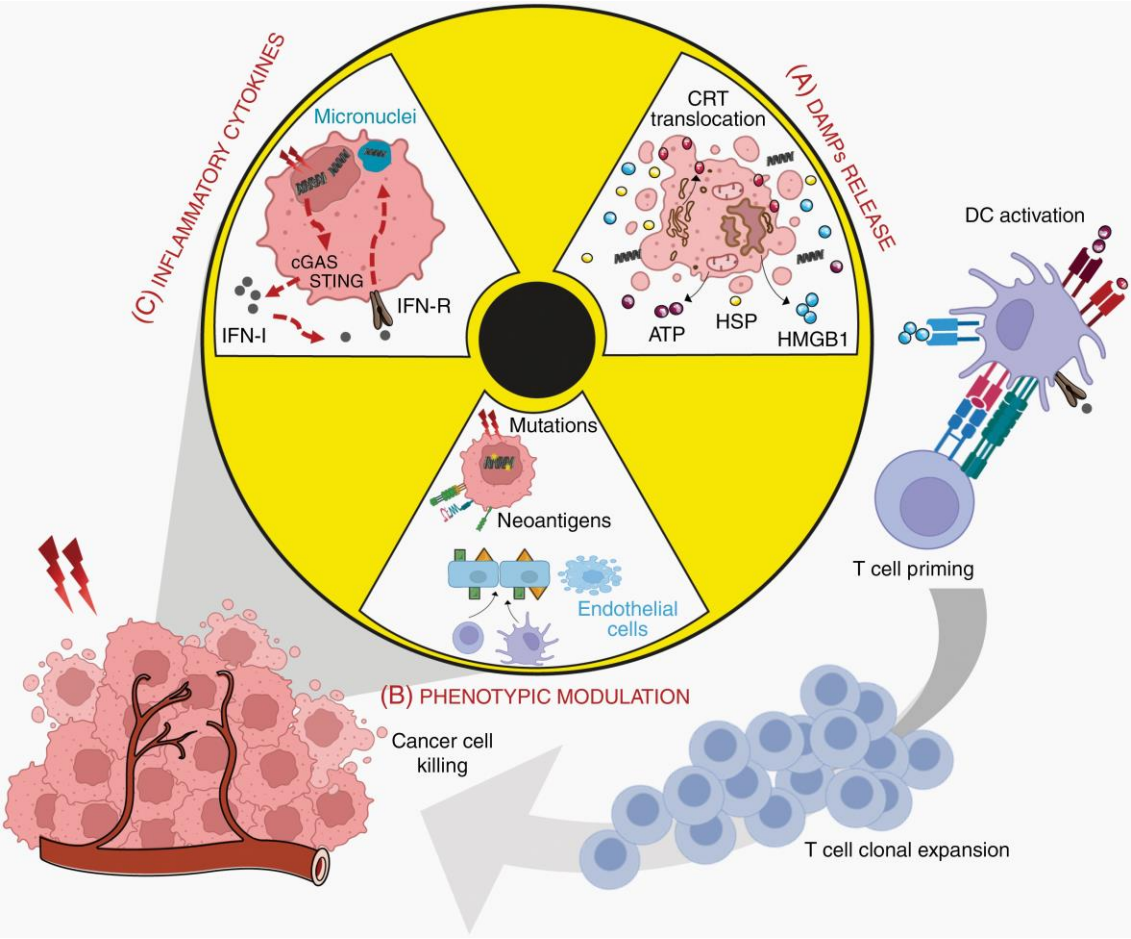

Figure 2: Overview of events in the tumor microenvironment of irradiated solid tumors.

Irradiation-induced immunogenic cell death of tumor cells leads to the release of DAMPs, neoantigens and inflammatory cytokines which triggers the activation of antigen presenting cells and priming of T cells and results in antitumoral T cell responses. With permission adapted from Awada et al. (Awada et al., 2023).

1.5 Radio- and immunotherapy combinations

The immunogenic modulation of the tumor microenvironment and recruitment of T cells make radiotherapy, in theory, an ideal partner for combinations with immunotherapies. Various preclinical studies in murine glioma models have already been performed to confirm an enhanced therapeutic effect of radio- and immunotherapy combinations. Zeng et al. showed that the combination of a PD-1 checkpoint inhibitor in combination with stereotactic radiation induced long-term survival in mice with the preclinical glioma model GL261. At the same time, mice treated only with anti PD-1 or radiotherapy alone only showed a minimal response and no significant increase in median survival (Zeng et al., 2013). They also showed a significant increase in CD8+ T cell infiltration and decreased numbers of regulatory T cells in the combined group (Zeng et al., 2013). Similarly, Kim et al. and Belcaid et al. also showed effective combination of radiotherapy with various other checkpoint inhibitor combinations with anti PD-1, CTLA-4, TIM-3 and 4-1BB which led to increased long-term survival and reduced tumor growth in mice (Belcaid et al., 2014; Kim et al., 2017). Also, studies combining therapeutic vaccinations and radiotherapy have been performed on preclinical glioma models and showed significant benefits of the combination (Newcomb et al., 2006; Tran et al., 2020). Even cellular therapies such as CAR T cells against preclinical glioma models benefited from the combination with radiotherapy (Weiss, Weller, et al., 2018).

At the same time, clinical studies fail to demonstrate this combinatorial effect. The large CheckMate-498 randomized phase III trial, in which standard-of-care radiotherapy was combined with the anti-PD1 checkpoint inhibitor Nivolumab, in patients with unmethylated newly diagnosed glioblastoma, failed to demonstrate a significant benefit in overall survival compared to the patients treated with standard radio-chemotherapy (Omuro et al., 2023). CheckMate-548, another phase III clinical trial for methylated newly diagnosed glioblastoma, compared the efficacy of standard-of-care radiotherapy with temozolomide with or without Nivolumab (Lim et al., 2022). Also this trial failed to demonstrate improved survival in patients treated with the combination (Lim et al., 2022). Moreover, a meta-analysis of nine phase II and III clinical trials showed no statistically significant increase in overall survival nor progression free survival in patients with newly diagnosed glioblastoma treated with the combination of radio-chemotherapy and immunotherapy (Lara-Velazquez et al., 2021). The reasons behind this failure in clinical trials might be multifactorial. A major difference between preclinical and clinical studies is the use of Temozolomide. While most preclinical studies focus on the pure combination of radiotherapy and immunotherapy, clinical studies utilize the standard-of-care treatment protocols which combine radiotherapy with Temozolomide (Lim et al., 2022;

Omuro et al., 2023; Stupp et al., 2005). However, the effects of Temozolomide on the immune response in gliomas and especially in combination with radiotherapy and immunotherapy are not well understood. Another major difference is the dosage and fractionation used in these studies. The above-mentioned preclinical studies make use of a single dose of 4-10 Gy, while standard-of-care radiotherapy in above mentioned clinical trials followed the Stupp protocol of 30x 2 Gy (Belcaid et al., 2014; Kim et al., 2017; Lim et al., 2022; Omuro et al., 2023; Stupp et al., 2005; Zeng et al., 2013). It has been shown that the standard-of-care radio-chemotherapy of 30x 2 Gy and TMZ induced a immunosuppressive tumor microenvironment rather than modulating it towards a favorable milieu for a potent and sustainable immune response (Grossman et al., 2011). Therefore, the sequential timing and dosage of administering radiotherapy for the combination with immunotherapy might be crucial for efficacy. As it is known that radiation also kills immune cells, if fractions are delivered in too close sequential proximity to each other, the following fractions might diminish the triggered immune response and thus dampen the immune-driven therapeutic effect. It might therefore be beneficial to modify the dosage and decrease the frequency of radiotherapy and apply hypofractionated regimens in combination with immunotherapy. Thus, further studies are needed to investigate the longitudinal effect of different dosages of radiotherapy on immune cells, in order to determine, not only the best dosage, but potentially also the ideal timing from which the immune response takes the best benefit. I therefore aimed to address this issue in this dissertation by investigating the longitudinal tumor immune microenvironment of a preclinical glioma model after radiotherapy with different dosages and fractionations.

1.6 Aims of this study

Since the combination of immunotherapies with radiotherapies only showed limited clinical efficacy, I aimed to decipher possible reasons behind the failure of these trials. In order to optimize radiotherapy dosage and timing, I aimed to investigate how immune cells behave after radiotherapy in a dose- and time-dependent manner (Part 1).

Additionally, I have discovered a novel perivascular T cell niche, which I aimed to comprehensively characterize in terms of structure, cellular composition and development (Part 2).

Overall, the following aims were addressed in this dissertation:

- Investigate the effect of different dosages of radiotherapy on immune cells in the brain tumor microenvironment
- Determine the optimal irradiation dosage for stimulating successful anti-tumor immune responses in the tumor microenvironment of gliomas
- Investigate the development, cellular composition and structure of perivascular T cell niches.

2 Material and methods

2.1 Material

2.1.1 Antibodies

Table 1: Antibodies and dyes used for flow cytometry.

Target	Conjugate	Ref#	Company
CD11b	PE-Dazzle	101256	BioLegend
CD16/CD32 block	unconjugated	14-0161-86	Invitrogen
CD3	FITC	100204	BioLegend
CD3	BV510	100234	BioLegend
CD31	BV785	102435	BioLegend
CD4	BV421	100438	BioLegend
CD45	BV510	103138	BioLegend
CD8	AF700	100730	BioLegend
Donkey anti-goat	AF488	A32814	Invitrogen
Galectin-1	unconjugated	AF1245	Bio-Techne
Live/Dead Fixable Viability Dye	eFluor780	65-0865-18	Invitrogen

Table 2: Antibodies used for cell hashing.

Antibody	Barcode sequence	Ref#	Company
TotalSeq™-C0301	ACCCACCAGTAAGAC	155861	BioLegend
TotalSeq™-C0302	GGTCGAGAGCATTCA	155863	BioLegend
TotalSeq™-C0303	CTTGCCGCATGTCAT	155865	BioLegend
TotalSeq™-C0304	AAAGCATTCTTCACG	155867	BioLegend
TotalSeq™-C0305	CTTTGTCTTTGTGAG	155869	BioLegend
TotalSeq™-C0306	TATGCTGCCACGGTA	155871	BioLegend
TotalSeq™-C0307	GAGTCTGCCAGTATC	155873	BioLegend
TotalSeq™-C0308	TATAGAACGCCAGGC	155875	BioLegend
TotalSeq™-C0309	TGCCTATGAAACAAG	155877	BioLegend
TotalSeq™-C0310	CCGATTGTAACAGAC	155879	BioLegend

Table 3: *In vivo* antibodies.

Target	Clone	Ref#	Company
InVivoMAb anti-mouse CD4	YTS 191	BE0119	Bio X Cell
InVivoMAb anti-mouse CD8α	YTS 169.4	BE0117	Bio X Cell
InVivoMAb rat IgG2b isotype control, anti-keyhole limpet hemocyanin	LTF-2	BE0090	Bio X Cell

Table 4: Primary antibodies used for immunofluorescence confocal and light sheet microscopy.

Target	Host species	Target species	Conjugate	Ref#	Company
B220	-	mouse	FITC	130110845	Miltenyi Biotec
CD3	rabbit	mouse/human	-	A0452	Dako
CD3	mouse	human	-	M7254	Dako
CD31	rat	mouse	-	550274	BD Pharmingen
CD31	rat	mouse	AF647	102516	BioLegend
CD31	goat	human	-	AF3628	Bio-Techne
DARC	sheep	mouse	-	AF6695	Bio-Techne
Iba1	goat	mouse	-	011-27991	Fujifilm Wako
Iba1	rabbit	mouse/human	-	019-19741	Fujifilm Wako

Table 5: Secondary antibodies used for immunofluorescence confocal and light sheet microscopy.

Host species	Target species	Conjugate	Ref#	Company
donkey	goat	AF647	A21447	Invitrogen
donkey	mouse	AF488	A21202	Invitrogen
donkey	rabbit	AF546	A10040	Invitrogen
donkey	rat	AF647	A78947	Invitrogen
donkey	sheep	AF488	A11015	Invitrogen
donkey	goat	AF488	A32814	Invitrogen
donkey	rabbit	AF488	A21206	Invitrogen
goat	rabbit	AF633	A21070	Invitrogen
goat	rat	AF546	A11081	Invitrogen
goat	rabbit	AF546	A11010	Invitrogen

2.1.2 Chemicals, reagents and others

Table 6: Overview of used plasmids.

Plasmid	Ref#	Company
LeGo-G2	25917	Addgene
pLC-ZsGreen-P2A-Puro	124302	Addgene

Table 7: Overview of used chemicals and other reagents.

Item	Ref#	Company
1-step fix lyse solution	00-5333-57	Invitrogen
Accutase®	A6964-100ML	Sigma-Aldrich
ACK lysis buffer	A1049201	Gibco
Benzyl alcohol	108006	Sigma-Aldrich
Benzyl benzoate	B6630	Sigma-Aldrich
BSA	T844.2	Carl Roth
CC1 buffer	05279801001	Roche
DMEM	D6429-500ml	Sigma-Aldrich
Donkey serum	S2170	Biowest
EDTA (0.5 M)	AM9260G	Invitrogen
Ethanol	9065.4	Carl Roth
FBS Superior	20041	Sigma-Aldrich
Fluoromount G™	00-4959-52	Invitrogen
HBSS	H6648-500mL	Sigma-Aldrich
HEPES	H0887-100ml	Sigma-Aldrich
IL-2	130-120-662	Miltenyi Biotec
InVivoPure pH 7.0 Dilution Buffer	IP0070	Bio X Cell
L-Glutamine	25030-024	Gibco
Liberase™	5401119001	Roche
Non-essential amino acids	M7145-100ml	Sigma-Aldrich
Normal goat serum	5425S	Cell Signaling Technologies
OneComp eBeads™	01-1111-42	Invitrogen
PBS	L0615-500	Sigma-Aldrich or Capricorn
Penicillin-Streptomycin	15140122	Gibco
Percoll®	GE17-0891-01	Cytiva
PFA (4%)	sc281692	ChemCruz
Puromycin	P8833	Sigma-Aldrich

RPMI-1640	P04-18500	Pan Biotech
Sodium pyruvate	11360-070	Gibco
Sucrose	84097-1kg	Sigma-Aldrich
Tissue-Tek® O.C.T. Compound	14291	Sakura Finetek USA, Inc.
TRITC-Dextran	52194	Sigma-Aldrich
Triton-X100	648466-50ml	Merck Millipore
Trypsin-EDTA (0.25%)	20100	ThermoFisher Scientific
Xylol	4436.1	Carl Roth

Table 8: Overview of used animal medications.

Product name	**Active substance**	**Company**
Antisedan ®	Atipamezolhydrochloride	Orion Pharma
Dorbene ® vet	Medetomidinhydrochloride	Zoetis Deutschland
Flumazenil Kabi	Flumazenil	Fresenius Kabi
Ketabel	Ketamin	Bela-pharm
Midazolam-ratiopharm ®	Midazolam	Ratiopharm
Rimadyl ®	Carprofen	Zoetis Deutschland
Rompun ®	Xylazinhydrochloride	Bayer Animal Health

2.1.3 Other items

Table 9: Overview of various used items.

Item	**Ref#**	**Company**
Ethilon sutures	EH7761H	Ethicon
Glass window	-	In-house production
Hamilton syringe 701 SN	80308	Hamilton
LS columns	130-042-401	Miltenyi Biotec
Superfrost™ Plus adhesion microscope slides	J1800AMNZ	Epredia
Titan ring	-	In-house production

2.1.4 Kits

Table 10: Overview of used kits

Kit	Ref#	Company
CD8a+ T Cell Isolation Kit, mouse	130-104-075	Miltenyi Biotec
Chromium Next GEM Single Cell 5' Kit v2	1000265	10x Genomics
eBioscience™ Intracellular Fixation & Permeabilization Buffer Set	88-8824-00	Invitrogen
Pan T Cell Isolation Kit II, mouse	130-095-130	Miltenyi Biotec
T Cell Activation/Expansion Kit, mouse	130-093-627	Miltenyi Biotec

2.1.5 Instruments

Table 11: Overview of used instruments.

Instrument name	Application	Company
10x Chromium controller	scRNA seq.	10x Genomics
4200 Tapestation	scRNA seq. quality control	Agilent
BD Aria II	FACS	BD Biosciences
BD Fusion	FACS	BD Biosciences
BioSpec 3 Tesla	MRI imaging	Bruker BioSpin
BioSpec 94/20 USR	MRI imaging	Bruker BioSpin
C170i Incubator	Cell culture	Eppendorf
Cryostat CM3050S	Sectioning of tissue	Leica
Electric drill	Stereotactic tumor cell injection	Foredom
Gammacell40	Irradiation	Best Theratronics
LSM 7MP	Multiphoton laser scanning microscopy	Zeiss
LSM700	Confocal microscopy	Zeiss
Mastercycler X50s	PCR cycler; scRNA seq. preparation	Eppendorf
Multirad225	Irradiation	Precision X-Ray
Stereotactic injector	Stereotactic tumor cell injection	Stoelting
Ultramicroscope II	Light sheet fluorescence microscopy	Miltenyi Biotec
ZE5	Flow cytometry analysis	BioRad

2.2 Methods

2.2.1 Mice

6-10 weeks old female Specific and Opportunistic Pathogen Free (SOPF) C57BL/6J mice were purchased from Janvier Labs, France. Lck-Cre x LSL-tdTomato (B6.Tg(Lck-cre)548Jxm x Gt(ROSA)26Sor$^{tm14(CAG.tdTomato)Hze}$) mice for *in vivo* multiphoton laser scanning microscopy were bred and provided by the group of Prof. Dr. Frank Winkler (CCU Neuro-oncology, German Cancer Research Center).

All animal experiments were performed at the animal facilities of the German Cancer Research Center, Heidelberg, Germany. All experiments were reviewed and approved by the responsible local governmental authorities (Regierungspräsidium Karlsruhe).

2.2.2 Cell lines

The murine glioma cell line GL261 was kindly provided by Dr. David Reuss (Department of Neuropathology, University Hospital Heidelberg) and the murine glioma cell line CT-2A was obtained from Sigma-Aldrich.

GL261 GFP cell line was generated by lentiviral transduction with the LeGO-G2 vector (Plasmid #25917; Addgene). After transduction, GFP positive cells were sorted using fluorescence activated cell sorting (FACS) and cultured in normal medium.

GL261 ZsGreen cell line was generated by lentiviral transduction with the pLC-ZsGreen-P2A-Puro vector (Plasmid #124302; Addgene). After transduction, cells were selected for successful transduction by adding 10 µg/ml puromycin to the culture media.

All cell lines were cultured in cell culture treated flasks in Dulbeccos' modified Eagle's medium (DMEM) supplemented with 10 % fetal bovine serum (FBS) and 100 U/ml penicillin and 100 µg/ml streptomycin at 37 °C and 5 % CO2.

2.2.3 Human samples

Anonymized human FFPE sections and tissue pieces of glioma patients for the detection of perivascular T cell niches were provided by the Department of Neuropathology, University Hospital Heidelberg and the Department of Neurosurgery, University Hospital Mannheim. Samples were covered under 2017-589N-MA and 2018-614N-MA ethical approvals.

2.2.4 Stereotactic tumor cell injection

Cell lines were detached using Accutase® at a confluency of 50-70 %. Cells were counted using a hemocytometer and cell number was adjusted to 25.000 cells/µl in sterile PBS. Mice were anesthetized using ketamine (100 mg/kg) and xylazin (10 mg/kg), the skin was opened using a scalpel and a hole was drilled into the skull using an electric drill (coordinates: 2 mm right lateral of the bregma and 1 mm anterior to the coronal suture). 50.000 cells in a total volume of 2 µl were injected in a depth of 3 mm below the dural surface at a rate of 1 µl/minute using a Hamilton micro-syringe mounted in a fine-step stereotactic device (Stoelting). After injection, the skin was stitched using surgical self-absorbing sutures. As analgesic, mice received two subcutaneous injections with 10 mg/kg Carprofen as well as 48 h of 10 mg/kg/day Carprofen in their drinking water.

For multiphoton laser scanning microscopy mice with an implanted titan ring and cranial window were fixated by fixing the titan ring into a custom adaptor on the stereotactic device. The glass window was removed and 25.000 GL261 GFP cells were injected in an angle of 45 degrees and 0.3-1 mm depth. After injection, a new glass window was glued into the titan ring (see also 2.2.16).

2.2.5 Irradiation of mice and cell lines

Mice were anesthetized by subcutaneous injection using an antagonizable anesthesia with Medetomidin (0,5 mg/kg) and Midazolam (5 mg/kg). Mice were irradiated with 2, 5 or 8 Gy using a Multirad225 (Precision X-Ray) device. Only the tumor-bearing brain hemisphere was irradiated. The rest of the body was protected by a custom-made lead shielding. After the irradiation, mice were given the antagonist consisting of Atipamezol (2,5 mg/kg) and Flumazenil (0,5 mg/kg) to wake them up from anesthesia. Cell lines and primary T cells were irradiated with 2, 5 or 8 Gy using GammaCell40 (Best Theratronics) or MultiRad225 (Precision X-Ray) device. After each irradiation, the media was exchanged.

2.2.6 Magnetic resonance imaging (MRI)

MRI was performed by the staff of the small animal imaging core facility at DKFZ using a BioSpec 3 Tesla (Bruker BioSpin) with ParaVision software 360 V1.1 or at the Radiology Department, University Clinic Heidelberg using a BioSpec 94/20 USR (Bruker BioSpin). For imaging, mice were anesthetized with Isoflurane inhalable narcosis. For lesion detection, T2 weighted imaging was performed using a T2_TurboRARE

sequence: TE = 48 ms, TR = 3350 ms, FOV 20x20 mm, slice thickness 1.0 mm, averages = 3, Scan Time 3 m 21 s, echo spacing 12 ms, rare factor 8, slices 20, image size 192x192. Tumor volume was determined by manual segmentation using Bruker ParaVision software 6.0.1 or 3D slicer 4.1 (Kilian et al., 2022).

2.2.7 *In vivo* T cell depletion

In order to deplete T cells *in vivo*, mice were injected with 1000 µg anti-CD4 and 500 µg anti-CD8a *in vivo* depletion antibodies (Bio X Cell). Control mice received 1500 µg rat IgG2b isotype control antibody (Bio X Cell). The injection with antibodies was repeated every 3-4 days for up to three times. In order to confirm the depletion, 48 hours after the first injection, blood was taken by puncturing the *Vena facialis* using a blood lancet. Blood was collected in EDTA-coated tubes and blood was stained for CD45, CD3, CD4, CD8 and CD11b. Using the 1-step Fix/Lyse solution (Invitrogen) cells were fixated and red blood cells lysed. After a final wash, cells were resuspended in FACS buffer and subsequently analyzed using flow cytometry.

2.2.8 Tumor harvest and processing

Mice were anesthetized with ketamine/xylazine and were cardially perfused using 30 ml PBS and tumor-bearing brains were resected. The tumor-bearing hemisphere was mechanically dissected using a scalpel and subsequently enzymatically digested in HBSS containing 50 µg/ml Liberase™ (Roche) for 30 minutes at 37°C. Next, the tissue was meshed through a 100 µm and 70 µm cell strainer (Miltenyi Biotec) to obtained single-cell suspensions. Myelin was removed by a 30 % continuous Percoll® (Cytiva) gradient.

2.2.9 T cell isolation and culture

In order to isolate T cells, spleens and lymph nodes (LN) from C57BL/6J were surgically resected. Spleens and LNs were then mashed through 70 µm strainer and flushed with PBS to obtain single-cell suspensions. The cell suspension was spanned down and the cell pellet was resuspended in 5 ml ACK lysis buffer (Gibco) to lyse red blood cells. After lysis the falcon is filled with 45 ml PBS and then filtered through a 70 µm strainer again. Cells were then counted and further used for magnetic activated cell sorting (MACS) using the Pan T cell isolation kit or CD8+ T cell isolation kit (both Miltenyi Biotec). Cells were stained with antibody cocktails and microbeads according to manufacturer's

protocol and then loaded onto LS columns (Miltenyi Biotec) mounted on the QuadroMACS separator (Miltenyi Biotec). As both kits are a negative selection, the flow through contains the untouched and unstained T cells which are then further used for experiments.

Isolated T cells are then cultured in T cell proliferation media (RPMI-1640 media + 10% FBS, 1% P/S, 50 µM β-mercaptoethanol, 2 mM L-Glutamine, 25 mM HEPES, 1 mM sodium pyruvate, 0.1 mM non-essential amino acids and 50 U/ml IL-2). For activation of T cells, cells were activated using the “T Cell Activation/Expansion Kit” (Miltenyi Biotec) according to manufacturer’s protocol.

2.2.10 Flow cytometry analysis and fluorescence activated cell sorting

After tissue processing or after harvest of cells from *in vitro* cultivation, cells were resuspended in 200 µl PBS and transferred to 96-well U-bottom plates. Unspecific binding of antibodies was blocked by incubation with anti-CD16/CD32 antibody mix (Invitrogen) and extracellular targets were subsequently stained using antibodies, listed in table 2.1.1, for 30-45 minutes at 4°C. Intracellular targets were stained after fixation and permeabilization using the IC fixation buffer kit (Invitrogen) for 45 minutes at 4°C. As control, fluorescence minus one (FMO) samples were generated. Stained cells were analyzed on a ZE5 flow cytometer (BioRad). For data analysis, FlowJo (version 10.8.1) software was used.

For sorting CD45+ immune cells, only extracellular staining using CD45-BV510 (BioLegend) and Fixable Viability Dye AF780 (Invitrogen) was performed. Cells were sorted using BD Aria Fusion or BD Aria II (both BD Biosciences) sorters with a 100 µm nozzle. Sorted cells were collected in BSA-coated 1,5 ml Eppendorf tubes and further processed for single-cell RNA-seq.

2.2.11 Cell hashing

Prior to FACS, samples subject to single-cell RNA sequencing, were stained with TotalSeq™-C hashing antibodies #1-10 (BioLegend). Hashing antibodies label all cells with a DNA-barcode sequence, which allows for the pooling of samples. Each sample from each group was assigned to two hashing antibodies. Then, four samples from different treatment groups were pooled and loaded onto Chromium Next GEM K Chips (10x Genomics) (see below).

2.2.12 Single-cell RNA sequencing and analysis

Hashed and sorted CD45+ cells were loaded on Chromium Next GEM Chip K microfluidics chips (10x Genomics) according to manufacturer's protocol. The further processing and library preparations were also performed according to manufacturer's protocol. Sequencing was performed by the core facility for next generation sequencing at DKFZ using NovaSeq 6000 (Illumina). Sequencing data was processed using 10x Genomics cell ranger platform (version 6.0) by Julius Michel. The data was aligned to the GRCm38 reference genome with all default settings. The resulting files were further processed and analyzed using Seurat package (version 4.3.0) and further specialized packages as described below on R (version 4.2.0) by Clara Tejido Dierssen (Stuart et al., 2019). The analysis and interpretation of data was performed together with Clara Tejido Dierssen.

Cells with unique feature counts over 4000 or less than 500, as well as cells with more than 10 % mitochondrial counts, were excluded from downstream analysis. Genes detected in fewer than three cells were excluded from downstream analysis. Doublet scores were generated using the scDblFinder package (version 1.10.0) (Germain et al., 2022). Cells labeled as "doublet" were not used for downstream analysis. Cells were classified as Hashtag positive singlets, doublets or unassigned cells using the HTODemux command to demultiplex cells and assign to the correct mice based on their hashtags (Stoeckius et al., 2018). In order to eliminate biases from different samples, batch correction was performed using the Harmony package (version 1.1.0) (Korsunsky et al., 2019). Annotation of cell clusters was performed using SingleR (version 1.10.0) with the "MouseRNAseqData" as a reference dataset from the celldex package (version 1.6.0) (Aran et al., 2019). The annotation was then further refined and corrected by manual curation of the differential gene expression of individual cell clusters. The data was divided into two subsets to separate myeloid and lymphoid cells. The clustering resolution was 1.4 and 0.9 for myeloid and lymphoid subsets, respectively. The enrichment of specific gene signatures was assessed by calculating UCell scores for each cell using the UCell package (version 2.2.0) (Andreatta & Carmona, 2021). To infer pseudotime trajectories of CD8 T cells, the monocle3 package (version 1.3.4) was utilized (Trapnell et al., 2014). Cells were ordered in pseudotime with the root node set in the "Naive CD8 T cells" cluster. The cell-to-cell interaction analysis was conducted using the CellChat package (version 1.6.1) (Jin et al., 2021). Plots were generated using Seurat package (version 4.3.0), the SCpubr package (version 2.0.2) and ggplot2 (version 3.5.1) (Blanco-Carmona, 2022).

2.2.13 Immunofluorescence imaging

Murine brains were resected as a whole and fixed in 4 % PFA in PBS for 24 hours at 4°C. Brains were then transferred into 30 % (w/v) Sucrose in PBS until full perfusion is reached and brains sink down. In order to freeze brains, they were transferred into a Tissue-Tek® O.C.T. compound (Sakura Finetek) filled mold and then placed on dry ice until completely frozen. For storage, frozen brains were stored at -80°C. 5-10 µm thick sections were then made by cutting frozen tissue-blocks at the cryostat cryotome CM3050S (Leica) and placed on Superfrost™Plus adhesion microscope slides (Epredia). For long-term storage, sections were stored at -80°C. For staining, frozen sections were thawed at room temperature for 5-10 minutes. Afterwards, slides were washed for 5 minutes in PBS, followed by 3 washes with washing buffer (0.1 % (v/v) Triton X-100 in PBS). Sections were then blocked with blocking buffer (washing buffer + 4 % (v/v) serum of secondary antibody host species (goat or donkey)) for 1 hour at RT. After blocking, sections were stained with primary antibodies (diluted 1:100-1:400 in blocking buffer) overnight at 4°C inside a humid chamber tray. The next day, samples were washed three times with washing buffer and then stained with secondary antibodies (diluted 1:200 in blocking buffer) for one hour at RT. After staining, samples were washed again three times with washing buffer and then mounted with DAPI-containing Fluoromount-G (Invitrogen) and cover slips. Stained samples were then stored at 4°C in the dark until imaging.

Human FFPE sections were warmed for 1 hour at 60°C, incubated two times with xylol and were rehydrated by serial incubation with 100 %, 96 %, 70 %, 50 % and 0 % ethanol in H2O. Antigen retrieval was performed by steaming slides in CC1 retrieval buffer for 30 minutes. Afterwards, slides were processed, blocked and stained as described above.

Imaging was performed at a Zeiss LSM700 confocal laser-scanning microscope (Zeiss). Image processing and analysis was performed on ZEN 3.4 blue edition software (Zeiss) and ImageJ version 1.53k.

2.2.14 Tissue clearing and staining

Mice were anesthetized as described above and subsequent cardial perfusion was first done with 20 ml PBS and then with 20 ml 4 % PFA in PBS for fixation. Brains were resected and further fixed for 24 hours in 4 % PFA in PBS at 4°C. Human tissue samples were fixed in 4 % PFA in PBS for 24 to 48 hours. After fixation, murine brains and human tissue samples were stored in PBS until further processing. Clearing of samples was subsequently performed by Berin Boztepe (Department of Neuroradiology, Heidelberg

University Hospital) according to iDISCO protocol (Renier et al., 2014). During the iDISCO protocol, brains were stained with anti-CD3 (Dako) in order to stain T cells and anti-CD31 (BioLegend/Bio-Techne) to stain for endothelial cells. Subsequently, fluorescently-labeled secondary antibodies were used to target the anti-CD3 primary antibody. Cleared and stained brains where then stored at 4°C in the dark until imaging at a light sheet fluorescence microscope.

2.2.15 Light sheet fluorescence microscopy

Cleared and stained brains were fixated inside the light sheet fluorescence microscope Ultramicroscope II (Miltenyi Biotec) and submerged in benzyl alcohol, benzyl benzoate (BABB) medium. The brain was imaged at 4x magnification using the MI Plan 4x DC57 objective. Images were taken at a step size of 5 µm with a light sheet thickness of 3.78 µm. Images were processed using Fiji software (version 1.53q) and 3D reconstruction of images was done using Imaris software (version 8.0.2) (Oxford Instruments).

2.2.16 *In vivo* multiphoton laser scanning microscopy

Multiphoton laser scanning microscopy was performed together with the group of Prof. Dr. Frank Winkler (CCU Neuro-oncology, DKFZ & Department of Neurology, University Hospital Heidelberg). In order to allow the live imaging of the brain, mice subject to imaging received a window implant. In order to insert the implant, mice were anesthetized and the skull and dura mater were surgically removed. Then, a titan ring was glued to the skull and the glass window was glued into the ring to seal the hole. Mice are then treated with Carprofen as analgesic and are left for 14 days to allow proper healing and adaption to the cranial window. After this period, the glass was removed to allow the orthotopic injection of syngeneic tumor cells (see 2.2.4) into the brain. After injection, a new glass window was glued into the titan ring. For imaging, mice were anesthetized with inhalation of Isoflurane and then imaged on a Zeiss LSM 7MP microscope equipped with a Chameleon Ultra II or a Discovery NX laser and a 20x/1.0 W-Plan-Apochromat objective. In order to visualize the vasculature, mice were intravenously injected with 100 µl of 5 mg/ml of tetramethylrhodamine-isothiocyanate-dextran (TRITC-Dextran) prior to imaging. To image endogenous T cells in perivascular niches, cranial windows were implanted into Lck-Cre x LSL-tdTomato mice in which all T cell express tdTomato. In order to locate niches inside and outside of the tumor, GL261 GFP expressing cells were used in these experiments (see 2.2.2).

2.2.17 Statistics

Statistical analysis was performed using GraphPad Prism (version 8.0.1 and version 10.3.0) or for single-cell RNA seq. analysis by R (version 4.2.0). Significance was tested by unpaired t-test analysis, one-way ANOVA with subsequent Tukey test, or in the case of symptom-free survival experiments by Log-rank (Mantel-Cox) test. For the interactome analysis, the significance was assessed by a one-sided permutation test. Significance was defined as P-value ≤ 0.05. Significance is displayed as * = P-value ≤ 0.05; ** = P-value ≤ 0.005; *** = P-value ≤ 0.0005; **** = P-value ≤ 0.0001; ns = not significant. If no star (*) is displayed, the difference is not statistically significant or the individual P-values are directly displayed in the respective graph.

2.2.18 Illustrations

All figures were made using Affinity Designer 2 (version 2.4.0). Illustrations were made using BioRender.com.

3 Results

3.1 Part 1: Dose- and time-dependent immune cell dynamics in an irradiated glioma model

In this first part, I aimed to investigate how different dosages of radiotherapy influence the immune cell-mediated therapeutic effect in a preclinical glioma model. Additionally, I aimed to assess how immune cell dynamics and interactions in the brain are influenced by different dosages of radiotherapy. The overall aim was to identify the dosage that induces the most potent immune response to be utilized in combinatorial therapies.

3.1.1 Different dosages of radiotherapy and their impact on survival of preclinical glioma models

Here, I aimed at investigating the overall clinical response of the preclinical glioma model GL261 to different dosages of radiotherapy and the contribution of the adaptive immune response, specifically the induced response by T cells. Therefore, I orthotopically injected GL261 cells into C57BL/6J mice and subjected them to different dosages of radiotherapy and evaluated their symptom-free survival (Figure 3a). I chose to irradiate with a low dosage (2 Gy), a medium dosage (5 Gy), another medium high but fractionated dosage (3x 2 Gy) on three consecutive days and a high dosage (8 Gy). In order to assess the importance of the T cell response for prolonged survival after radiotherapy, mice were either treated with anti-CD4/anti-CD8a depletion antibodies or with isotype control antibodies. Due to the large number of mice (n = 120), this experiment had to be split in two rounds. Yet, the comparability and consistency between the two experiments was confirmed by comparing the untreated isotype control mice from both experiments (Supplementary Figure 1a). The successful depletion of T cells was confirmed by flow cytometry of blood samples from T cell depleted and isotype control mice (Supplementary Figure 1b-c). Untreated mice showed a median survival of 18 days, while irradiated mice showed a median survival of 20 (2 Gy), 26.5 (5 Gy), 25 (3x 2 Gy) and 35 days (8 Gy), respectively (Figure 3b-c). Overall, the symptom-free survival was significantly prolonged by all dosages with a survival benefit of 2 (2 Gy), 8.5 (5 Gy), 7.0 (3x 2 Gy) and 17 days (8 Gy) (Figure 3b-c & Supplementary Figure 1d). When comparing isotype control treated mice with T cell depleted mice without irradiation, an endogenous T cell response against GL261 can be observed, which accounts for a survival benefit of only 2 days (Supplementary Figure 1e). In order to assess the T cell-mediated survival benefit after radiotherapy, irradiated T cell depleted mice were compared with isotype control treated mice. This revealed that the survival benefit of 2 Gy was 100.0% T cell-mediated, while the T cell-mediated survival benefit of 5, 3x 2 and 8 Gy was 88.24%,

85.24% and 70.59%, respectively (Figure 3d-h & Supplementary Figure 1f-h). Interestingly, although not statistically significant, the single dose of 5 Gy seemed to outperform a higher dosage of 6 Gy fractionated by 3x 2 Gy in terms of median survival, survival benefit and T cell-mediated survival benefit (Figure 3c-h & Supplementary Figure 1d, f).

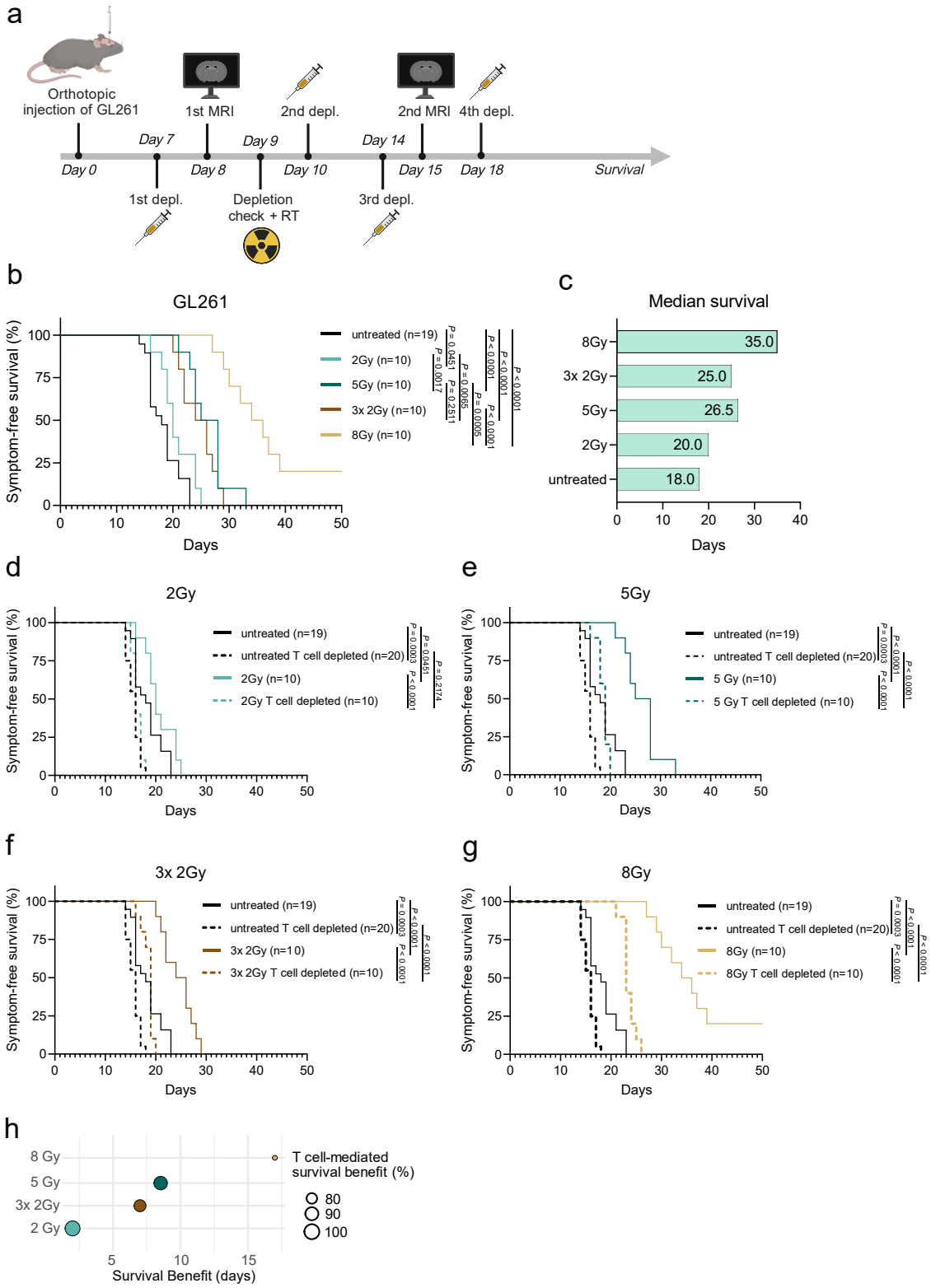

Figure 3: The dose- and T cell-dependent survival after radiotherapy.

(a) Schematic overview of performed survival experiments with GL261. Single dosages were applied on day 9. Mice treated with 3x 2Gy were treated on day 9, 10 and 11. (b) Symptom-free survival of C57BL/6J mice after receiving 2, 3x 2, 5, or 8 Gy radiotherapy displayed in a Kaplan-Meier curve. (c) Median survival of all experimental groups displayed in days. (d-g) Kaplan-Meier curve of symptom-free survival after 2 Gy (d), 5 Gy (e), 3x 2 Gy (f) or 8 Gy (g) radiotherapy +/- pan T cell depletion with anti-CD4 and anti-CD8 depletion antibodies. Non-T cell-depleted mice

received isotype control antibodies. (h) The overall survival benefit compared to untreated control mice in days (x-axis) displayed together with the T cell-mediated survival benefit (dot size) of all irradiated groups. All statistics were performed by Log-rank (Mantel-Cox) test. Individual *P*-values are displayed in the graph.

3.1.2 The longitudinal immune landscape of irradiated gliomas

In order to assess the longitudinal immune cell dynamics after different dosages of radiotherapy, I performed single-cell RNA sequencing of immune cells from untreated and 2, 5, 3x 2 and 8 Gy irradiated mice. For this, mice were orthotopically injected with GL261 cells on day 0 and on day 8 the tumor growth was confirmed by MRI (Figure 4a). On day 10, mice were irradiated with a single dose of 2, 5 or 8 Gy. Mice that received 3x 2 Gy also received additional dosages of 2 Gy on day 11 and 12. On day 13 (day 3 after initial irradiation) and on day 17 (day 7 after initial irradiation), mice were sacrificed, tumors resected and CD45+ immune cells were FACS sorted and subsequently single-cell RNA sequencing was performed. In order to increase the resolution on individual cell subtypes, immune cells of the myeloid and lymphoid lineage were identified (Supplementary Figure 2a-b) and further subclustered in two separate uniform manifold approximation and projections (UMAPs) (Figure 4b-c). On average, of all cells, myeloid cells made up for >85% on day 3 and >75% on day 7 (Supplementary Figure 2b). Lymphoid and myeloid cell clusters were annotated based on expression of cell-type specific markers and their abundancy was assessed among the different treatment groups and two timepoints (Figure 4b-e). In total, in the lymphoid lineage 21 clusters were identified and included activated CD4 T cells, memory CD4 T cells, exhausted CD4 T cells, T regulatory cells, proliferating T regulatory cells, naïve CD8 T cells, early activated CD8 T cells, proliferating CD8 T cells, IFN-stimulated CD8 T cells, cytotoxic CD8 T cells, memory CD8 T cells, exhausted CD8 T cells, gamma delta (gd) T cells, MAIT T cells, proliferating cells, NKT cells, NK cells, Ccl5 NK cells, Xcl1 NK cells, B cells and plasma cells (Figure 4b,d). Within the myeloid lineage, also 21 cell clusters were identified and included macrophages 1-4, M2-like macrophages, border-associated macrophages, IFN-stimulated macrophages, microglia, Plxna4 microglia, microglia-like cells, dendritic cells (DCs) 1-3, Ccr7 DCs, plasmacytoid DCs 1-2, Ly6d- plasmacytoid DCs, neutrophils, mast cells, basophils and as small contamination also neurons (Figure 4c, e).

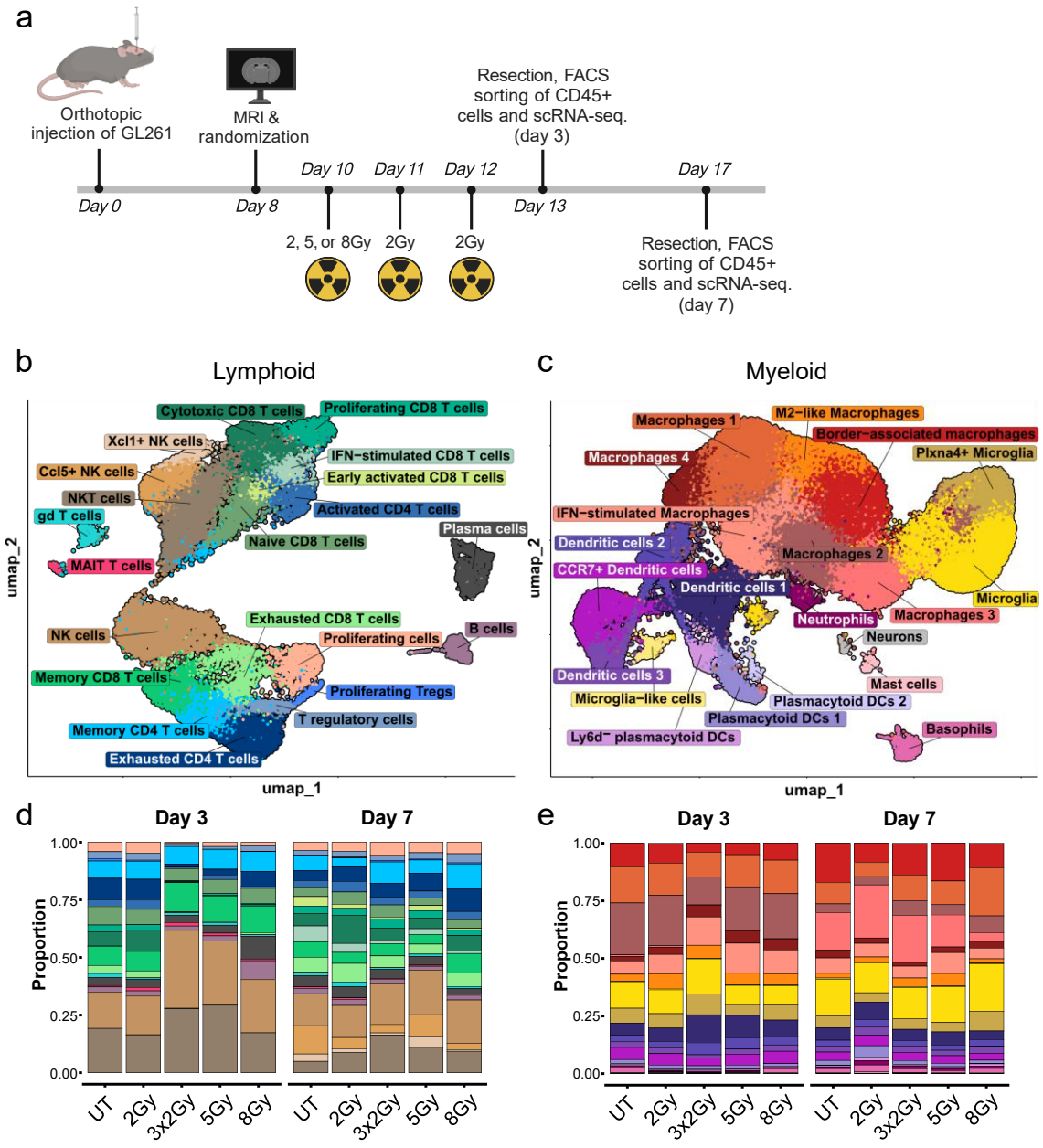

Figure 4: The tumor immune microenvironment of GL261.

(a) Experimental overview of performed irradiation experiments with 2, 3x 2, 5 and 8 Gy and subsequent FACS sorting for CD45+ immune cells and single-cell RNA sequencing on day 3 and day 7 after first treatment. n = 4 per group and per timepoint. (b) Uniform Manifold Approximation and Projection (UMAP) dimension reduction displaying all lymphoid cells and defined clusters in the TME of GL261. (c) UMAP of all myeloid cells and defined cluster in the TME of GL261. (d-e) Proportions of individual lymphoid (d) and myeloid (e) cell clusters on day 3 and day 7 in the individual treatment groups. Bioinformatic processing with Clara Tejido Dierssen.

Interestingly, after medium (5 and 3x 2 Gy) and high (8 Gy) dosages, a depletion of the T cell clusters cytotoxic CD8 T cells, proliferating CD8 T cells, proliferating cells, exhausted CD4 and CD8 T cells, and activated CD4 T cells was observed on day 3 after irradiation compared to untreated and low-dose treatment with 2 Gy (Figure 4d & 5a-b).

However, these clusters returned on day 7 after irradiation, indicating a depletion after treatment and replenishment with new cells at the later timepoint. In order to confirm the irradiation- and dosage-dependent T cell depletion, I irradiated T cells with 2, 5 and 8 Gy *in vitro*. *In vitro*, T cells showed a dose-dependent and significant reduction in viability already 24h after irradiation (Figure 5c). Meanwhile, other cell populations such as memory CD4 and CD8 T cells, NK cells and NKT cells seemed resistant to this depletion independently of the dosage. Comparing the cell composition between day 3 and day 7, certain cell clusters only appeared on day 7 but not on day 3 independently of the treatment. In the lymphoid compartment, these were Ccl5+ NK cells, Xcl1+ NK cells, IFN-stimulated CD8 T cells and early-activated CD8 T cells (Figure 4d & Figure 5a, d). Among the myeloid cells only the cluster Macrophages 3 appeared at day 7, but not day 3 (Figure 4e & Supplementary Figure 3a-b). At the same time, cluster Macrophages 2 only appeared on day 3, but was not observed on day 7. Overall, all other myeloid clusters showed no change in abundancy after different dosages of irradiation or time (Figure 4e & Supplementary Figure 3a-b).

In summary, I demonstrate time-dependent immune cell compositions of the tumor microenvironment independently of treatment. Irradiation with medium and high dosages lead to cluster-specific T cell depletion early after irradiation, but the depleted cells were replenished with newly infiltrating cells four days later. As there were no dosage-dependent changes in myeloid cluster abundancies, myeloid cells seem to be more radio-resistant than lymphoid cells.

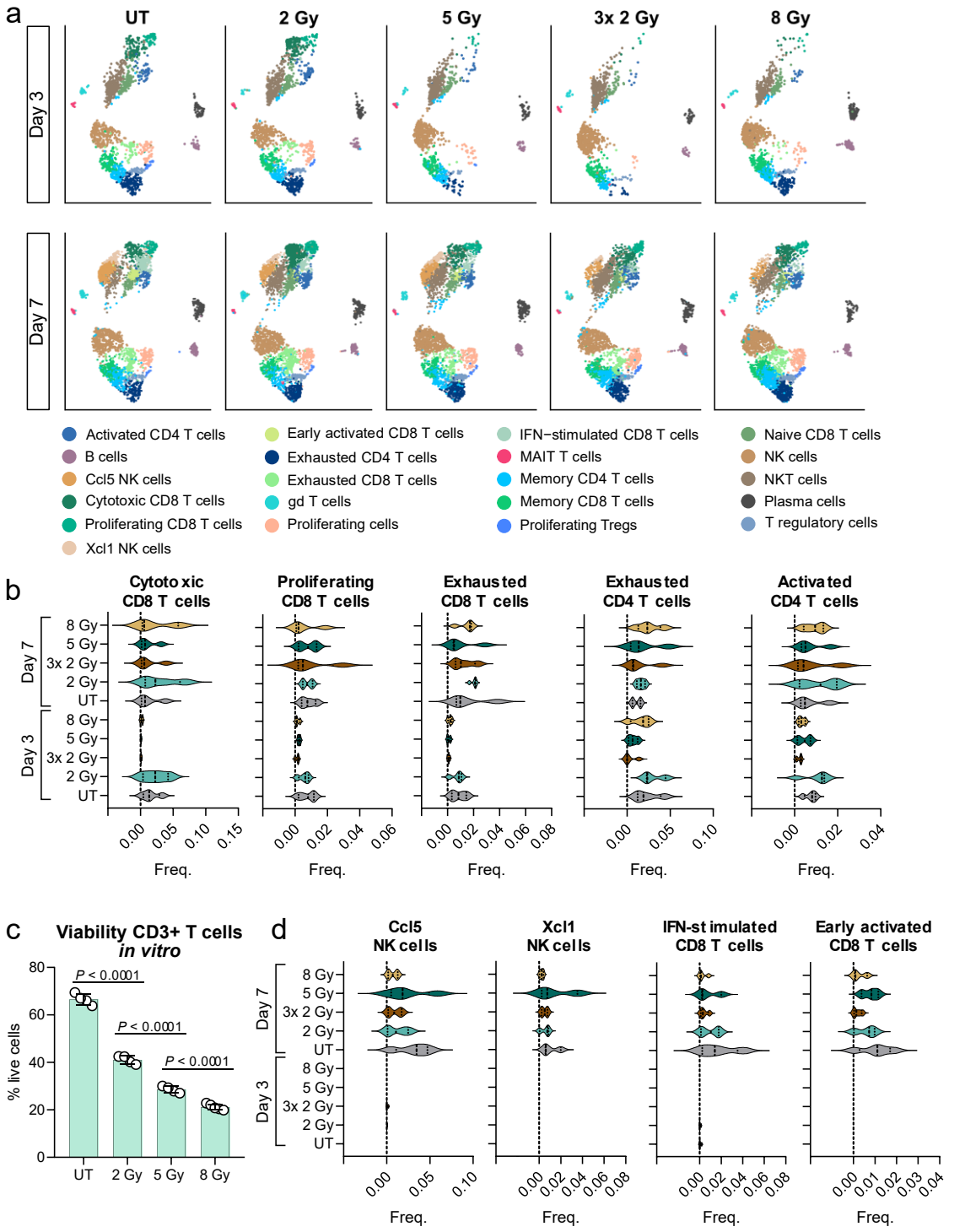

Figure 5: Overview and abundancies of lymphoid cell clusters.

(a) UMAP of all groups at day 3 and 7. (b) Frequency (Freq.) of selected lymphoid cell clusters that are affected by medium and high dosages at day 3 and 7 in the different treatment groups. (c) Viability of T cell 24h after different dosages of irradiation tested by staining with fixable viability dye and flow cytometry measurement. Percentage of all viability-dye negative cells among all CD3+ T cells. Statistics performed by unpaired t-test. Significance was defined as P-value ≤ 0.05. (d) Frequency of selected lymphoid cell clusters that are not present at day 3 but at day 7 in the different treatment groups. Bioinformatic processing with Clara Tejido Dierssen.

3.1.3 Immune signatures of different dosages of radiotherapy

In order to identify which dosage is inducing the best immune response, various literature-curated gene expression signatures were applied to cell clusters, in order to identify differences between the treatment groups at day 3 and day 7 after irradiation. At day 3, the T cell and NK cell response signatures were significantly enriched in both 3x 2 Gy and 5 Gy treatment groups (Figure 6a-b, e-f). However, both signatures only sustained their enrichment in the 5 Gy group at day 7 (Figure 6c-d, g-h). At the same time, the 8 Gy treated group demonstrated a significant downregulation of both response signatures compared to the lower dosages and even compared to the untreated group, both at day 3 and day 7 (Figure 6a-h). Next, I looked at the expression of inhibitory immune checkpoints on the cytotoxic CD8 T cell population. This revealed no significant differences among groups at day 3, but a significant downregulation in the 5 Gy treated group compared to untreated or 3x 2 Gy (Figure 6i-l). Overall, this indicates that both medium dosages induced a strong T cell and NK cell response, which was only sustained until day 7 in the 5 Gy group compared to the other regimen. A reason for the sustained response in the single-dose treated group could be the downregulation of immune checkpoints after 5 Gy and upregulation after 3x 2Gy. Altogether, 5 Gy irradiation is associated with the highest and most sustained expression of T and NK cell response signatures while reducing exhaustion of cytotoxic T cells at the late time point, indicating a favorable modulation of these cells in the TME.

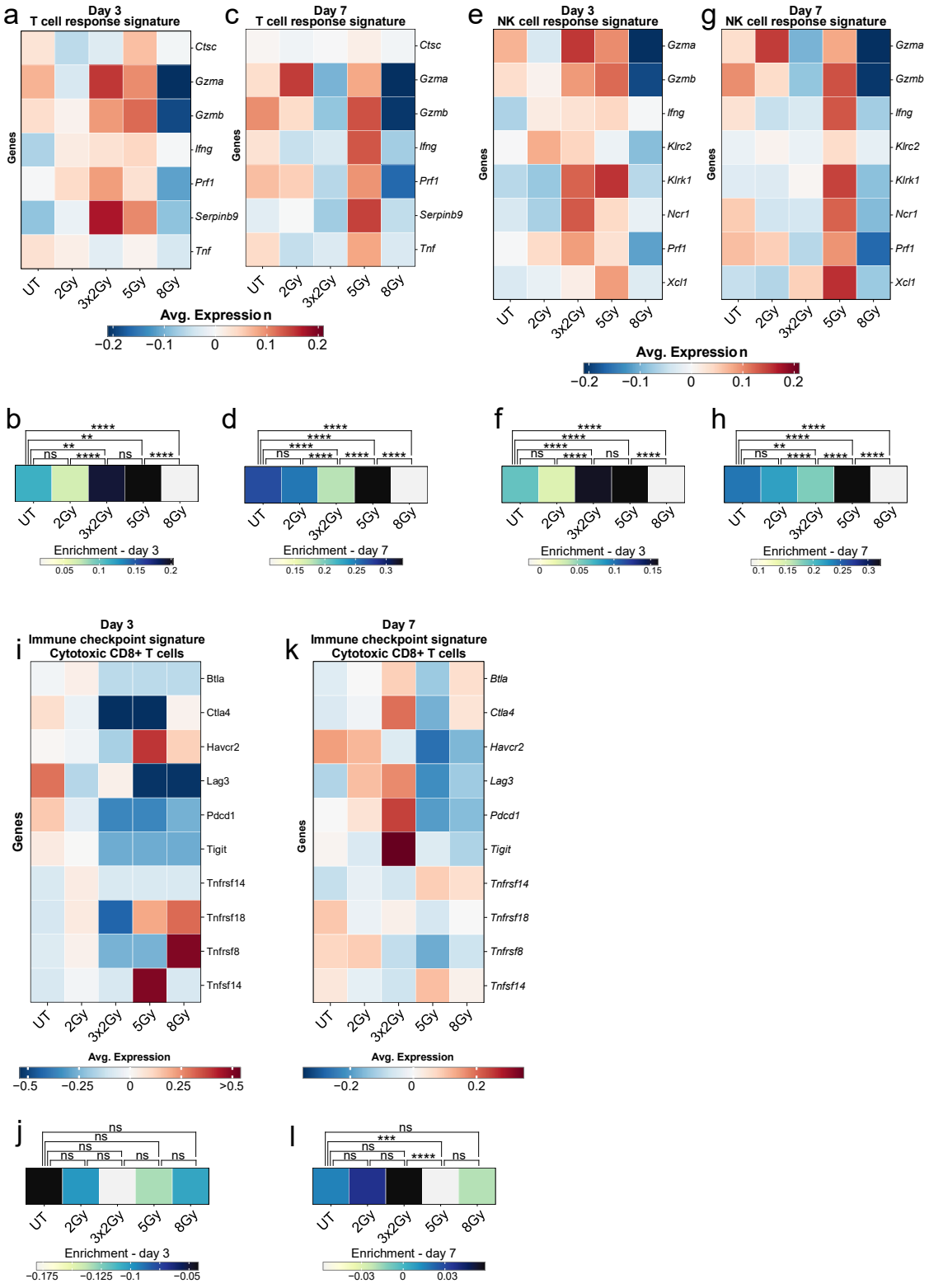

Figure 6: Gene signatures of T and NK cell responses.

(a) Heatmap of the T cell response signature and the average expression of genes in lymphoid cells at day 3. (b) Enrichment of the T cell response signature in lymphoid cells at day 3. (c) Heatmap of the T cell response signature and the average expression of genes in lymphoid cells at day 7. (d) Enrichment of the T cell response signature in lymphoid cells at day 7. (e) Heatmap of the NK cell response signature and the average expression of genes in lymphoid cells at day 3. (f) Enrichment of the NK cell response signature in lymphoid cells at day 3. (g) Heatmap of the

NK cell response signature and the average expression of genes in lymphoid cells at day 7. (h) Enrichment of the NK cell response signature in lymphoid cells at day 7. (i) Heatmap of the immune checkpoint signature and the average expression of genes in the cytotoxic CD8 T cell cluster at day 3. (j) Enrichment of the immune checkpoint signature in the cytotoxic CD8 T cells cluster at day 3. (k) Heatmap of the immune checkpoint signature and the average expression of genes in the cytotoxic CD8 T cell cluster at day 7. (l) Enrichment of the immune checkpoint signature in the cytotoxic CD8 T cells cluster at day 7. Statistical analysis in all enrichment plots was performed by one-way ANOVA with subsequent Tukey test. Significance was defined as P-value ≤ 0.05. Significance is displayed as * = P-value ≤ 0.05; ** = P-value ≤ 0.005; *** = P-value ≤ 0.0005; **** = P-value ≤ 0.0001. ns = not significant. Not all statistics are displayed in the enrichment plots. Bioinformatic processing with Clara Tejido Dierssen.

As irradiation is well-known for inducing type I IFN responses and since several studies have shown that a type I IFN response is crucial for a successful anti-tumor (T cell) response (Burnette et al., 2011; Deng et al., 2014; Diamond et al., 2011) , a type I IFN response signature was applied in order to evaluate the type I IFN response induction in lymphoid and myeloid cells in the different treatment groups. In lymphoid cells, at day 3, in all groups except for 2 Gy, a significant upregulation of the IFN response can be observed in comparison to the untreated group (Figure 7a-d). Yet, no dose-dependency could be observed as the medium high dosages of 3x 2 Gy and 5 Gy showed the highest enrichment, while 8 Gy demonstrated a significantly lower expression compared to 3x 2 Gy and 5 Gy. However, only in the 5 Gy treated group, a strong enrichment was observed at day 7 (Figure 7c-d). Among myeloid cells, the picture looked similar, with the highest enrichment in 3x 2 Gy and 5 Gy at day 3 and the highest enrichment in the 5 Gy treated group at day 7 (Figure 7e-g). Especially at day 7, in both myeloid and lymphoid cells, the major interferon stimulatory genes 15 (*Isg15*) and 20 (*Isg20*), as well as important signaling transducers of the type I IFN signaling pathway, such as signal transducer and activator of transcription 1 (*Stat1*) and 2 (*Stat2*), as well as interferon regulatory factor 7 (*Irf7*), which is responsible for inducing type I IFN expression, are most expressed in the 5 Gy treated group (Figure 7c, g). At the same time, the major T and NK cell chemoattractant C-X-C motif chemokine ligand 10 (*Cxcl10*) is most expressed in the 5 Gy group both in lymphoid and myeloid cells (Figure 7a, c, e, g). Microglia, macrophages and dendritic cells are among the most abundant cell types expressing *Cxcl10*. In all three cell types, *Cxcl10* was most expressed after 5Gy irradiation at day 7 (Figure 7i). This hints towards an enhanced induction of T and NK cell recruitment into the TME. Again, in line with activation and exhaustion signatures in T and NK cells, these data indicate the highest and most sustained induction of the type I IFN response after 5 Gy irradiation.

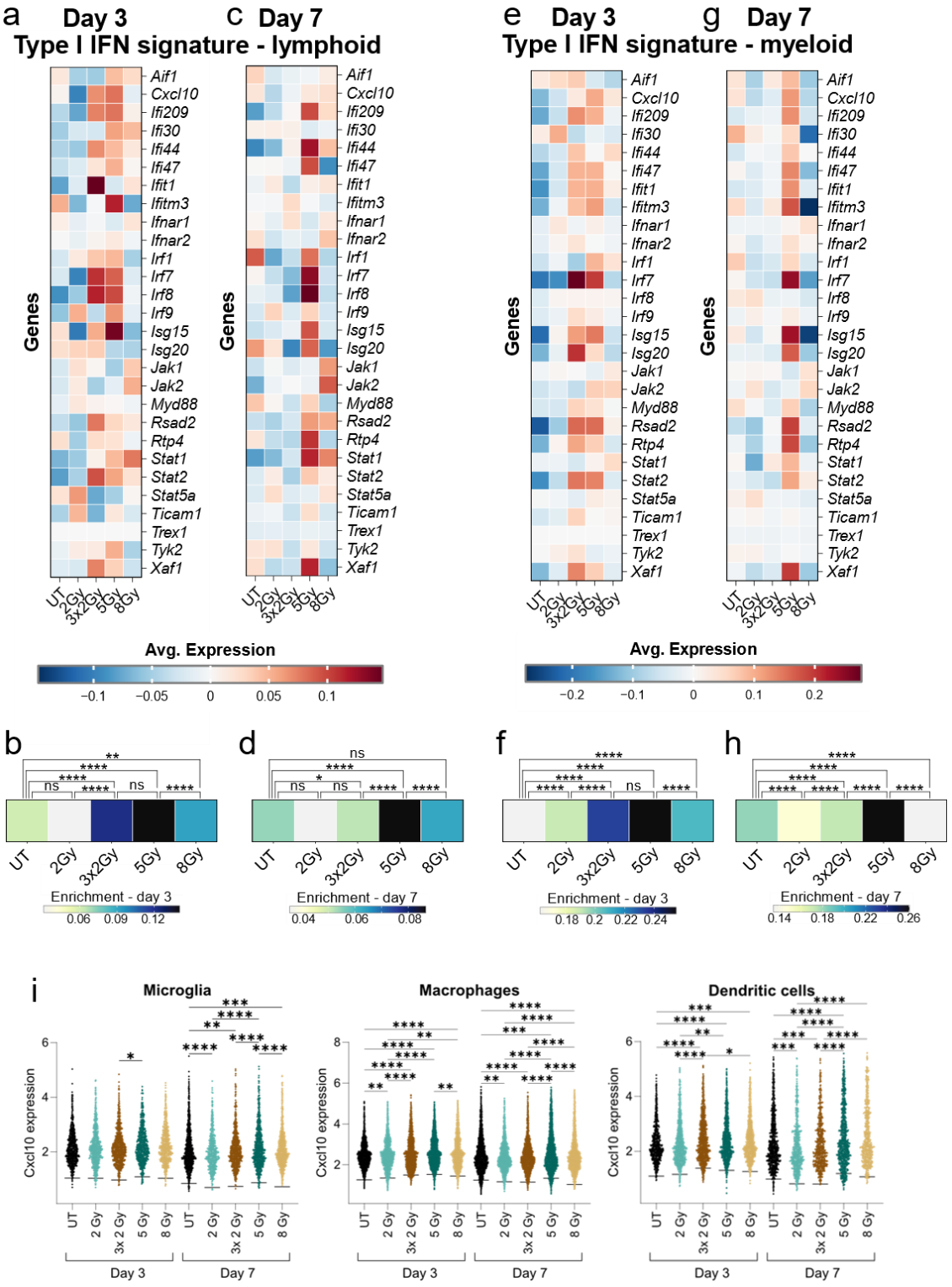

Figure 7: Type I IFN signature expression in lymphoid and myeloid cells.

(a) Heatmap of the type I IFN response signature and the average expression of genes in lymphoid cells at day 3. (b) Enrichment of the type I IFN response signature in lymphoid cells at day 3. (c) Heatmap of the type I IFN response signature and the average expression of genes in lymphoid cells at day 7. (d) Enrichment of the type I IFN response signature in lymphoid cells at day 7. (e) Heatmap of the type I IFN response signature and the average expression of genes in myeloid cells at day 3. (f) Enrichment of the type I IFN response signature in myeloid cells at day 3. (g) Heatmap of the type I IFN response signature and the average expression of genes in

myeloid cells at day 7. (h) Enrichment of the type I IFN response signature in myeloid cells at day 7. (i) Expression of Cxcl10 in microglia, macrophages and dendritic cells. Bars display the mean expression level. Cells without expression are not displayed. Statistical test was performed individually by timepoint with one-way ANOVA and subsequent Tukey test. Significance was defined as P-value ≤ 0.05. Significance is displayed as * = P-value ≤ 0.05; ** = P-value ≤ 0.005; *** = P-value ≤ 0.0005; **** = P-value ≤ 0.0001. Only significant differences are displayed. Bioinformatic processing with Clara Tejido Dierssen.

Next, I aimed to investigate the influence of the different treatment groups on antigen processing and presentation. Therefore, an antigen presentation signature, comprised of major histocompatibility (MHC) genes, as well as genes playing a role in antigen processing and loading, was applied to all myeloid cells and the dominant professional antigen presenting cell (APC) types in the glioma TME, namely dendritic cells, microglia and macrophages. Among all myeloid cells, at day 3, the 2 Gy treated group showed a significant upregulation of the signature compared to the untreated group, while 3x 2 Gy showed a significant downregulation and no significant changes in 5 Gy and 8 Gy compared to untreated were detected (Supplementary Figure 4a-b). At day 7, 2 Gy, 3x 2 Gy and 8 Gy showed a significant downregulation compared to the untreated group, while 5 Gy showed no significant difference (Supplementary Figure 4c-d). On a cell type specific level, in dendritic cells, the signature was significantly upregulated at day 3 in 2 Gy, 3x 2 Gy, and 5 Gy compared to the untreated group (Figure 8a-b). At day 7 on the other hand, 2 Gy, 3x 2 Gy and 8 Gy showed a significantly lower enrichment compared to UT (Figure 8c-d). Only 5 Gy maintained an upregulated enrichment compared to UT and all other treatment groups (Figure 8a-d). In Microglia, the highest enrichment was observed in the untreated group at day 3, but at day 7, the enrichment also significantly increased in the 5 Gy treated group compared to the other treatment groups, but no significant difference was observed between 5 Gy and the untreated group (Figure 8e-h). In macrophages the enrichment was highest in UT and 2 Gy at day 3 and only slightly increased in 3x 2Gy and 5 Gy at day 7, but was still lower than UT and 2 Gy (Supplementary Figure 4e-h). Taken together, irradiation seemed to have a rather negative impact on antigen presentation in all myeloid cells except for DCs at the early time point. The 5 Gy treated group demonstrated a superior antigen processing and presentation signature, in all APCs at day 7 after treatment, among all irradiated groups. Dendritic cells and microglia seem to play a major role for the antigen presentation after 5 Gy. Meanwhile, 8 Gy showed a highly negative impact on antigen presentation in all myeloid cell types.

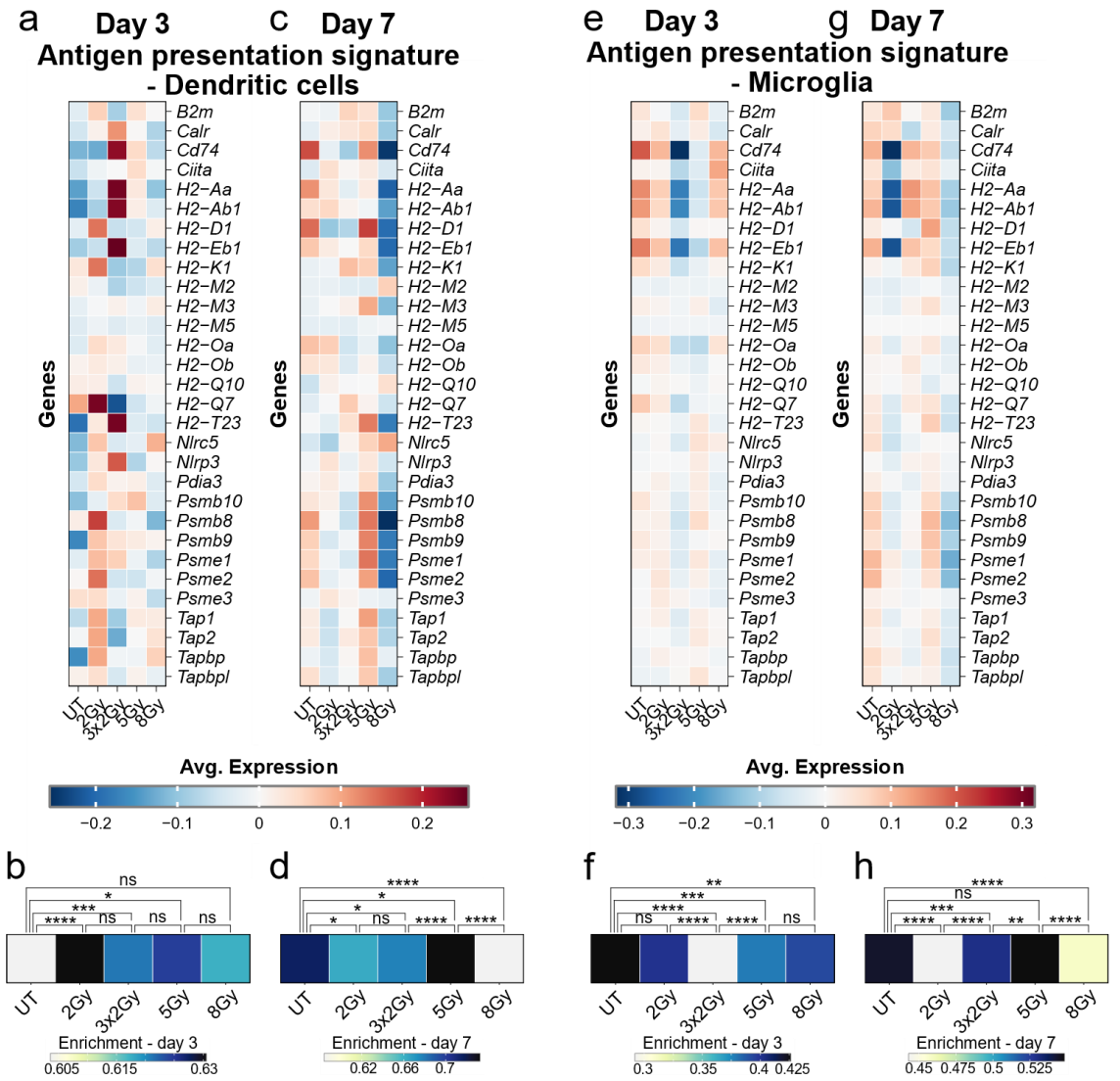

Figure 8: Antigen presentation signature in DCs and microglia.

(a) Heatmap of the antigen presentation signature and the average expression of genes in all dendritic cells at day 3. (b) Enrichment of the type antigen presentation signature in all dendritic cells at day 3. (c) Heatmap of the antigen presentation signature and the average expression of genes in dendritic cells at day 7. (d) Enrichment of the antigen presentation signature in all dendritic cells at day 7. (e) Heatmap of the antigen presentation signature and the average expression of genes in all microglia at day 3. (f) Enrichment of antigen presentation signature in all microglia at day 3. (g) Heatmap of the antigen presentation signature and the average expression of genes in all microglia at day 7. (h) Enrichment of the antigen presentation signature in all microglia at day 7. Statistical analysis was performed with one-way ANOVA and subsequent Tukey test. Significance was defined as P-value ≤ 0.05. Significance is displayed as * = P-value ≤ 0.05; ** = P-value ≤ 0.005; *** = P-value ≤ 0.0005; **** = P-value ≤ 0.0001; ns = not significant. Bioinformatic processing with Clara Tejido Dierssen.

In conclusion, both treatment groups applying medium dosages of 3x 2 Gy (6 Gy total) and 5 Gy were associated with strong T cell and NK cell response signatures, as well as type I IFN signatures and enhanced antigen presentation, as well as reduced exhaustion. However, these signatures were only sustained until the later timepoint in the single

dosage 5 Gy treatment group. Meanwhile, the application of 8 Gy induced rather negative effects by showing significantly lower T, NK and type I IFN responses as well as lower antigen presentation. Taken together, the single application of 5 Gy seems to be the superior dosage among the tested treatments in inducing anti-tumoral immune responses and shaping a favorable tumor microenvironment.

3.1.4 The irradiation-specific immune cell interactome

Next, I aimed at investigating how radiotherapy influences the cellular interaction within the tumor immune microenvironment and which interactions are crucial for mounting a successful anti-tumoral immune response induced or facilitated by irradiation. Therefore, the probability of cell to cell interaction in the untreated and 5 Gy treated group was evaluated and compared using the CellChat package (Jin et al., 2021). This analysis was only performed on the 5 Gy treated group, as the previous results indicated superiority over the other dosages (Figure 3-8). The complete immune interactomes of the untreated and 5 Gy treated group were compared and only those predicted interacting receptor-ligand pairs that were significantly upregulated or exclusively present in the 5 Gy treated group were filtered out and are presented (Figure 9a-d). At day 3 and day 7, 11 and 34 interacting receptor-ligand pairs, respectively, were detected to be either upregulated or exclusively present in the 5 Gy treated group solely at the respective timepoint (Figure 9a). 47 interacting receptor-ligand pairs were detected to be upregulated or exclusively present in the 5 Gy group both at day 3 and day 7 (Figure 9a). At day 3, lymphotoxin alpha (*Lta*) and various other cytokines and chemokines, such as IL-15 (*Il15*), CSF1 (*Csf1*), IL-4 (*Il4*), and CXCL2 (*Cxcl2*) with their respective receptors were among the exclusive interactions in the 5 Gy treated group (Figure 9b & Supplementary Figure 5a-c). Additionally, various other receptor ligand pairs interacting at day 3 in the 5 Gy treated group are related to cell-cell adhesion such as Cadherin 1 (*Cdh1*; E-Cadherin) with integrin subunit alpha 1 (*Itga1*) and beta 1 (*Itgb1*), intercellular adhesion molecule 1 (*Icam1*) with integrin subunit alpha M (*Itgam*) and beta 2 (*Itgb2*) or laminin subunit gamma 1 (*Lamc1*) with integrin subunit alpha 2 (*Itga2*) and *Itgb1* (Figure 9b & Supplementary Figure 5a-c). The day 7 exclusive interacting partners are in majority related to MHC interaction with lymphocytes such as Cd8b1, Cd8a or Cd4 with various MHC class I and II genes, but also again various pairs related to cell-cell adhesion (Figure 9c & Supplementary Figure 5a-c). Interestingly, the receptor-ligand pair with the highest probability of interaction to be exclusive to the 5 Gy group at day 7, in NK cells and Cd4 T cells, was interferon gamma (*Ifng*) with its receptors interferon gamma receptor 1 (*Ifngr1*) and 2 (*Ifngr2*) (Figure 9c & Supplementary Figure 5a-c). Among the

interactions that were significantly upregulated or exclusive in the 5 Gy treated group at both timepoints, were especially chemokines such as CC motif chemokine ligands 2-8 and 12 (*Ccl2, Ccl3, Ccl4, Ccl5, Ccl6, Ccl7, Ccl8, Ccl12*) but also many cell-cell adhesion pairs, with *Lamc1* and *Cd44* showing the highest probability (Figure 9d & Supplementary Figure 5a-c).

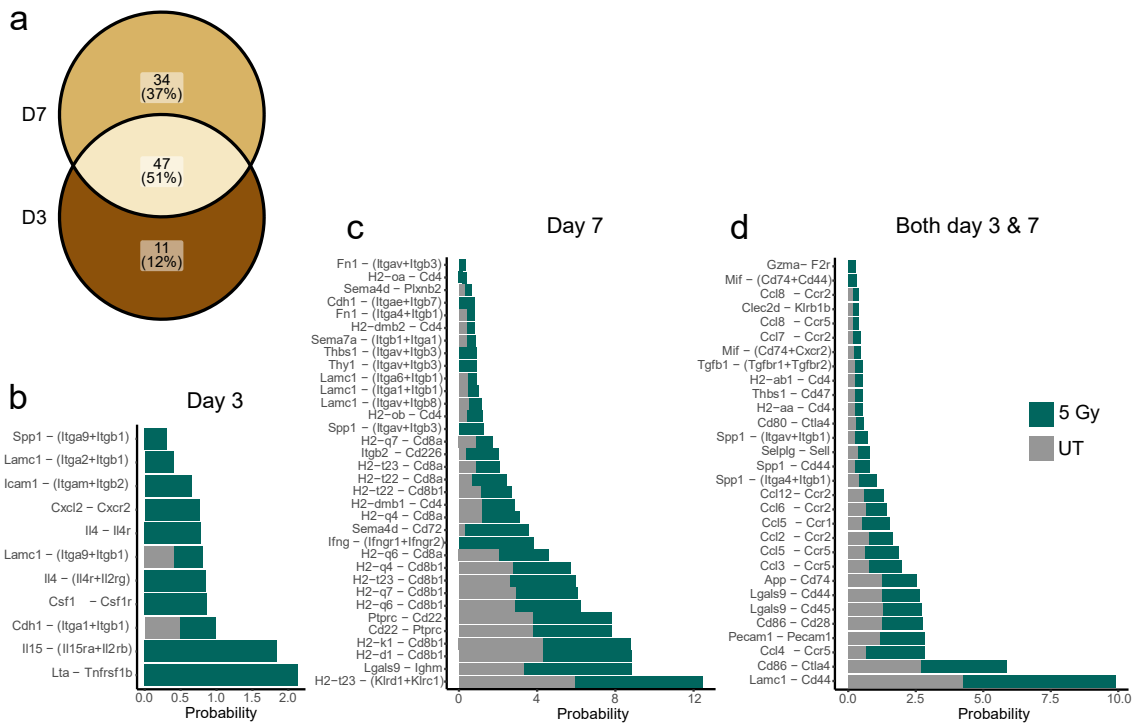

Figure 9: The irradiation-specific immune interactome.

(a) The number of predicted exclusive or significantly upregulated receptor-ligand interactions in the 5 Gy treated group compared to untreated at exclusively day 3 (11), exclusively day 7 (34), or both days (47). (b) Receptor-ligand pairs and their probability of interaction, which are exclusively only in the 5 Gy treated group or significantly upregulated compared to the untreated group at day 3. (c) Receptor-ligand pairs and their probability of interaction, which are exclusively only in the 5 Gy treated group or significantly upregulated compared to the untreated group at day 7. (d) Receptor-ligand pairs and their probability of interaction, which are exclusively only in the 5 Gy treated group or significantly upregulated compared to the untreated group on both days. Only statistically significant (P-value ≤ 0.05) interactions were included. Statistical testing was performed by a one-sided permutation test. Bioinformatic processing with Clara Tejido Dierssen.

Next, as some of the exclusive or upregulated genes in the 5 Gy treated group, *Ifng* and the cell adhesion molecules *Thy1, Pecam1* and *Icam1* were evaluated on their predicted interacting cell types within the tumor immune microenvironment in the untreated and 5 Gy treated groups. Interestingly, *Ifng* signaling from CD4 T cells and NK cells to various myeloid cells such as macrophages, microglia and DCs was exclusive to the 5 Gy treated

group (Figure 10a & Supplementary Figure 5a, c). *Thy1* expressed on various lymphoid cells, including CD4, CD8, and gamma delta T cells, interacted with various myeloid populations and its interactions were significantly enhanced in the 5 Gy treated group (Figure 9c & 10b). Exclusively in the 5 Gy treated group, *Thy1* expressed by NKT cells also interacted with the same populations (Figure 9c & 10b). The *Pecam1* interactions were upregulated in the 5 Gy treated group and interactions that included Tregs, proliferating cells and mast cells were exclusively detected in the irradiated group (Figure 10c). *Icam1* interaction was exclusively derived from microglia and the number of interacting cell types increased in the 5 Gy treated group (Figure 10d). In summary, radiotherapy enhances *Ifng* mediated signaling via CD4 T cells and NK cells and the upregulation of interactions with cell adhesion molecules may suggest a higher migration of cells within the TME.

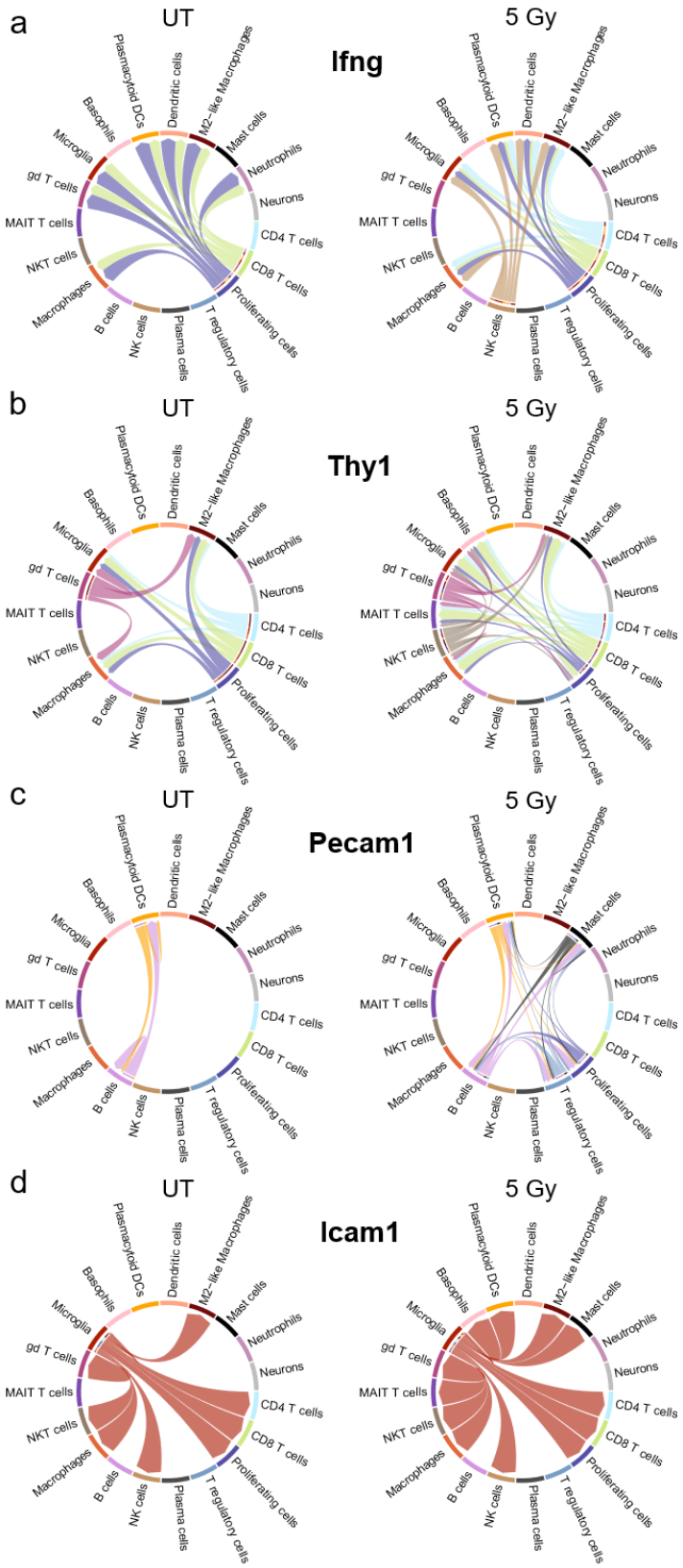

Figure 10: Cell-cell interactions of selected genes.

Chord plots displaying the CellChatDB predicted cell to cell interactions among immune cells in the TME of GL261 of *Ifng* (a), *Thy1* (b), *Pecam1* (c) and *Icam1* (d). Bioinformatic processing with Clara Tejido Dierssen.

3.1.5 Galectin-1 is expressed by activated CD8+ T cells and is potentially regulated by radiotherapy

As one of the longitudinally most differentially expressed genes in CD8+ T cells in all irradiated groups (Supplementary Figure 6), *Lgals1* (Galectin-1) expression was further assessed in all cell types. This revealed that Galectin-1 was predominantly expressed in cytotoxic CD8 T cells, type I IFN stimulated CD8 T cells, early-activated CD8 T cells and proliferating CD8 T cells compared to all other cell types (Figure 11a-b). As comparison, other galectins expressed in immune cells, such as *Lgals3,* were predominantly expressed in myeloid cells such as M2-like macrophages and IFN-stimulated macrophages and comparably low expressed in cytotoxic CD8 T cells (Supplementary Figure 7a). *Lgals9* was only low or not at all expressed in any cell type, but highest in myeloid cells such as IFN-simulated macrophages or microglia (Supplementary Figure 7b). Next, the trajectory of *Lgals1* expression among all CD8 T cell populations was evaluated based on pseudotime trajectory. The root node was set to naïve CD8 T cells, and based on pseudotime, the trajectory progressed to early activated CD8 T cells, followed by IFN-stimulated CD8 T cells, cytotoxic CD8 T cells, proliferating CD8 T cells, memory CD8 T cells and exhausted CD8 T cells in the named order (Figure 11c-e). Interestingly, the expression of *Lgals1* correlated with the activation status of the CD8 T cells, with the peak of expression in activated CD8 clusters, such as cytotoxic CD8 T cells, and a downregulation once exhaustion or the memory phenotype is reached along the trajectory (Figure 11e). To confirm *Lgals1* expression is upregulated upon activation, CD8 T cells were activated *in vitro* using CD3/CD28 microbeads and Galectin-1 expression was measured by flow cytometry. Upon activation, CD8 T cells significantly upregulated Galectin-1 expression, which peaked at 48 hours post-activation (Figure 11f-g). This indicates that *Lgals1*/Galectin-1 expression could serve as robust surrogate marker for activated CD8 T cells *in vivo* and *in vitro.* Next, the impact of irradiation on *Lgals1* expression was evaluated among the different treatment groups. Due to the depletion of cytotoxic CD8 T cells at day 3 in the groups treated with 3x 2 Gy, 5 Gy and 8 Gy, it was not possible to properly evaluate *Lgals1* levels in these groups (Figure 11h-i). Yet, in the 2 Gy treated group a downregulation in the average expression of *Lgals1* was observed at day 3 compared to untreated control (Figure 11h-i). At day 7, an overall increase in *Lgals1* expression was observed in the untreated and 2 Gy treated groups compared to day 3 (Figure 11h-i). At the same time, a significant dose-dependent downregulation of *Lgals1* expression with increasing irradiation dosage was observed at day 7 (Figure 11h-i).

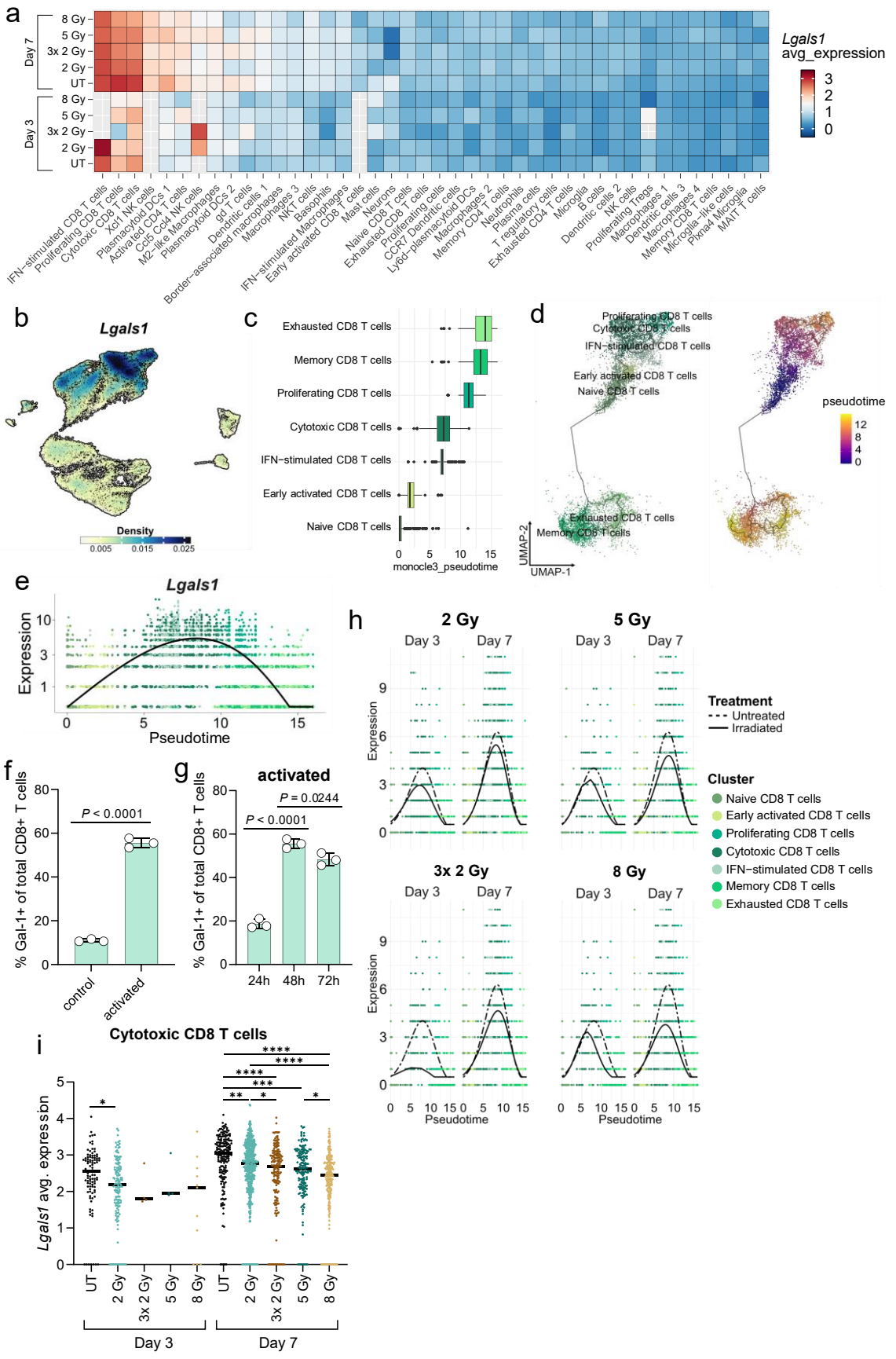

Figure 11: Galectin-1 dynamics in CD8+ T cells.

(a) Overview of average *Lgals1* expression among all cell types in the different treatment groups at day 3 and day 7. Grey boxes indicate no detectable *Lgals1* expression. (b) Lymphoid UMAP displaying *Lgals1* expression density across cell populations. (c-d) Pseudotime trajectory analysis among CD8 T cells based on expression of *Lgals1* and the root node set to naïve CD8 T cells. (e) Expression level of *Lgals1* across CD8 T cells along the pseudotime trajectory. (f) Flow cytometry analysis of Galectin-1 expression of activated CD8 T cells and non-activated control CD8 T cells 48h post-activation. (g) Flow cytometry analysis of Galectin-1 expression in activated CD8 T cells over time (24-72h post-irradiation). Statistical test performed in f and g by unpaired t-test. (h) Pseudotime analysis and expression of *Lgals1* among treatment groups. (i) Expression levels of *Lgals1* in cytotoxic CD8 T cells among treatment groups and timepoints. Bars indicate the median expression level. Significance was defined as P-value ≤ 0.05. Significance is displayed as * = P-value ≤ 0.05; ** = P-value ≤ 0.005; *** = P-value ≤ 0.0005; **** = P-value ≤ 0.0001. Bioinformatic processing with Clara Tejido Dierssen.

3.2 Part 2: Perivascular T cell niches (PVTNs) in gliomas

In this second part, I am reporting the discovery of so far undescribed perivascular T cell niches in the brain and investigated their cellular composition, structure and migration of T cells into and out of the niche. In addition, I investigated the tumor-antigen uptake by endothelial cells (ECs) for their potential role in PVTN development.

3.2.1 T cells develop perivascular niches around CD31+ blood vessels

In order to assess the infiltration of T cells in untreated and irradiated gliomas, I performed immunofluorescence imaging of CD3+ T cells on fixed-frozen sections of GL261-bearing mouse brains. During imaging, I observed that CD3+ T cells tightly accumulate in high numbers at certain positions within the tumor, but also outside of the tumor (Figure 12a-b). These T cells always form these accumulations around CD31+ blood vessels, thereby forming what I termed the perivascular T cell niche (PVTN). PVTNs outside of the tumor seem more organized in their structure, while intratumoral PVTNs appear more dissociated or diffuse, which is likely due to the overall remodeled tissue environment within the tumor (Figure 12a-b). Even though, the number of intact vessels decreases with irradiation (Supplementary Figure 8a-b), the number of intratumoral PVTNs significantly increased after treatment with 1x 5 Gy irradiation (Figure 12c). Interestingly, extratumoral PVTNs can not only be found in the very near proximity to the tumor but also at distant sites and at the meninges (Supplementary Figure 9a-b). In order to confirm that the phenomenon of PVTNs is not only specific to mice, I performed CD3 and CD31 immunofluorescence stainings on FFPE-fixated tumor sections of glioma patients and was able to confirm the existence of PVTNs in humans (Figure 12d).

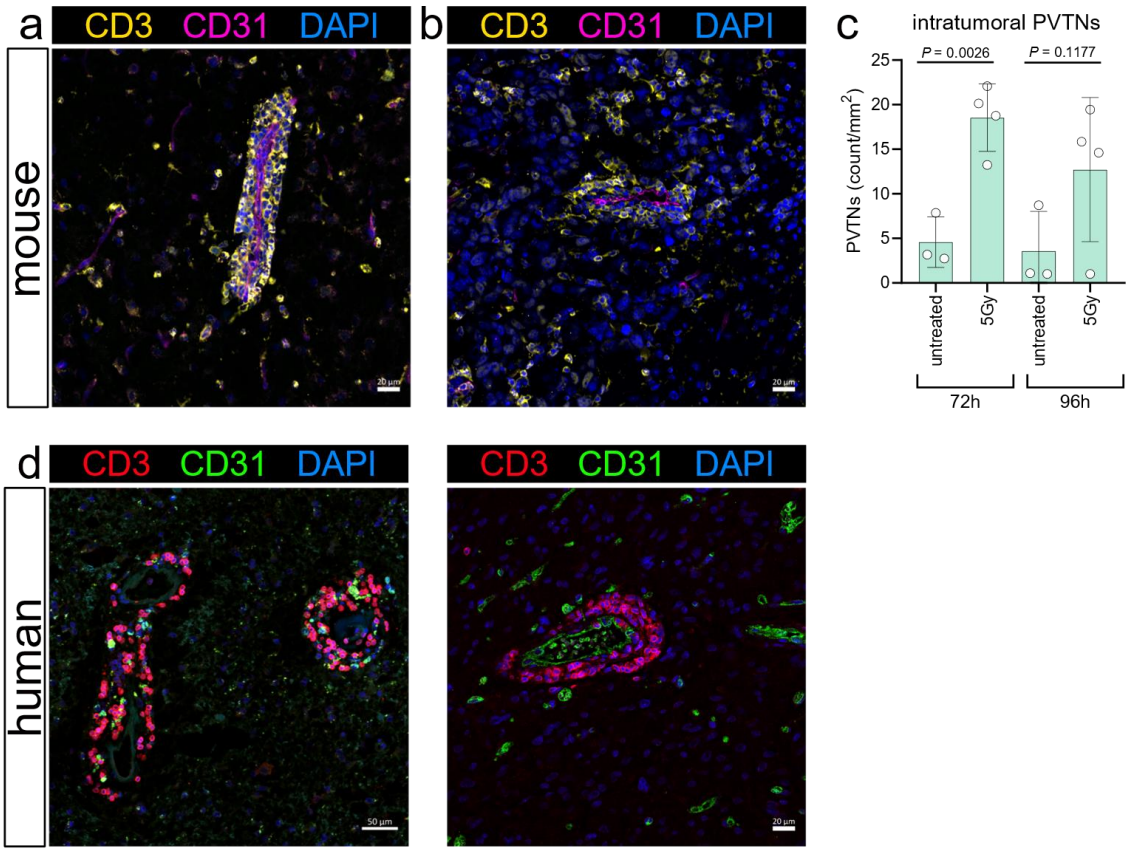

Figure 12: Discovery of perivascular T cell niches (PVTNs) in gliomas.

Representative example images of PVTNs outside (a) or inside (b) of GL261 tumors by immunofluorescence (IF) staining with anti-CD3 (yellow), anti-CD31 (magenta) and DAPI (blue) and subsequent laser scanning confocal microscopy. (c) Quantification of intratumoral PVTNs in untreated or 1x 5 Gy irradiated GL261 tumors 72 and 96 hours after treatment (13 and 14 days after tumor inoculation) from IF images. Statistical test performed by unpaired t-test. (d) Representative example images of PVTNs in human glioma patient samples by IF staining with anti-CD3 (red), anti-CD31 (green) and DAPI (blue) and subsequent laser scanning confocal microscopy.

Next, I wanted to investigate whether other immune cells infiltrate or surround PVTNs. I therefore stained for the CD45 isoform B220 as a B cell marker, but was not able to confirm relevant numbers of B cells in or around the niches (data not shown). Next, in order to stain for myeloid cells, I stained for Ionized calcium-binding adaptor molecule 1 (Iba1) as a marker for macrophages and microglia. In both murine and human samples, Iba+ macrophages/microglia were detected to cluster within PVTNs (Figure 13a-d). Even in dense niches, these Iba1+ cells would be found between the CD3+ T cells. The location of the PVTN did not influence the occurrence of Iba+ cells within the niche as they were detected both in PVTNs at the tumor (Figure 13a) and at the meninges (Figure 13b). However, whether these cells are macrophages or microglia, whether they are

newly infiltrated or tissue-resident cells, still needs to be determined. Also, their phenotype as well as their functional role within the niche remains unknown.

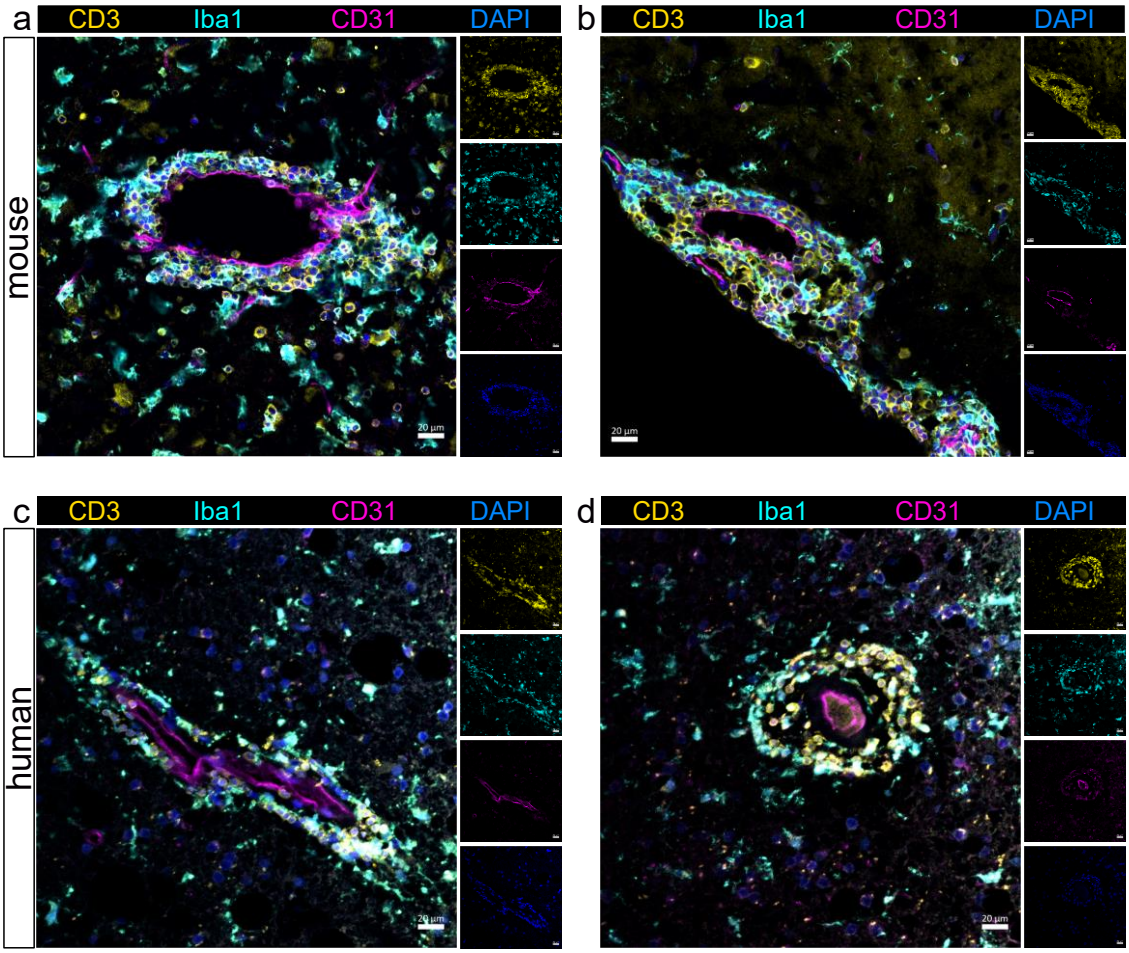

Figure 13: Myeloid cells in PVTNs.

Evaluation of myeloid cell localization in and around PVTNs. Representative images of PVTNs and their cellular composition with CD3+ T cells (yellow), Iba+ Macrophages/Microglia (cyan), CD31+ ECs (magenta) and DAPI (blue) by immunofluorescence staining and subsequent confocal laser scanning microscopy in (a) murine samples near the GL261 tumor, (b) murine samples at the meninges, (c-d) human glioma samples at unknown location. Mouse samples were fixed-frozen (day 13 past tumor cell injection). Human samples were FFPE fixed. Scale bars 20 µm.

3.2.2 Identity of endothelial vessel phenotype in PVTNs

Furthermore, I aimed to identify the vessel type of endothelial vessels contributing in PVTNs. High endothelial venules (HEV) are a type of blood vessels known to be involved in lymphocyte trafficking and T cell entry into solid tumors outside of the brain and into lymph nodes (Blanchard & Girard, 2021; Martinet et al., 2012). One of the well-established markers for HEVs is the *Duffy antigen receptor for chemokines* (DARC) (Thiriot et al., 2017). I therefore stained for DARC on murine sections of GL261 in order

to investigate whether the vessels in PVTNs are HEV-like vessels. And indeed, all PVTNs, both at the tumor and the meninges, were found to be around CD31+ DARC+ vessels (Figure 14a-b). All PVTNs were found to be around CD31+ DARC+ HEV-like vessels, but not all HEV-like vessels were surrounded by PVTNs. Only at the meninges also CD31+ DARC- vessels were observed to be present within large PVTNs, but were always alongside or between CD31+ DARC+ HEV-like vessels (Figure 14b).

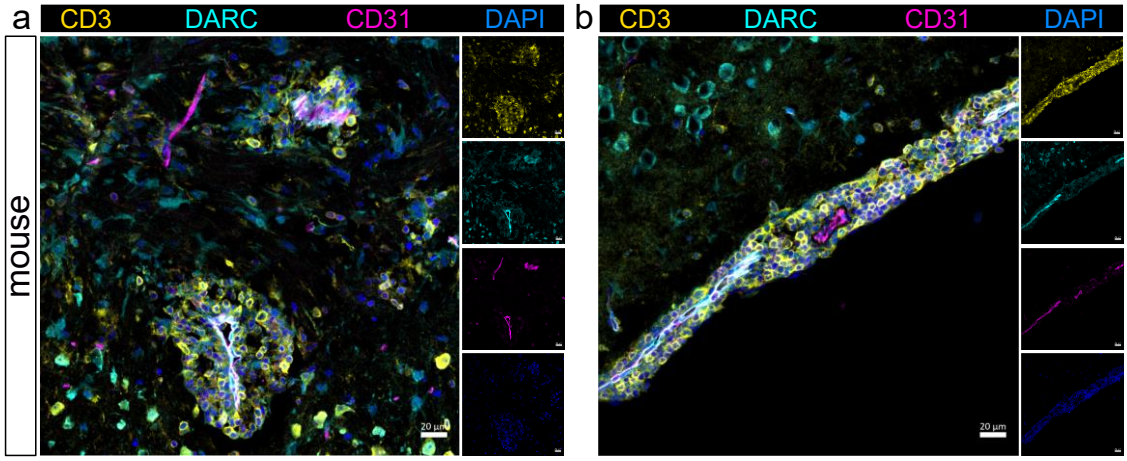

Figure 14: Identification of PVTN vessels.

Representative immunofluorescences images of PVTNs with CD31+ (magenta) and DARC+ (cyan) vessels and surrounding CD3+ T cells (yellow) taken by confocal laser scanning microscopy. (a) PVTNs in or near GL261 tumor and (b) PVTN at the meninges of a GL261-bearing mouse. Day 13 past tumor cell injection. Scale bars 20 µm.

3.2.3 3D structure and size of PVTNs

In order to assess the size and structure of PVTNs, tissue clearing with subsequent light sheet fluorescence microscopy was performed on brains of tumor-bearing mice and human brain tumor samples. Tissue clearing makes the brain transparent and subsequent staining with fluorescently labeled antibodies enables the use of a light sheet fluorescence microscope to image the entire brain with the markers of interest layer by layer. Using advanced imaging software, such as Imaris (version 8.0.2), the generated single layer images can be stitched together to a 3D image of the imaged area. This allowed us to investigate the 3D structure and course of vessels and PVTNs in the brain and the tumor. After clearing and light sheet fluorescence microscopy of the preclinical murine glioma models GL261 and CT-2A, I could show that PVTNs can extend along entire vessels starting from the meninges all the way to and around the tumor (Figure 15a-b & Supplementary Figure 10b). In the contralateral hemisphere, although in

relatively low numbers and with seemingly lower CD3+ T cell density, PVTNs can also be observed (Supplementary Figure 10a). In untreated mice, a low infiltration of T cells into the tumor can be observed. At the same time, seemingly more T cells are present in PVTNs outside of the tumor than T cells inside the tumor (Figure 15a). In mice irradiated with 1x 5 Gy on the other hand, a high number of T cells and PVTNs can be observed inside the tumor, while extratumoral PVTNs demonstrate a seemingly lower T cell density (Figure 15b). However, quantification of this data will be needed for making quantitative statements on the density of T cells and PVTNs in untreated and irradiated tumors.

In order to also assess the 3D structure of PVTNs in human glioma patients, freshly resected glioma samples were obtained and subsequently fixed, cleared, stained and imaged with a light sheet fluorescence microscope. PVTNs were also found in these samples and extend around CD31+ vessels (Supplementary Figure 11a-b). In the samples analyzed, PVTNs were only locally observed and did not extend along entire vessels which is in line with my observation of intratumoral PVTNs within murine tumors, but not with extratumoral PVTNs. However, the original localization of the tissue piece analyzed within the original tumor or peritumoral tissue was not available.

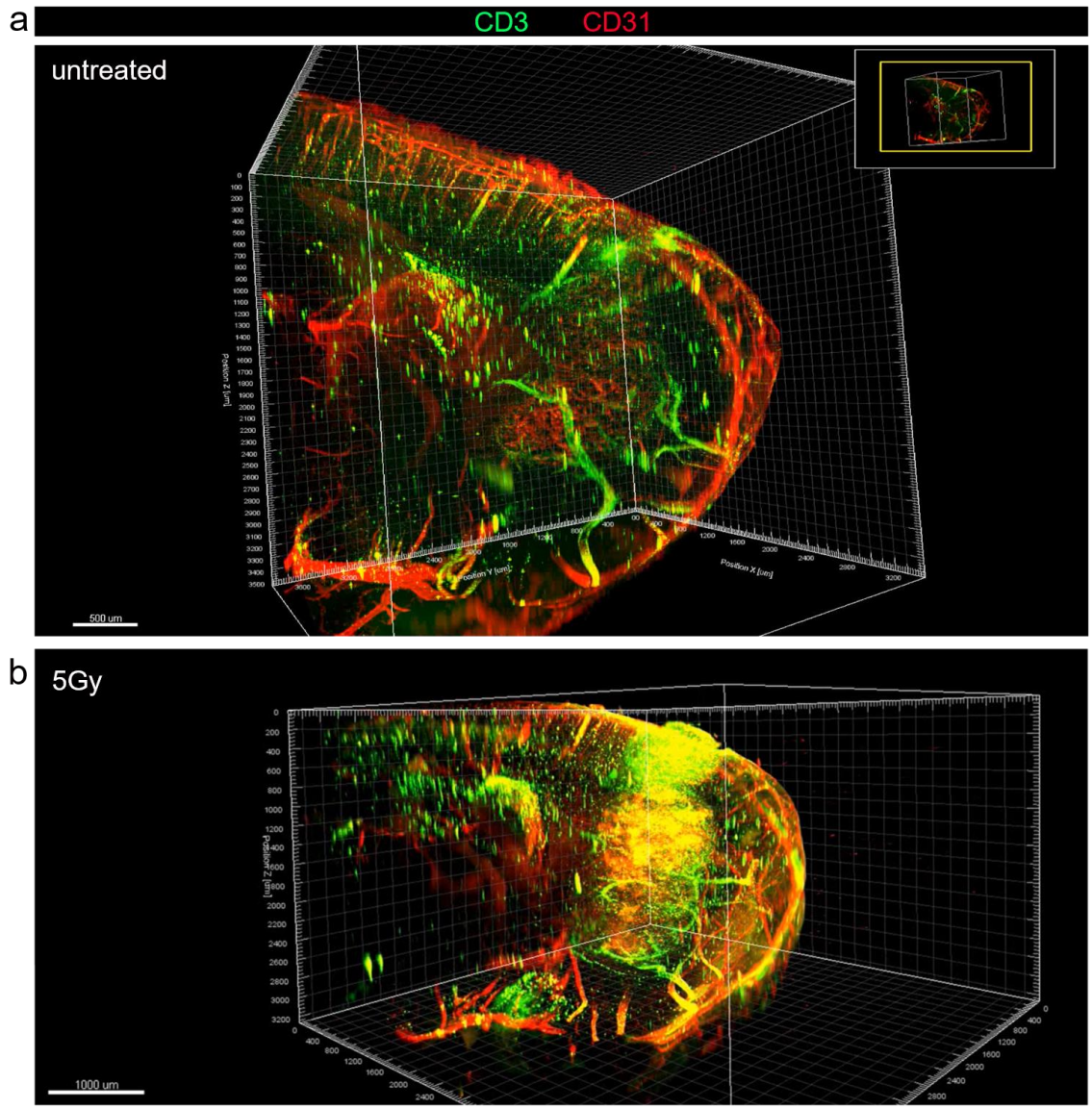

Figure 15: 3D structure of PVTNs.

3D reconstruction of images taken by light sheet fluorescence microscopy of cleared brains of a (a) untreated and (b) 1x 5 Gy treated mouse bearing GL261 tumors on day 13 past tumor cell injection and day 3 past irradiation. CD3+ T cells (green) and CD31+ vessels (red).

3.2.4 *In vivo* T cell migration and development of PVTNs

Next, I wanted to investigate the migration behavior of T cells into and out of PVTNs, in order to assess their ability to transmigrate towards or into the tumor. Together with our collaborators Dr. Matthia Karreman and Calvin Thommek (both DKFZ and Department of Neurology, University Hospital Heidelberg), we performed multiphoton laser scanning imaging of PVTNs in order to track T cell migration in a longitudinal fashion. Starting from day 5 after orthotopic tumor injection of GL261-GFP cells, first PVTNs were detectable (Figure 16a). Interestingly, when the same PVTN was imaged on day 5 and day 7 after

tumor injection, an increase in size was observed (Figure 16a). This indicates that PVTNs develop over time and grow in size, which also indicates that more T cells might be migrating into the niche than out of the niche. In order to investigate whether T cells are trapped inside of PVTNs, at day 10 after tumor injection, a PVTN outside of the tumor was live imaged over a time frame of up to one hour. T cells within the niche did not move, while T cells outside of the niche moved around freely in the tissue, indicating an entrapment of T cells within PVTNs (Figure 16b).

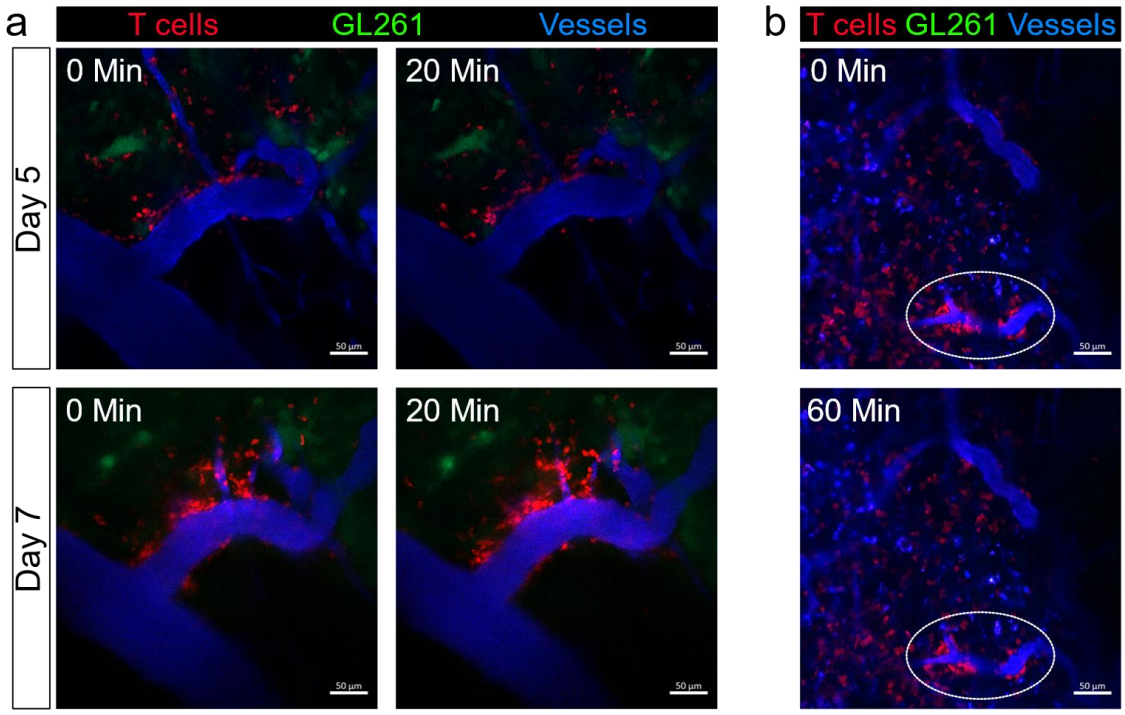

Figure 16: Niche development and T cell migration behavior.

Live in vivo multiphoton laser scanning microscopy of PVTNs in GL261 GFP bearing Lck-Cre x LSL tdTomato mice. (a) Live imaging for 20 minutes at day 5 and day 7 past tumor cell injection. tdTomato+ endogenous T cells (red) in an early stage of a PVTNs in close proximity to the GL261 GFP+ tumor (green). Vessels were stained by i.v. injection of TRITC-labeled dextran prior to imaging. (b) Live imaging of a PVTN and tracking of tdTomato+ T cells (red) over a timeframe of approximately 60 minutes at day 10 after tumor cell injection. The PVTN was located distant to the tumor (green; not visible). Scale bars 50 µm. Experiments performed together with Calvin Thommek, DKFZ.

3.2.5 Brain endothelial cells are capable to take up tumor antigens

If T cells are trapped within PVTNs, it is vital for the improvement and success of immunotherapies to decipher the underlying mechanism that hinder T cells from their successful migration into the tumor. In autoimmune diseases of the CNS, such as MS, it has been shown that presentation of auto-antigens by endothelial cells (ECs) trapped T cells at the blood-brain barrier, which ultimately resulted in the breakdown of the BBB

(Aydin et al., 2023). I therefore wanted to investigate, whether endothelial cells in the brain are capable of taking up and presenting tumor antigens. As surrogate antigen, I utilized the fluorescent protein ZsGreen which remains stable even after being taken up by antigen presenting cells (Yi et al., 2022). ZsGreen is also multiple times brighter than other commonly used fluorescent proteins such as GFP, which allows for the detection even at low levels (Nakamura et al., 2013; Yi et al., 2022). Expression of ZsGreen as surrogate antigen in our preclinical glioma model GL261, allows tracking of tumor-derived antigens in non-malignant cells. GL261 ZsGreen and GL261 control cells were orthotopically implanted into C57BL/6J mice and after 14 days, the antigen uptake in CD31+ ECs in the tumor-bearing hemisphere was analyzed by flow cytometry (Figure 17a). This revealed, that on average, ~33% of CD31+ ECs were ZsGreen positive in GL261 ZsGreen+ tumor-bearing mice (Figure 17a-b). At the same time, the amount of ZsGreen+ ECs decreased after irradiation with 1x 5 Gy, which could be explained with the general reduction of vessels after irradiation (Figure 17c & Supplementary Figure 8a-b). In order to confirm the antigen uptake by CD31+ endothelial cells, I additionally performed immunofluorescence staining of brains bearing ZsGreen expressing GL261 tumors, which confirmed the uptake of ZsGreen in vessels outside of the tumor (Figure 17d) and also in PVTNs (Figure 17e). In summary, I provide evidence that endothelial cells are able to take up tumor antigens in the brain. However, whether the endothelial cells are also capable of presenting these antigens needs to be further investigated.

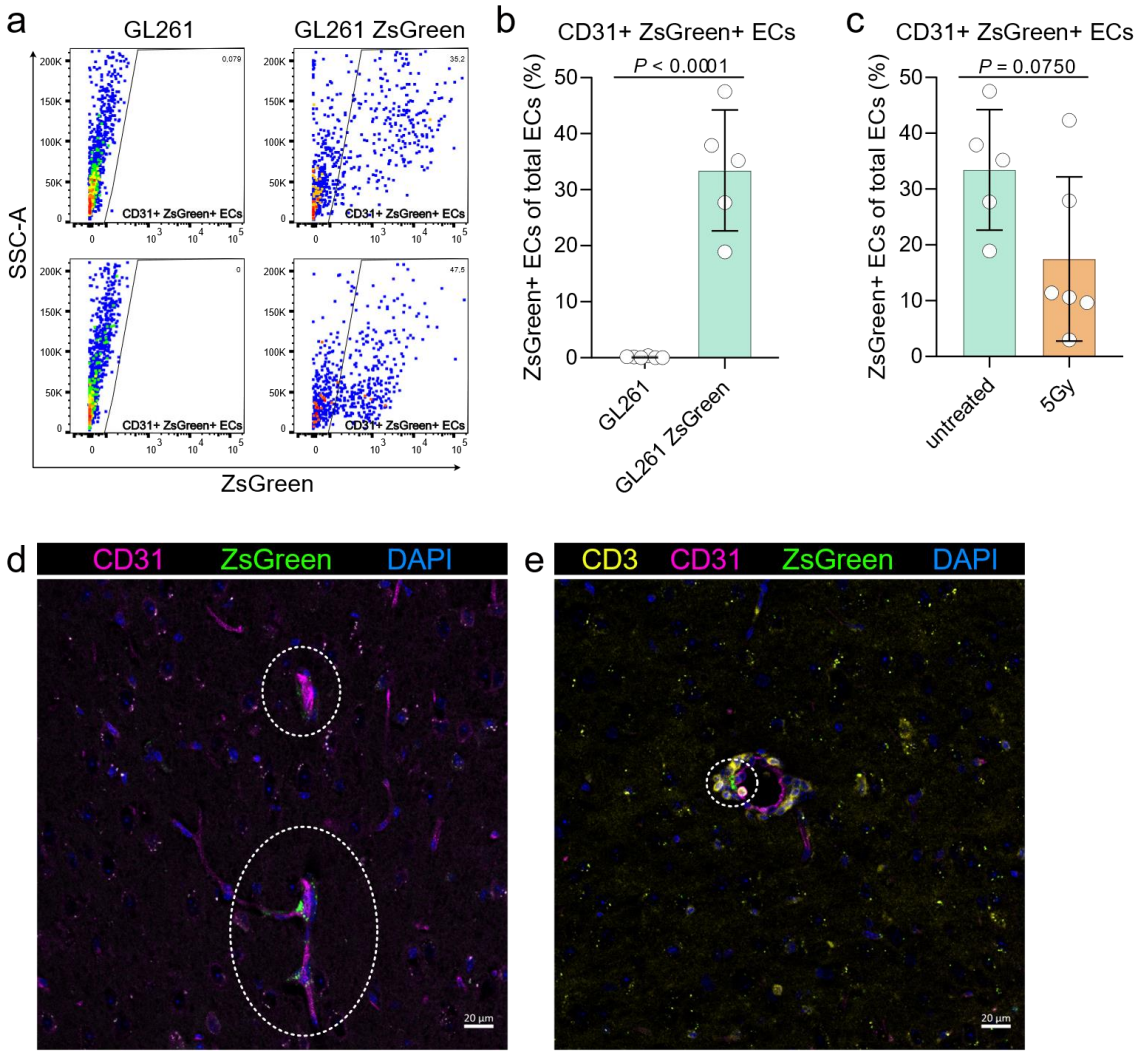

Figure 17: Assessment of tumor-antigen uptake by endothelial cells.

(a) Flow cytometry analysis of ZsGreen uptake in CD45- CD31+ endothelial cells in GL261 (left) and GL261 ZsGreen (right) tumor-bearing brain hemispheres 13 days after tumor cell injection. (b-c) Quantification of ZsGreen uptake by CD45- CD31+ endothelial cells in GL261 and GL261 ZsGreen tumor-bearing hemispheres (c) in untreated and irradiated mice by flow cytometry on day 13 after tumor cell injection (3 days after irradiation). Statistical analysis performed by unpaired t-test. (d-e) Confocal laser scanning microscopy of GL261 ZsGreen bearing tumor hemispheres and immunofluorescence staining of CD31+ ECs (magenta), ZsGreen (green), CD3+ T cells (yellow) and DAPI (blue) on day 13 after tumor cell injection. (d) Demonstration of ZsGreen uptake by ECs distant to the tumor. (e) ZsGreen+ ECs in PVTNs outside of the tumor. Scale bars 20 µm.

4 Discussion

4.1 Radiotherapy modulates the tumor immune microenvironment

Radiotherapy and its potential to favorably modulate the tumor microenvironment is a promising combination partner for immunotherapeutic approaches targeting solid tumors. While preclinical studies show a strong combinatorial benefit (Belcaid et al., 2014; Kim et al., 2017; Zeng et al., 2013), large clinical trials combining standard-of-care radiotherapy with immunotherapies failed to show significant benefits in gliomas (Lara-Velazquez et al., 2021; Lim et al., 2022; Omuro et al., 2023). The direct and indirect effects of radiotherapy on immune cells were not comprehensively evaluated in these clinical trials and the mechanisms behind the lack of efficiency remain elusive. It is difficult to investigate the effects on immune cells in the glioma tumor microenvironment of patients, as radiotherapy is always applied as adjuvant therapy after surgical resection and no tissue shortly after irradiation is available for analysis. Therefore, further preclinical research is needed to understand the underlying immune cell dynamics after irradiation and improve radiotherapy dosage and regimens that would support immunotherapies in the most efficient way. Here, I provided insights on how different dosages and fractionations of localized radiotherapy affect immune cells in the tumor microenvironment of a preclinical glioma model. I investigated the influence of a low dosage (2 Gy), two medium high dosages (5 and 6 Gy total), one of which was fractionated (3x 2 Gy), and a high dosage (8 Gy). While there was a dose-dependent response observable and 8Gy showed the overall highest survival benefit, 8 Gy also demonstrated the lowest percentage in terms of T cell-mediated survival benefit. At the same time, 8 Gy also showed the lowest enrichment in all applied immune signatures, with low T and NK cells responses, low antigen presentation and a low type I IFN response. The downregulation of the immune response compared to the untreated and other treatment groups, indicates negative effects of too high dosages on immune responses in the brain. Although completely T cell-mediated, low dosage irradiation with 2 Gy showed only a small survival benefit of 2 days and also only low enrichment in immune signatures. Despite the overall higher total dosage of 6 Gy compared to 5 Gy, the fractionation of 3x 2 Gy performed worse than the single application of 5 Gy. 5 Gy induced and sustained a strong T cell, NK cell and type I IFN response signature until day 7. Overall, the single application of 5 Gy has been shown to be the superior dose among all tested dosages in regards to T cell and NK cell responses, type I IFN response, expression of chemokines, low expression of inhibiting immune checkpoints on cytotoxic CD8 T cells and also in antigen processing and presentation.

Other preclinical studies investigating different dosages and fractionations have been performed. However, most of these studies were performed in subcutaneous flank tumors models of other entities and some results may be contradicting. A study using the colon carcinoma model MCA38, demonstrated that the fractionation of 3x 8 Gy in combination with anti-CTLA-4 checkpoint inhibition, induced a better response compared to a single application of 20 Gy (Dewan et al., 2009). Yet, another study using the B16-F0 melanoma model, demonstrated a better immune activation after a single application of 15 Gy compared to 3x 5 Gy (Lugade et al., 2005). In the glioma models GL261 and CT-2A, an interesting study was performed to compare a regimen of 10x 2 Gy, which supposedly models the Stupp protocol, with a hypofractionated regimen of 4x 5 Gy applied every third day. The authors demonstrated that both regimens induced similar levels of radiotherapy-mediated DNA damage and cell death, but the 4x 5 Gy regimen resulted in a significantly better median survival (McKelvey et al., 2022). A phase I clinical trial in melanoma and metastatic renal cell carcinoma assessed the use of one, two or three applications of 20 Gy in combination with IL-2. Although a low number of patients was assessed, their data suggests a higher percentage of complete response (CR) in the cohorts treated with only one or two applications of 20 Gy (Seung et al., 2012). High dosages of 1x 25 Gy or 15x 4 Gy (total 60 Gy) have been shown to induce a pro-tumorigenic phenotype in macrophages (Tsai et al., 2007), while low dosages have shown to induce a pro-inflammatory phenotype in macrophages (Klug et al., 2013). Dosages above 10 Gy have been shown to induce significant vascular damage which resulted in impaired T cell recruitment to the tumor (Park et al., 2012). Taken together, the existing preclinical data of different dosages and fractionations can be contradictory and seems dependent on the model. Due to the unique environment of the brain, the relevance of findings in subcutaneous models for the translation into gliomas is debatable. Another inherent limitation, that makes the comparison with other findings difficult, is the seemingly arbitrary decision on used dosages in other studies. Still, the preexisting data and the data provided by this study suggest better tumor microenvironment modulation properties of low to medium high dosages. The better performance of the single dosage or hypofractionated regimens compared to the conventional fractionated applications puts the currently used Stupp protocol, which utilizes the daily application of 2 Gy for 30 days, in question as suitable combination partner for immunotherapy (McKelvey et al., 2022; Stupp et al., 2005). However, due to the unavailability of samples, little to no evidence has been provided on the tumor microenvironmental changes in glioma patients following the treatment with the Stupp protocol, but the failure to provide a combinatorial effect with this regimen hints towards an unfavorable modulation of the TME (Lim et al., 2022; Omuro et al., 2023). Additionally,

studies which longitudinally monitored peripheral immune cells in glioma patients treated with the Stupp protocol, showed induced immune suppression by a significant und durable decrease in T , NK and B cell numbers during and after the treatment for up to 48 weeks, which was also correlated with poor outcome (Campian et al., 2017; Grossman et al., 2011; Saeed et al., 2024). However, in about 42 % of patients with concurrent glioma and multiple sclerosis, standard-of-care radiotherapy led to increased inflammatory activity and progression of multiple sclerosis lesions, indicating a radiation-induced pro-inflammatory response (Sahm et al., 2023).

Furthermore, the potential effects of TMZ are not considered in this, and most other preclinical studies, as those studies often only evaluate radiotherapy alone in combination with immunotherapy. However, the larger phase III clinical trials that evaluated the combination of radiotherapy and immunotherapy, which did not meet their endpoints, also included the application of TMZ according to the Stupp protocol (Lim et al., 2022; Omuro et al., 2023). TMZ has been shown to also induce immunogenic cell death in tumor cells, but since it is applied systemically, it can also have detrimental effects on the entire (peripheral) immune system by inducing long-lasting systemic lymphopenia (Di Ianni et al., 2021; Mathios et al., 2016). This would again question the use of the Stupp protocol as a suitable combination partner for immunotherapeutic approaches.

I demonstrated T cell depletion by medium and high dosages at the early timepoint, but a replenishment with new T cells already four days later. This local depletion can have the advantage that exhausted and unspecific bystander T cells are depleted from the TME and are replaced by a fresh pool of activated antigen-specific T cells. Lymphodepletion, through the application of a chemotherapeutic agent, has been shown to be crucial for the success of cellular immunotherapies such as CAR T cell therapy (Lickefett et al., 2023). Lymphodepletion led to enhanced CAR T cell expansion and persistence and was crucial for a therapeutic response to cell therapy in preclinical glioma models (Sampson et al., 2014; Suryadevara et al., 2018). This data suggests that radiotherapy-induced lymphodepletion could redundantize chemically induced lymphodepletion when combined with cellular therapies, but this needs further investigation.

Next to the T cell-driven anti-tumor response, my data also suggests a strong NK cell response after the treatment with 5 Gy. NK cells have been shown to populate gliomas, and are crucial for control of tumor cells with downregulated or absent expression of MHC class I (Burster et al., 2021). Yet, the immunosuppressive TME of treatment-naïve

gliomas dampens their functionality (Kozlowska et al., 2016). Radiotherapy has been shown to induce NK cell responses against solid tumors (Canter et al., 2017; Walle et al., 2022) and human and murine glioma cells have been shown to upregulate NK cell ligands, such as NKG2DL, which initiated NK cell mediated killing (Weiss, Schneider, et al., 2018). The here presented data shows a significant and sustained upregulation of the NK cell receptors *Ncr1* (NKp46), *Klrc2* (NKG2C) and *Klrk1* (NKG2D) after the treatment with 5 Gy. These receptors are essential for the engagement and recognition of tumor cells by NK cells (Meza Guzman et al., 2020). In combination with the expression of markers of cytotoxic activity, such as granzymes (*Gzma* & *Gzmb*), perforin (*Prf1*) and interferon gamma (*Ifng*), this provides evidence for a strong NK cell response. By utilizing NK cell depleting antibodies, we will assess role of NK cells in tumor control after radiotherapy in future investigations.

This study focused solely on ionizing irradiation using X-rays. The potential differential effects on the tumor microenvironment, and in particular immune cells, by different types of radiation are so far poorly investigated. In clinical practice for the management of gliomas, external beam radiation therapy (EBRT) using photon-based radiation like X-rays or gamma rays is commonly used (Koka et al., 2022). EBRT, that utilizes charged particles like protons, helium ions or carbon ions, is an emerging field due to their increased accuracy (Fernandez-Gonzalo et al., 2017). However, the differential impact on immune cells and the entire tumor microenvironment induced by photons like X-rays and charged particles like protons or carbon ions remains largely unexplored and should be considered in future studies. Some recent studies suggest that radiotherapy using charged particles has higher immune modularity effects compared to photons (Ando et al., 2013; Imadome et al., 2008), while others reported comparable effects (Gameiro et al., 2016). In a model of pulmonary metastases, the combination of carbon ion radiotherapy in combination with a DC immunotherapy led to the suppression of lung metastases, while the combination with photon radiotherapy showed no synergistic effects (Ando et al., 2013). Another study using carbon ion radiotherapy reported enhanced immunogenicity and beneficial effects in combination with CTLA-4 checkpoint inhibitors in subcutaneous tumor models (Hartmann et al., 2022; Hartmann et al., 2020). Another emerging approach is FLASH radiotherapy (FLASH-RT). FLASH-RT utilizes ultra-high-dosages that are applied within milliseconds (Matuszak et al., 2022). With current technical possibilities, FLASH-RT primarily uses very high energy electrons (VHEE) or protons (Matuszak et al., 2022). FLASH-RT has been praised for its reduced off-target toxicity, while providing similar effects on tumor control and the immune response (Favaudon et al., 2014; Liljedahl et al., 2022). A recent study comparing

FLASH-RT with conventional radiotherapy in murine models of lung adenocarcinoma and glioma, concluded no differential effects on the immune response, but a higher immune-independent delay of tumor growth after FLASH-RT (Almeida et al., 2024). Another study in rat glioma came to the same conclusion, but additionally showed that FLASH-RT had neuroprotective properties compared to conventional radiotherapy (Iturri et al., 2023). Yet, another study using a murine model of diffuse midline glioma, showed similar clinical results comparing FLASH-RT with conventional RT, but demonstrated a higher type I IFN response in the conventionally treated mice (Padilla et al., 2024). In conclusion, all different types of radiotherapy possess the ability to modulate the tumor microenvironment and all might be suitable for the combination with immunotherapies. But the underlying mechanism influencing the responses might be multifactorial. Therefore, the optimal dosage, fractionation and timing of individual approaches need to be evaluated for each individual entity, to account for the underlying heterogeneity and differential responses.

While this study focused solely on immune cells, a comprehensive characterization on the direct and indirect effects on tumor cells, vasculature as well as other cell types in the brain such as astrocytes and neurons, should be performed. Future research should also consider the underlying heterogeneity among different tumor types and patients. The differential mutational profile and load, varying extracellular matrix, vascularization, hypoxic regions, cellular composition and overall location of the tumor might significantly influence the response to radio- and immunotherapy. Therefore, reliable predictive markers need to be identified to tailor the optimal personalized therapy for each individual patient or patient group to maximize the clinical outcome. Still, the here presented results provide valuable insights into the immune response following radiotherapy in gliomas and will potentially help to shape and improve future radiotherapy and immunotherapy combinatorial trials.

4.2 The role of *Lgals1* expression in activated CD8+ T cells

By differential gene expression and pseudotime trajectory analysis of CD8+ T cells, *Lgals1* (Galectin-1) expression was identified as specific marker of activated cytotoxic CD8+ T cells. Radiotherapy differentially regulated the expression of *Lgals1* in a dosage-dependent manner. However, the mechanisms behind this regulation are unknown and need to be further investigated. The overall function of Galectin-1, which is a beta-galactoside-binding lectin, is still subject to investigation as not all binding partners are yet known either (Yu et al., 2023). This is also the reason why no interactome analysis

on *Lgals1* could be performed, as the underlying databases used by cell interaction algorithms lack the information on known *Lgals1* receptor-ligand pairs. *Lgals1* can also be highly expressed in glioma cells and endothelial cells and has been shown to induce an immunosuppressive tumor microenvironment or T cell exclusion (Q. Chen et al., 2019; Corapi et al., 2018; Verschuere et al., 2014). The function of *Lgals1* expression in activated CD8+ T cells remains incompletely understood, but studies suggest rather regulatory effects of Galectin-1 on T cell functionality. A study by Sharanek et al. demonstrated that *Lgals1* transcription is regulated by signal transducer and activator of transcription 3 (STAT3) (Sharanek et al., 2021). STAT3 is crucial for many cytokine signaling pathways and in CD8+ T cells, it plays a crucial role in developing memory phenotypes (Hillmer et al., 2016). Some older studies on the effects of Galectin-1 on CD8+ T cells suggest that Galectin-1 regulates the proliferation, modulates TCR binding, negatively regulates subsequent effector activity and induces T cell apoptosis (Liu et al., 2009; Perillo et al., 1995; Vespa et al., 1999). Therefore, activated CD8+ T cells might express *Lgals1* during activation as an autocrine regulatory mechanism to prevent overshooting or chronic immune activity, or to transition into a memory phenotype. If Galectin-1 serves as inhibitory regulator of T cell activation, *Lgals1* knockout (KO) in T cells used for cellular immunotherapies might provide a beneficial modification to enhance the proliferation and activity or to prevent exhaustion. In ongoing work, I therefore investigate CRISPR/Cas9-mediated KOs of *Lgals1* in wildtype and OT-1 TCR transgenic T cells and its impact on their phenotype *in vitro* and *in vivo*. Furthermore, I aim to evaluate *Lgals1* KO OT1 TCR transgenic T cells for adoptive cell transfer (ACT) in preclinical glioma models such as GL261 OVA and CT-2A OVA. We aim to investigate how *Lgals1* KO influences the migration of T cells into the brain and their ability to sustain anti-tumoral responses and memory compared to unmodified control cells. Uncovering the functional role of Galectin-1 in activated CD8+ T cells could lead to the improvement of cellular immunotherapies for enhanced therapeutic efficacy in patients with gliomas and other solid tumors.

4.3 T cells form perivascular niches in the brain

The priming and migration of T cells that infiltrate into the brain and especially into the glioma tumor microenvironment has been a prominent topic in neuroimmunology. Yet, the unique anatomical features, environment and location of the brain still make it difficult to understand the complex immune dynamics within this organ. It has been well established that one of the locations of T cell priming for responses to the brain are

cervical lymph nodes, where soluble antigens drain via the CSF, but also dendritic cells migrate from the brain to these lymph nodes to present CNS antigens (Laaker et al., 2023). Once primed, peripheral T cells still have to overcome potential barriers such as the BBB. Even though the BBB is often compromised in gliomas (Kadry et al., 2020), the treatment naïve tumor microenvironment is still comparably low infiltrated with T cells (Luce et al., 2024). Recent studies suggest additional possible locations of T cell priming and routes of homing to the brain. One study demonstrated a hub of tumor-reactive T cells in the skull of glioma patients that are able to infiltrate the brain (Dobersalske et al., 2024). Another study demonstrated that antigens in the CSF were also shown to be presented to CSF-patrolling T cells at the outside of the dural sinus (Rustenhoven et al., 2021). The outside of bridging veins connecting the dura with the brain have been shown to serve as migration paths for immune cells (Smyth et al., 2024). It has also recently been reported that in the healthy choroid plexus a population of cDC1 dendritic cells and CD8+ T cells are present, and upon local injection with TLR-agonist lipopolysaccharide (LPS), an increase in CD8+ T cell infiltration into the choroid plexus was observed (Xu et al., 2024). In Alzheimer's disease and multiple sclerosis, clonally expanded populations of T cells can be found within the CSF (Gate et al., 2020; Gottlieb et al., 2024). Overall the CSF has been shown to be a major T cell trafficking route in the CNS in health and disease (Strazielle et al., 2016). Still, the overall dynamics of T cell priming and migration paths for responses against gliomas are incompletely understood.

Here, I have shown a so far unknown perivascular T cell niche, which develops already within 5-7 days after tumor formation. Within this niche, T cells appear to be potentially detained from further migration into the tumor. However, the mechanism of entrapment remains unexplored and will be subject of my further research. I have shown that apart from T cells, the niche is also highly populated with macrophages and/or microglia. However, their functional relevance in niche development or maintenance remains elusive. Macrophages are highly plastic cells which can obtain either an immunosuppressive or immune stimulatory phenotype depending on their environment (Shapouri-Moghaddam et al., 2018). If they are immune stimulatory, these myeloid cells would have the potential to present antigens to T cells and prime them. In this case, PVTNs would serve as a so far unknown hub of T cell priming in the brain. This would be supported by observations made in perivascular spaces of multiple sclerosis patients, in which activated and proliferative T cells were observed alongside antigen-presenting macrophages (Fabriek et al., 2005; Fransen et al., 2020; Smolders et al., 2020). However, others have reported that perivascular macrophages in murine glioma and brain metastases models obtain an anti-inflammatory phenotype and form perivascular

cuffs that limit T cell infiltration (Sun et al., 2023). Interestingly, upon treatment with immune checkpoint inhibitors, perivascular cuffs in brain metastases were resolved and immune cells migrated into the tumor (Sun et al., 2023). It has also yet to be explored what kind of T cells are populating PVTNs. Whether they are cytotoxic T cells, T helper or regulatory T cells, and whether they are tumor-specific or rather unspecific bystander T cells will be important to understand the dynamics within the niche. Next, I will explore the complete cellular composition and phenotype of all cells within and surrounding the niche by spatial transcriptomics. By applying spatial TCR sequencing we will be able to identify the T cells specificity as well as clonality, which will provide insights on local priming and expansion (Engblom et al., 2023). Additionally, spatial transcriptomics will also allow us to evaluate cell to cell interactions of neighboring cells and will provide clues to help decipher the potential mechanism of T cell entrapment. Once potential candidate genes are identified, we will functionally evaluate each candidate and its role in niche formation. Literature and my results already provide one potential mechanism of T cell entrapment at the endothelial wall. Aydin et al. have shown that in experimental autoimmune encephalitis (EAE), a preclinical model used for multiple sclerosis research, endothelial cells presented autoantigens to CD8+ T cells which led to their entrapment and subsequently to the destruction of the BBB (Aydin et al., 2023). As part of this dissertation, I have shown that endothelial cells are also capable to uptake tumor antigens inside the tumor, but also at distant sites outside of the tumor. Even though I have shown that also endothelial cells in PVTNs take up antigens, I did not provide proof for their presentation so far. I will further investigate the role of tumor antigen presentation by endothelial cells for the development of the perivascular niche. For this, I am currently in the process of generating a VE-cadherin-CreERT2 Tap1$^{floxed/floxed}$ transgenic mouse. In this mouse, the antigen presentation of endothelial cells can be specifically deactivated upon treatment with tamoxifen, which leads to the Cre recombinase-mediated knockout of the *transporter associated with antigen processing 1* (*Tap1*) gene, which is crucial for MHC antigen loading and MHC complex assembly (Kelly et al., 1992; Spies et al., 1992). Using this model, we will evaluate the role of antigen presentation and co-stimulation by endothelial cells in niche formation and entrapment of T cells in the perivascular space. The presentation of antigen, but the possible absence of the necessary co-stimulatory signals, that are lacking on endothelial cells, might lead to T cell anergy and thereby induce their inactivation and reduce their potential to further migrate (Crespo et al., 2013).

Another potential mechanism might not lie within the niche, but rather within the surrounding microenvironment of the niche. The surrounding environment, which is likely

comprised of pericytes, microglia, astrocytes and neurons, might provide a physical barrier which blocks the further transmigration of T cells and other immune cells. It has been shown that a desmoplastic stroma highly limits the T cell migration and can exclude T cells from entering the tumor microenvironment (Xiao et al., 2023). Perivascular fibroblast-like cells and pericytes in the brain might render the extracellular matrix unfavorably for T cell transmigration (Dinevska et al., 2023; Zarodniuk et al., 2023). The cellular composition of the niche-surrounding microenvironment will be analyzed by spatial transcriptomics (see above).

Another open question to investigate, is the route of influx of T cells into PVTNs. The obvious answer to this question would be through the HEV-like blood vessels that they are surrounding. However, during intravital multiphoton laser scanning imaging, the transmigration of T cells through the vessel wall was only rarely observed. Also, in ongoing preliminary work, in which I intravenously injected fluorescently-labeled T cells into the blood stream, labeled T cells were not observed to infiltrate into PVTNs (data not shown). This opens up the hypothesis that T cells make use of an alternative route by which they enter the niche. I am proposing that T cells in the CSF might enter from the meningeal subarachnoid space through the Virchow-Robin perivascular spaces into the niche. This theory would be supported by the observation, I made with light sheet fluorescence microscopy and 3D reconstruction of niches, which showed that niches can extend from the distant meninges to the tumor and would serve as explanation why large PVTNs can be observed at the meninges. T cells might migrate along vessels like a street as shown by Smyth et al., which demonstrated that immune cells were migrating along the outside of vessels from the dura to the brain and vice versa (Smyth et al., 2024). The opening that the Virchow-Robin space provides at the interface of the meninges, would allow T cells to enter the brain and move along a path with potentially the lowest resistance. T cells would also not need to overcome the migration-limiting BBB. It has also been shown that interstitial and cerebrospinal fluids would drain along vessels out of the brain (Ma et al., 2017; Smyth et al., 2024). These fluids potentially also contain chemokines (Lok et al., 2014; Pashenkov et al., 2003) that are draining from the tumor microenvironment which would provide a hypothesis why T cells would enter the Virchow-Robin space in the first place. Additionally, I have shown that vessels inside PVTNs are expressing the Duffy antigen receptor for chemokines (DARC), a receptor which a variety of chemokines bind to unspecifically, which serves as presentation tool for chemokines to line the vessel (Novitzky-Basso & Rot, 2012; Thiriot et al., 2017). I will evaluate this alternative route by injecting fluorescently-labeled T cells into the CSF via the cisterna magna and cerebral ventricle, methods which are currently being

established in our lab. The migration of these T cells will then be tracked longitudinally using intravital multiphoton laser scanning microscopy and light sheet fluorescence microscopy, which could provide novel insights into the route of T cell migration into the brain. Furthermore, the applied spatial transcriptomics will potentially reveal the necessary chemokine receptors which facilitate the migration of T cells into the niche. By blocking these receptors, further functional mechanisms can be evaluated. Overall, these investigations will provide novel insights into the migration behavior and routes of T cells and would have a substantial impact on the understanding of immune cell dynamics in the brain.

Tertiary lymphoid structures (TLS) have been reported in preclinical glioma models and glioma patients and are suggested as possible location of local T cell priming (van de Walle et al., 2021; L. van Hooren et al., 2021). They share characteristics with PVTNs, but whether PVTNs are a developmental stage of TLS or whether they are an independently forming structure needs to be further investigated. The reported TLS are also formed around HEV-like vessels, but besides T cells also contain high numbers of B cells, or depending on the developmental stage even specialized T and B cell zones similar to those found in secondary lymphoid organs (van de Walle et al., 2021). However, in PVTNs, no significant numbers of B cells were observed, which would lead to the conclusion that they are not TLS or TLS-like structures.

Radiotherapy with 1x 5 Gy induced the formation of intratumoral PVTNs, but no difference in the number of extratumoral PVTNs was observed. This correlates with the increased infiltration of T cells after radiotherapy. Furthermore, it appears that after radiotherapy the T cell density in extratumoral PVTNs is lower, indicating a possible breakdown or leakage of the niche. The release of T cells from the niche after radiotherapy could serve as a possible mechanism of radiotherapy-induced immune responses and T cell infiltration into the tumor microenvironment. However, a major limitation is our ability to accurately quantify the obtained 3D images from light sheet fluorescence microscopy at this point. Collaborators are working on accurate machine learning algorithms that are capable to quantify PVTNs, T cell numbers and T cell density in these large datasets of 100 gigabytes and more per image. This will allow us to accurately investigate and quantify the influence of radiotherapy and other therapies on PVTNs. Understanding the potential mechanisms of T cell entrapment in PVTNs and developing therapeutic options that allows T cells to leave PVTNs towards the tumor will be crucial for successful anti-tumor immune responses and immunotherapies for glioma patients.

4.4 Conclusions and outlook

In summary, I have demonstrated that a single medium dose of 5 Gy photon radiotherapy led to the most beneficial T cell-mediated survival and overall higher pro-inflammatory modulation of the tumor microenvironment compared to other tested dosages and fractionations. Based on the here provided results, 5 Gy would be the recommended dosage to be used in future combinatorial studies. The sustained response seven days after treatment suggests that repeated applications of radiotherapy should be made in a hypofractionated fashion with >7 days apart from each other, to not deplete the ongoing responses. The optimal timing of applying immunotherapies such as peptide vaccinations, checkpoint inhibitors or adoptive cell therapy with TCR-transgenic T cells, in between the applications of radiotherapy, will be investigated in future studies. This will become crucial for translating radio- and immunotherapy combinations into the clinical management for glioma patients. Additionally, *Lgals1* expression was identified as marker for activated CD8+ T cells in the brain, hence the functional role of *Lgals1* in T cells and the potential therapeutic implications of a *Lgals1* knockout are investigated in ongoing work. Furthermore, I have discovered the formation of perivascular T cell niches (PVTNs) in the context of gliomas. Further investigations will focus on the origin of T cells and their migration behavior within PVTNs. Additionally, the cellular composition and crosstalk within the niche will be investigated in order to understand the mechanism behind niche formation and potential T cell entrapment. Understanding the functional relevance of this niche in T cell entrapment and the tumor-directed migration and anti-tumoral response by T cells, will be crucial for the understanding T cell dynamics in the brain and will be crucial for the successful advancement of immunotherapeutic strategies against brain tumors.

5 Literature

Acharya, M. M., Green, K. N., Allen, B. D., Najafi, A. R., Syage, A., Minasyan, H., Le, M. T., Kawashita, T., Giedzinski, E., Parihar, V. K., West, B. L., Baulch, J. E., & Limoli, C. L. (2016). Elimination of microglia improves cognitive function following cranial irradiation. *Scientific Reports*, *6*(1). https://doi.org/10.1038/srep31545

Akhavan, D., Alizadeh, D., Wang, D., Weist, M. R., Shepphird, J. K., & Brown, C. E. (2019). CAR T cells for brain tumors: Lessons learned and road ahead. *Immunological Reviews*, *290*(1). https://doi.org/10.1111/imr.12773

Allen, N. J., & Lyons, D. A. (2018). Glia as architects of central nervous system formation and function. *Science*, *362*(6411). https://doi.org/10.1126/science.aat0473

Almeida, A., Godfroid, C., Leavitt, R. J., Montay-Gruel, P., Petit, B., Romero, J., Ollivier, J., Meziani, L., Sprengers, K., Paisley, R., Grilj, V., Limoli, C. L., Romero, P., & Vozenin, M.-C. (2024). Antitumor Effect by Either FLASH or Conventional Dose Rate Irradiation Involves Equivalent Immune Responses. *International Journal of Radiation Oncology, Biology, Physics*, *118*(4). https://doi.org/10.1016/j.ijrobp.2023.10.031

Ando, K., Fujita, H., Hosoi, A., Nakawatari, M., Nakamura, E., Kakimi, K., Nakano, T., Imai, T., & Shimokawa, T. (2013). Effective Suppression of Pulmonary Metastasis in Combined Carbon Ion Radiation Therapy With Dendritic-Cell Immunotherapy in Murine Tumor Models. *International Journal of Radiation Oncology Biology Physics*, *87*(2), S642-S642. https://doi.org/10.1016/j.ijrobp.2013.06.1700

Andreatta, M., & Carmona, S. J. (2021). UCell: Robust and scalable single-cell gene signature scoring. *Comput Struct Biotechnol J*, *19*, 3796-3798. https://doi.org/10.1016/j.csbj.2021.06.043

Aran, D., Looney, A. P., Liu, L., Wu, E., Fong, V., Hsu, A., Chak, S., Naikawadi, R. P., Wolters, P. J., Abate, A. R., Butte, A. J., Bhattacharya, M., Aran, D., Looney, A. P., Liu, L., Wu, E., Fong, V., Hsu, A., Chak, S., . . . Bhattacharya, M. (2019). Reference-based analysis of lung single-cell sequencing reveals a transitional profibrotic macrophage. *Nature Immunology 2019 20:2*, *20*(2). https://doi.org/10.1038/s41590-018-0276-y

Aslan, K., Turco, V., Blobner, J., Sonner, J. K., Liuzzi, A. R., Núñez, N. G., De Feo, D., Kickingereder, P., Fischer, M., Green, E., Sadik, A., Friedrich, M., Sanghvi, K., Kilian, M., Cichon, F., Wolf, L., Jähne, K., von Landenberg, A., Bunse, L., . . . Platten, M. (2020). Heterogeneity of response to immune checkpoint blockade in hypermutated experimental gliomas. *Nature Communications 2020 11:1*, *11*(1). https://doi.org/10.1038/s41467-020-14642-0

Awada, H., Paris, F., & Pecqueur, C. (2023). Exploiting radiation immunostimulatory effects to improve glioblastoma outcome. *Neuro Oncol*, *25*(3), 433-446. https://doi.org/10.1093/neuonc/noac239

Aydin, S., Pareja, J., Schallenberg, V. M., Klopstein, A., Gruber, T., Page, N., Bouillet, E., Blanchard, N., Liblau, R., Korbelin, J., Schwaninger, M., Johnson, A. J., Schenk, M., Deutsch, U., Merkler, D., & Engelhardt, B. (2023). Antigen recognition detains CD8(+) T cells at the blood-brain barrier and contributes to its breakdown. *Nat Commun*, *14*(1), 3106. https://doi.org/10.1038/s41467-023-38703-2

Bachiller, S., Jiménez-Ferrer, I., Paulus, A., Yang, Y., Swanberg, M., Deierborg, T., & Boza-Serrano, A. (2018). Microglia in Neurological Diseases: A Road Map to Brain-Disease Dependent-Inflammatory Response. *Frontiers in Cellular Neuroscience*, *12*. https://doi.org/10.3389/fncel.2018.00488

Beach, C., MacLean, D., Majorova, D., Arnold, J. N., & Olcina, M. M. (2022). The effects of radiation therapy on the macrophage response in cancer. *Frontiers in Oncology*, *12*. https://doi.org/10.3389/fonc.2022.1020606

Belcaid, Z., Phallen, J. A., Zeng, J., See, A. P., Mathios, D., Gottschalk, C., Nicholas, S., Kellett, M., Ruzevick, J., Jackson, C., Albesiano, E., Durham, N. M., Ye, X., Tran,

P. T., Tyler, B., Wong, J. W., Brem, H., Pardoll, D. M., Drake, C. G., & Lim, M. (2014). Focal Radiation Therapy Combined with 4-1BB Activation and CTLA-4 Blockade Yields Long-Term Survival and a Protective Antigen-Specific Memory Response in a Murine Glioma Model. *PLOS ONE*, *9*(7). https://doi.org/10.1371/journal.pone.0101764

Betlazar, C., Middleton, R. J., Banati, R. B., & Liu, G. J. (2016). The impact of high and low dose ionising radiation on the central nervous system. *Redox Biol*, *9*, 144-156. https://doi.org/10.1016/j.redox.2016.08.002

Blanchard, L., & Girard, J.-P. (2021). High endothelial venules (HEVs) in immunity, inflammation and cancer. *Angiogenesis*, *24*(4). https://doi.org/10.1007/s10456-021-09792-8

Blanco-Carmona, E. (2022). Generating publication ready visualizations for Single Cell transcriptomics using SCpubr. *bioRxiv*. https://doi.org/10.1101/2022.02.28.482303

Boschert, T., Kromer, K., Lerner, T., Lindner, K., Haltenhof, G., Tan, C. L., Jähne, K., Poschke, I., Bunse, L., Eisele, P., Grassl, N., Mildenberger, I., Sahm, K., Platten, M., Lindner, J. M., & Green, E. W. (2024). H3K27M neoepitope vaccination in diffuse midline glioma induces B and T cell responses across diverse HLA loci of a recovered patient. *Science Advances*, *10*(5). https://doi.org/10.1126/sciadv.adi9091

Bowman-Kirigin, J. A., Desai, R., Saunders, B. T., Wang, A. Z., Schaettler, M. O., Liu, C. J., Livingstone, A. J., Kobayashi, D. K., Durai, V., Kretzer, N. M., Zipfel, G. J., Leuthardt, E. C., Osbun, J. W., Chicoine, M. R., Kim, A. H., Murphy, K. M., Johanns, T. M., Zinselmeyer, B. H., & Dunn, G. P. (2023). The Conventional Dendritic Cell 1 Subset Primes CD8+ T Cells and Traffics Tumor Antigen to Drive Antitumor Immunity in the Brain. *Cancer Immunology Research*, *11*(1). https://doi.org/10.1158/2326-6066.CIR-22-0098

Boydell, E., Sandoval, J. L., Michielin, O., Obeid, M., Addeo, A., & Friedlaender, A. (2023). Neoadjuvant Immunotherapy: A Promising New Standard of Care. *Int J Mol Sci*, *24*(14). https://doi.org/10.3390/ijms241411849

Braganza, M. Z., Kitahara, C. M., Berrington de Gonzalez, A., Inskip, P. D., Johnson, K. J., & Rajaraman, P. (2012). Ionizing radiation and the risk of brain and central nervous system tumors: a systematic review. *Neuro Oncol*, *14*(11), 1316-1324. https://doi.org/10.1093/neuonc/nos208

Brown, C. E., Alizadeh, D., Starr, R., Weng, L., Wagner, J. R., Naranjo, A., Ostberg, J. R., Blanchard, M. S., Kilpatrick, J., Simpson, J., Kurien, A., Priceman, S. J., Wang, X., Harshbarger, T. L., D'Apuzzo, M., Ressler, J. A., Jensen, M. C., Barish, M. E., Chen, M., . . . Badie, B. (2016). Regression of Glioblastoma after Chimeric Antigen Receptor T-Cell Therapy. *New England Journal of Medicine*, *375*(26). https://doi.org/10.1056/NEJMoa1610497

Brown, C. E., Badie, B., Barish, M. E., Weng, L., Ostberg, J. R., Chang, W.-C., Naranjo, A., Starr, R., Wagner, J., Wright, C., Zhai, Y., Bading, J. R., Ressler, J. A., Portnow, J., D'Apuzzo, M., Forman, S. J., & Jensen, M. C. (2015). Bioactivity and Safety of IL13Rα2-Redirected Chimeric Antigen Receptor CD8+ T Cells in Patients with Recurrent Glioblastoma. *Clinical Cancer Research*, *21*(18). https://doi.org/10.1158/1078-0432.CCR-15-0428

Brown, N. F., Ottaviani, D., Tazare, J., Gregson, J., Kitchen, N., Brandner, S., Fersht, N., & Mulholland, P. (2022). Survival Outcomes and Prognostic Factors in Glioblastoma. *Cancers*, *14*(13). https://doi.org/10.3390/cancers14133161

Burnette, B. C., Liang, H., Lee, Y., Chlewicki, L., Khodarev, N. N., Weichselbaum, R. R., Fu, Y.-X., & Auh, S. L. (2011). The Efficacy of Radiotherapy Relies upon Induction of Type I Interferon–Dependent Innate and Adaptive Immunity. *Cancer Research*, *71*(7). https://doi.org/10.1158/0008-5472.CAN-10-2820

Burster, T., Gärtner, F., Bulach, C., Zhanapiya, A., Gihring, A., & Knippschild, U. (2021). Regulation of MHC I Molecules in Glioblastoma Cells and the Sensitizing of NK Cells. *Pharmaceuticals*, *14*(3). https://doi.org/10.3390/ph14030236

Buttmann, M., Berberich-Siebelt, F., Serfling, E., & Rieckmann, P. (2007). Interferon-β Is a Potent Inducer of Interferon Regulatory Factor-1/2-Dependent IP-10/CXCL10 Expression in Primary Human Endothelial Cells. *Journal of Vascular Research*, *44*(1). https://doi.org/10.1159/000097977

Byun, Y. H., & Park, C.-K. (2022). Classification and Diagnosis of Adult Glioma: A Scoping Review. *Brain & Neurorehabilitation*, *15*(3). https://doi.org/10.12786/bn.2022.15.e23

Cai, Y., Chen, R., Gao, S., Li, W., Liu, Y., Su, G., Song, M., Jiang, M., Jiang, C., & Zhang, X. (2022). Artificial intelligence applied in neoantigen identification facilitates personalized cancer immunotherapy. *Frontiers in Oncology*, *12*. https://doi.org/10.3389/fonc.2022.1054231

Campian, J. L., Piotrowski, A. F., Ye, X., Hakim, F. T., Rose, J., Yan, X. Y., Lu, Y., Gress, R., & Grossman, S. A. (2017). Serial changes in lymphocyte subsets in patients with newly diagnosed high grade astrocytomas treated with standard radiation and temozolomide. *J Neurooncol*, *135*(2), 343-351. https://doi.org/10.1007/s11060-017-2580-z

Canter, R. J., Grossenbacher, S. K., Foltz, J. A., Sturgill, I. R., Park, J. S., Luna, J. I., Kent, M. S., Culp, W. T. N., Chen, M., Modiano, J. F., Monjazeb, A. M., Lee, D. A., & Murphy, W. J. (2017). Radiotherapy enhances natural killer cell cytotoxicity and localization in pre-clinical canine sarcomas and first-in-dog clinical trial. *Journal for ImmunoTherapy of Cancer*, *5*(1). https://doi.org/10.1186/s40425-017-0305-7

Chen, J., Cao, Y., Markelc, B., Kaeppler, J., Vermeer, J. A., & Muschel, R. J. (2019). Type I IFN protects cancer cells from CD8+ T cell-mediated cytotoxicity after radiation. *J Clin Invest*, *129*(10), 4224-4238. https://doi.org/10.1172/JCI127458

Chen, Q., Han, B., Meng, X., Duan, C., Yang, C., Wu, Z., Magafurov, D., Zhao, S., Safin, S., Jiang, C., & Cai, J. (2019). Immunogenomic analysis reveals LGALS1 contributes to the immune heterogeneity and immunosuppression in glioma. *Int J Cancer*, *145*(2), 517-530. https://doi.org/10.1002/ijc.32102

Cloughesy, T. F., Mochizuki, A. Y., Orpilla, J. R., Hugo, W., Lee, A. H., Davidson, T. B., Wang, A. C., Ellingson, B. M., Rytlewski, J. A., Sanders, C. M., Kawaguchi, E. S., Du, L., Li, G., Yong, W. H., Gaffey, S. C., Cohen, A. L., Mellinghoff, I. K., Lee, E. Q., Reardon, D. A., . . . Prins, R. M. (2019). Neoadjuvant anti-PD-1 immunotherapy promotes a survival benefit with intratumoral and systemic immune responses in recurrent glioblastoma. *Nature Medicine 2019 25:3*, *25*(3). https://doi.org/10.1038/s41591-018-0337-7

Corapi, E., Carrizo, G., Compagno, D., & Laderach, D. (2018). Endogenous Galectin-1 in T Lymphocytes Regulates Anti-prostate Cancer Immunity. *Frontiers in Immunology*, *9*. https://doi.org/10.3389/fimmu.2018.02190

Crespo, J., Sun, H., Welling, T. H., Tian, Z., & Zou, W. (2013). T cell anergy, exhaustion, senescence and stemness in the tumor microenvironment. *Current opinion in immunology*, *25*(2). https://doi.org/10.1016/j.coi.2012.12.003

Croese, T., Castellani, I., & Schwartz, M. (2021). Immune cell compartmentalization for brain surveillance and protection. *Nature Immunology*, *22*(9), 1083-1092. https://doi.org/10.1038/s41590-021-00994-2

Deng, L., Liang, H., Xu, M., Yang, X., Burnette, B., Arina, A., Li, X. D., Mauceri, H., Beckett, M., Darga, T., Huang, X., Gajewski, T. F., Chen, Z. J., Fu, Y. X., & Weichselbaum, R. R. (2014). STING-Dependent Cytosolic DNA Sensing Promotes Radiation-Induced Type I Interferon-Dependent Antitumor Immunity in Immunogenic Tumors. *Immunity*, *41*(5), 843-852. https://doi.org/10.1016/j.immuni.2014.10.019

Dewan, M. Z., Galloway, A. E., Kawashima, N., Dewyngaert, J. K., Babb, J. S., Formenti, S. C., & Demaria, S. (2009). Fractionated but Not Single-Dose Radiotherapy Induces an Immune-Mediated Abscopal Effect when Combined with Anti–CTLA-4 Antibody. *Clinical Cancer Research*, *15*(17). https://doi.org/10.1158/1078-0432.CCR-09-0265

Di Ianni, N., Maffezzini, M., Eoli, M., & Pellegatta, S. (2021). Revisiting the Immunological Aspects of Temozolomide Considering the Genetic Landscape and the Immune Microenvironment Composition of Glioblastoma. *Front Oncol*, *11*, 747690. https://doi.org/10.3389/fonc.2021.747690

Diamond, M. S., Kinder, M., Matsushita, H., Mashayekhi, M., Dunn, G. P., Archambault, J. M., Lee, H., Arthur, C. D., White, J. M., Kalinke, U., Murphy, K. M., & Schreiber, R. D. (2011). Type I interferon is selectively required by dendritic cells for immune rejection of tumors. *Journal of Experimental Medicine*, *208*(10). https://doi.org/10.1084/jem.20101158

Dinevska, M., Widodo, S. S., Furst, L., Cuzcano, L., Fang, Y., Mangiola, S., Neeson, P. J., Darcy, P. K., Ramsay, R. G., Hutchinson, R., MacKay, F., Christie, M., Stylli, S. S., & Mantamadiotis, T. (2023). Cell signaling activation and extracellular matrix remodeling underpin glioma tumor microenvironment heterogeneity and organization. *Cell Oncol (Dordr)*, *46*(3), 589-602. https://doi.org/10.1007/s13402-022-00763-9

Dizdaroglu, M., & Jaruga, P. (2012). Mechanisms of free radical-induced damage to DNA. *Free Radic Res*, *46*(4), 382-419. https://doi.org/10.3109/10715762.2011.653969

Dobersalske, C., Rauschenbach, L., Hua, Y., Berliner, C., Steinbach, A., Gruneboom, A., Kokkaliaris, K. D., Heiland, D. H., Berger, P., Langer, S., Tan, C. L., Stenzel, M., Landolsi, S., Weber, F., Darkwah Oppong, M., Werner, R. A., Gull, H., Schroder, T., Linsenmann, T., . . . Scheffler, B. (2024). Cranioencephalic functional lymphoid units in glioblastoma. *Nat Med*. https://doi.org/10.1038/s41591-024-03152-x

Ehrend, E., Manns, P., Herkt, S. C., Lee, S., Romanski, A., Burger, M., Steinbach, J., Wels, W. S., Bönig, H., & Tonn, T. (2024). Real World Product Quality Data of Car-Engineered Nk Cells for Intracranial Injection in Patients with Recurrent Her2-Positive Glioblastoma from the Ongoing Car2brain Clinical Trial. *Cytotherapy*, *26*(6), S9-S10. <Go to ISI>://WOS:001282333600062

Eide, P. K., Vatnehol, S. A. S., Emblem, K. E., & Ringstad, G. (2018). Magnetic resonance imaging provides evidence of glymphatic drainage from human brain to cervical lymph nodes. *Scientific Reports*, *8*(1). https://doi.org/10.1038/s41598-018-25666-4

Engblom, C., Thrane, K., Lin, Q., Andersson, A., Toosi, H., Chen, X., Steiner, E., Lu, C., Mantovani, G., Hagemann-Jensen, M., Saarenpää, S., Jangard, M., Saez-Rodriguez, J., Michaëlsson, J., Hartman, J., Lagergren, J., Mold, J. E., Lundeberg, J., & Frisén, J. (2023). Spatial transcriptomics of B cell and T cell receptors reveals lymphocyte clonal dynamics. *Science*, *382*(6675). https://doi.org/10.1126/science.adf8486

Engelhardt, B., Vajkoczy, P., & Weller, R. O. (2017). The movers and shapers in immune privilege of the CNS. *Nature Immunology*, *18*(2). https://doi.org/10.1038/ni.3666

Fabriek, B. O., Van Haastert, E. S., Galea, I., Polfliet, M. M. J., Döpp, E. D., Van den Heuvel, M. M., Van den Berg, T. K., De Groot, C. J. A., Van der Valk, P., & Dijkstra, C. D. (2005). CD163-positive perivascular macrophages in the human CNS express molecules for antigen recognition and presentation. *Glia*, *51*(4), 297-305. https://doi.org/10.1002/glia.20208

Favaudon, V., Caplier, L., Monceau, V., Pouzoulet, F., Sayarath, M., Fouillade, C., Poupon, M.-F., Brito, I., Hupé, P., Bourhis, J., Hall, J., Fontaine, J.-J., & Vozenin, M.-C. (2014). Ultrahigh dose-rate FLASH irradiation increases the differential

response between normal and tumor tissue in mice. *Science Translational Medicine*, *6*(245). https://doi.org/10.1126/scitranslmed.3008973

Feng, X., Jopson, T. D., Paladini, M. S., Liu, S., West, B. L., Gupta, N., & Rosi, S. (2016). Colony-stimulating factor 1 receptor blockade prevents fractionated whole-brain irradiation-induced memory deficits. *Journal of Neuroinflammation 2016 13:1*, *13*(1). https://doi.org/10.1186/s12974-016-0671-y

Feng, X., Tubbs, A., Zhang, C., Tang, M., Sridharan, S., Wang, C., Jiang, D., Su, D., Zhang, H., Chen, Z., Nie, L., Xiong, Y., Huang, M., Nussenzweig, A., & Chen, J. (2020). ATR inhibition potentiates ionizing radiation-induced interferon response via cytosolic nucleic acid-sensing pathways. *The EMBO Journal*, *39*(14). https://doi.org/10.15252/embj.2019104036

Fernandez-Gonzalo, R., Baatout, S., & Moreels, M. (2017). Impact of Particle Irradiation on the Immune System: From the Clinic to Mars. *Frontiers in Immunology*, *8*. https://doi.org/10.3389/fimmu.2017.00177

Fransen, N. L., Hsiao, C. C., van der Poel, M., Engelenburg, H. J., Verdaasdonk, K., Vincenten, M. C. J., Remmerswaal, E. B. M., Kuhlmann, T., Mason, M. R. J., Hamann, J., Smolders, J., & Huitinga, I. (2020). Tissue-resident memory T cells invade the brain parenchyma in multiple sclerosis white matter lesions. *Brain*, *143*(6), 1714-1730. https://doi.org/10.1093/brain/awaa117

Friedrich, M., Hahn, M., Michel, J., Sankowski, R., Kilian, M., Kehl, N., Günter, M., Bunse, T., Pusch, S., von Deimling, A., Wick, W., Autenrieth, S. E., Prinz, M., Platten, M., & Bunse, L. (2023). Dysfunctional dendritic cells limit antigen-specific T cell response in glioma. *Neuro-oncology*, *25*(2). https://doi.org/10.1093/neuonc/noac138

Gameiro, S. R., Jammed, M. L., Wattenberg, M. M., Tsang, K. Y., Ferrone, S., & Hodge, J. W. (2014). Radiation-induced immunogenic modulation of tumor enhances antigen processing and calreticulin exposure, resulting in enhanced T-cell killing. *Oncotarget*, *5*(2). https://doi.org/10.18632/oncotarget.1719

Gameiro, S. R., Malamas, A. S., Bernstein, M. B., Tsang, K. Y., Vassantachart, A., Sahoo, N., Tailor, R., Pidikiti, R., Guha, C. P., Hahn, S. M., Krishnan, S., & Hodge, J. W. (2016). Tumor Cells Surviving Exposure to Proton or Photon Radiation Share a Common Immunogenic Modulation Signature, Rendering Them More Sensitive to T Cell-Mediated Killing. *Int J Radiat Oncol Biol Phys*, *95*(1), 120-130. https://doi.org/10.1016/j.ijrobp.2016.02.022

Gangoso, E., Southgate, B., Bradley, L., Rus, S., Galvez-Cancino, F., McGivern, N., Guc, E., Kapourani, C. A., Byron, A., Ferguson, K. M., Alfazema, N., Morrison, G., Grant, V., Blin, C., Sou, I., Marques-Torrejon, M. A., Conde, L., Parrinello, S., Herrero, J., . . . Pollard, S. M. (2021). Glioblastomas acquire myeloid-affiliated transcriptional programs via epigenetic immunoediting to elicit immune evasion. *Cell*, *184*(9), 2454-2470 e2426. https://doi.org/10.1016/j.cell.2021.03.023

Gate, D., Saligrama, N., Leventhal, O., Yang, A. C., Unger, M. S., Middeldorp, J., Chen, K., Lehallier, B., Channappa, D., De Los Santos, M. B., McBride, A., Pluvinage, J., Elahi, F., Tam, G. K., Kim, Y., Greicius, M., Wagner, A. D., Aigner, L., Galasko, D. R., . . . Wyss-Coray, T. (2020). Clonally expanded CD8 T cells patrol the cerebrospinal fluid in Alzheimer's disease. *Nature*, *577*(7790), 399-404. https://doi.org/10.1038/s41586-019-1895-7

Gehrke, N., Mertens, C., Zillinger, T., Wenzel, J., Bald, T., Zahn, S., Tuting, T., Hartmann, G., & Barchet, W. (2013). Oxidative damage of DNA confers resistance to cytosolic nuclease TREX1 degradation and potentiates STING-dependent immune sensing. *Immunity*, *39*(3), 482-495. https://doi.org/10.1016/j.immuni.2013.08.004

Gellert, J., Agardy, D. A., Kumar, S., Kourtesakis, A., Boschert, T., Jaehne, K., Breckwoldt, M. O., Bunse, L., Wick, W., Davies, M. A., Platten, M., & Bunse, T. (2024). Tumoral Interferon Beta Induces an Immune-Stimulatory Phenotype in

Tumor-Associated Macrophages in Melanoma Brain Metastases. *Cancer Res Commun*. https://doi.org/10.1158/2767-9764.CRC-24-0024

Germain, P.-L., Lun, A., Garcia Meixide, C., Macnair, W., & Robinson, M. D. (2022). Doublet identification in single-cell sequencing data using scDblFinder. *F1000Research*, *10*. https://doi.org/10.12688/f1000research.73600.2

Ginhoux, F., Greter, M., Leboeuf, M., Nandi, S., See, P., Gokhan, S., Mehler, M. F., Conway, S. J., Ng, L. G., Stanley, E. R., Samokhvalov, I. M., & Merad, M. (2010). Fate Mapping Analysis Reveals That Adult Microglia Derive from Primitive Macrophages. *Science*, *330*(6005). https://doi.org/10.1126/science.1194637

Gomez-Nicola, D., & Perry, V. H. (2015). Microglial Dynamics and Role in the Healthy and Diseased Brain: A Paradigm of Functional Plasticity. *The Neuroscientist*, *21*(2). https://doi.org/10.1177/1073858414530512

Gomez Perdiguero, E., Klapproth, K., Schulz, C., Busch, K., Azzoni, E., Crozet, L., Garner, H., Trouillet, C., de Bruijn, M. F., Geissmann, F., & Rodewald, H.-R. (2014). Tissue-resident macrophages originate from yolk-sac-derived erythro-myeloid progenitors. *Nature*, *518*(7540). https://doi.org/10.1038/nature13989

Goodhead, D. T. (1994). Initial events in the cellular effects of ionizing radiations: clustered damage in DNA. *Int J Radiat Biol*, *65*(1), 7-17. https://doi.org/10.1080/09553009414550021

Gottlieb, A., Pham, H. P. T., Saltarrelli, J. G., & Lindsey, J. W. (2024). Expanded T lymphocytes in the cerebrospinal fluid of multiple sclerosis patients are specific for Epstein-Barr-virus-infected B cells. *Proc Natl Acad Sci U S A*, *121*(3), e2315857121. https://doi.org/10.1073/pnas.2315857121

Goubau, D., Schlee, M., Deddouche, S., Pruijssers, A. J., Zillinger, T., Goldeck, M., Schuberth, C., Van der Veen, A. G., Fujimura, T., Rehwinkel, J., Iskarpatyoti, J. A., Barchet, W., Ludwig, J., Dermody, T. S., Hartmann, G., & Reis e Sousa, C. (2014). Antiviral immunity via RIG-I-mediated recognition of RNA bearing 5'-diphosphates. *Nature*, *514*(7522), 372-375. https://doi.org/10.1038/nature13590

Grassl, N., Poschke, I., Lindner, K., Bunse, L., Mildenberger, I., Boschert, T., Jähne, K., Green, E. W., Hülsmeyer, I., Jünger, S., Kessler, T., Suwala, A. K., Eisele, P., Breckwoldt, M. O., Vajkoczy, P., Grauer, O. M., Herrlinger, U., Tonn, J.-C., Denk, M., . . . Sahm, K. (2023). A H3K27M-targeted vaccine in adults with diffuse midline glioma. *Nature Medicine*, *29*(10). https://doi.org/10.1038/s41591-023-02555-6

Grossman, S. A., Ye, X., Lesser, G., Sloan, A., Carraway, H., Desideri, S., Piantadosi, S., & Consortium, f. t. N. C. (2011). Immunosuppression in Patients with High-Grade Gliomas Treated with Radiation and Temozolomide. *Clinical Cancer Research*, *17*(16). https://doi.org/10.1158/1078-0432.CCR-11-0774

Guipaud, O., Jaillet, C., Clément-Colmou, K., François, A., Supiot, S., & Milliat, F. (2018). The importance of the vascular endothelial barrier in the immune-inflammatory response induced by radiotherapy. *The British Journal of Radiology*, *91*(1089). https://doi.org/10.1259/bjr.20170762

Hallahan, D., Kuchibhotla, J., & Wyble, C. (1996). Cell adhesion molecules mediate radiation-induced leukocyte adhesion to the vascular endothelium. *Cancer Res*, *56*(22), 5150-5155. https://www.ncbi.nlm.nih.gov/pubmed/8912850

Hambardzumyan, D., Gutmann, D. H., & Kettenmann, H. (2015). The role of microglia and macrophages in glioma maintenance and progression. *Nature Neuroscience*, *19*(1). https://doi.org/10.1038/nn.4185

Haroun, R., Naasri, S., & Oweida, A. J. (2023). Toll-Like Receptors and the Response to Radiotherapy in Solid Tumors: Challenges and Opportunities. *Vaccines (Basel)*, *11*(4). https://doi.org/10.3390/vaccines11040818

Hartmann, L., Osen, W., Eichmuller, O. L., Kordass, T., Furkel, J., Dickes, E., Reid, C., Debus, J., Brons, S., Abdollahi, A., Moustafa, M., Rieken, S., & Eichmuller, S. B. (2022). Carbon ion irradiation plus CTLA4 blockade elicits therapeutic immune

responses in a murine tumor model. *Cancer Lett*, *550*, 215928. https://doi.org/10.1016/j.canlet.2022.215928

Hartmann, L., Schroter, P., Osen, W., Baumann, D., Offringa, R., Moustafa, M., Will, R., Debus, J., Brons, S., Rieken, S., & Eichmuller, S. B. (2020). Photon versus carbon ion irradiation: immunomodulatory effects exerted on murine tumor cell lines. *Sci Rep*, *10*(1), 21517. https://doi.org/10.1038/s41598-020-78577-8

Hillmer, E. J., Zhang, H., Li, H. S., & Watowich, S. S. (2016). STAT3 signaling in immunity. *Cytokine Growth Factor Rev*, *31*, 1-15. https://doi.org/10.1016/j.cytogfr.2016.05.001

Himburg, H. A., Sasine, J., Yan, X., Kan, J., Dressman, H., & Chute, J. P. (2016). A Molecular Profile of the Endothelial Cell Response to Ionizing Radiation. *Radiat Res*, *186*(2), 141-152. https://doi.org/10.1667/RR14444.1

Hohsfield, L. A., Najafi, A. R., Ghorbanian, Y., Soni, N., Hingco, E. E., Kim, S. J., Jue, A. D., Swarup, V., Inlay, M. A., & Green, K. N. (2020). Effects of long-term and brain-wide colonization of peripheral bone marrow-derived myeloid cells in the CNS. *Journal of Neuroinflammation*, *17*(1). https://doi.org/10.1186/s12974-020-01931-0

Hou, A. J., Chen, L. C., & Chen, Y. Y. (2021). Navigating CAR-T cells through the solid-tumour microenvironment. *Nature Reviews Drug Discovery*, *20*(7). https://doi.org/10.1038/s41573-021-00189-2

Ignarro, R. S., Bombeiro, A. L., Chiarotto, G. B., Cartarozzi, L. P., Coser, L. O., Ghizoni, E., Tedeschi, H., Cendes, F., Lopes-Cendes, I., Rogerio, F., & Oliveira, A. L. R. (2022). Interferon-beta induces major histocompatibility complex of class I (MHC-I) expression and a proinflammatory phenotype in cultivated human astrocytes. *Differentiation*, *128*, 43-56. https://doi.org/10.1016/j.diff.2022.10.004

Iliff, J. J., Wang, M., Liao, Y., Plogg, B. A., Peng, W., Gundersen, G. A., Benveniste, H., Vates, G. E., Deane, R., Goldman, S. A., Nagelhus, E. A., & Nedergaard, M. (2012). A paravascular pathway facilitates CSF flow through the brain parenchyma and the clearance of interstitial solutes, including amyloid beta. *Sci Transl Med*, *4*(147), 147ra111. https://doi.org/10.1126/scitranslmed.3003748

Imadome, K., Iwakawa, M., Nojiri, K., Tamaki, T., Sakai, M., Nakawatari, M., Moritake, T., Yanagisawa, M., Nakamura, E., Tsujii, H., & Imai, T. (2008). Upregulation of stress-response genes with cell cycle arrest induced by carbon ion irradiation in multiple murine tumors models. *Cancer Biology & Therapy*, *7*(2). https://doi.org/10.4161/cbt.7.2.5255

Iturri, L., Bertho, A., Lamirault, C., Juchaux, M., Gilbert, C., Espenon, J., Sebrie, C., Jourdain, L., Pouzoulet, F., Verrelle, P., Marzi, L. D., & Prezado, Y. (2023). Proton FLASH Radiation Therapy and Immune Infiltration: Evaluation in an Orthotopic Glioma Rat Model. *International Journal of Radiation Oncology, Biology, Physics*, *116*(3). https://doi.org/10.1016/j.ijrobp.2022.12.018

Jacquelot, N., Yamazaki, T., Roberti, M. P., Duong, C. P. M., Andrews, M. C., Verlingue, L., Ferrere, G., Becharef, S., Vétizou, M., Daillère, R., Messaoudene, M., Enot, D. P., Stoll, G., Ugel, S., Marigo, I., Foong Ngiow, S., Marabelle, A., Prevost-Blondel, A., Gaudreau, P.-O., . . . Zitvogel, L. (2019). Sustained Type I interferon signaling as a mechanism of resistance to PD-1 blockade. *Cell Research*, *29*(10). https://doi.org/10.1038/s41422-019-0224-x

Jin, S., Guerrero-Juarez, C. F., Zhang, L., Chang, I., Ramos, R., Kuan, C.-H., Myung, P., Plikus, M. V., Nie, Q., Jin, S., Guerrero-Juarez, C. F., Zhang, L., Chang, I., Ramos, R., Kuan, C.-H., Myung, P., Plikus, M. V., & Nie, Q. (2021). Inference and analysis of cell-cell communication using CellChat. *Nature Communications 2021 12:1*, *12*(1). https://doi.org/10.1038/s41467-021-21246-9

Johnston, M., Zakharov, A., Papaiconomou, C., Salmasi, G., & Armstrong, D. (2004). Evidence of connections between cerebrospinal fluid and nasal lymphatic vessels in humans, non-human primates and other mammalian species. *Cerebrospinal Fluid Research*, *1*(1). https://doi.org/10.1186/1743-8454-1-2

Kadry, H., Noorani, B., & Cucullo, L. (2020). A blood-brain barrier overview on structure, function, impairment, and biomarkers of integrity. *Fluids Barriers CNS*, *17*(1), 69. https://doi.org/10.1186/s12987-020-00230-3

Kang, C., Jeong, S.-Y., Song, S. Y., & Choi, E. K. (2020). The emerging role of myeloid-derived suppressor cells in radiotherapy. *Radiation Oncology Journal*, *38*(1). https://doi.org/10.3857/roj.2019.00640

Karim, A. B., Maat, B., Hatlevoll, R., Menten, J., Rutten, E. H., Thomas, D. G., Mascarenhas, F., Horiot, J. C., Parvinen, L. M., van Reijn, M., Jager, J. J., Fabrini, M. G., van Alphen, A. M., Hamers, H. P., Gaspar, L., Noordman, E., Pierart, M., & van Glabbeke, M. (1996). A randomized trial on dose-response in radiation therapy of low-grade cerebral glioma: European Organization for Research and Treatment of Cancer (EORTC) Study 22844. *Int J Radiat Oncol Biol Phys*, *36*(3), 549-556. https://doi.org/10.1016/s0360-3016(96)00352-5

Kelly, A., Powis, S. H., Kerr, L.-A., Mockridge, I., Elliott, T., Bastin, J., Uchanska-Ziegler, B., Ziegler, A., Trowsdale, J., & Townsend, A. (1992). Assembly and function of the two ABC transporter proteins encoded in the human major histocompatibility complex. *Nature*, *355*(6361). https://doi.org/10.1038/355641a0

Kilian, M., Bunse, T., Wick, W., Platten, M., & Bunse, L. (2021). Genetically Modified Cellular Therapies for Malignant Gliomas. *Int J Mol Sci*, *22*(23). https://doi.org/10.3390/ijms222312810

Kilian, M., Friedrich, M., Sanghvi, K., Green, E., Pusch, S., Kawauchi, D., Lower, M., Sonner, J. K., Kramer, C., Zaman, J., Jung, S., Breckwoldt, M. O., Willimsky, G., Eichmuller, S. B., von Deimling, A., Wick, W., Sahm, F., Platten, M., & Bunse, L. (2022). T-cell Receptor Therapy Targeting Mutant Capicua Transcriptional Repressor in Experimental Gliomas. *Clin Cancer Res*, *28*(2), 378-389. https://doi.org/10.1158/1078-0432.CCR-21-1881

Kim, J. E., Patel, M. A., Mangraviti, A., Kim, E. S., Theodros, D., Velarde, E., Liu, A., Sankey, E. W., Tam, A., Xu, H., Mathios, D., Jackson, C. M., Harris-Bookman, S., Garzon-Muvdi, T., Sheu, M., Martin, A. M., Tyler, B. M., Tran, P. T., Ye, X., . . . Lim, M. (2017). Combination Therapy with Anti-PD-1, Anti-TIM-3, and Focal Radiation Results in Regression of Murine Gliomas. *Clinical Cancer Research*, *23*(1). https://doi.org/10.1158/1078-0432.CCR-15-1535

Klug, F., Prakash, H., Huber, P. E., Seibel, T., Bender, N., Halama, N., Pfirschke, C., Voss, R. H., Timke, C., Umansky, L., Klapproth, K., Schakel, K., Garbi, N., Jager, D., Weitz, J., Schmitz-Winnenthal, H., Hammerling, G. J., & Beckhove, P. (2013). Low-dose irradiation programs macrophage differentiation to an iNOS(+)/M1 phenotype that orchestrates effective T cell immunotherapy. *Cancer Cell*, *24*(5), 589-602. https://doi.org/10.1016/j.ccr.2013.09.014

Koka, K., Verma, A., Dwarakanath, B. S., & Papineni, R. V. L. (2022). Technological Advancements in External Beam Radiation Therapy (EBRT): An Indispensable Tool for Cancer Treatment. *Cancer Management and Research*, *14*. https://doi.org/10.2147/CMAR.S351744

Korsunsky, I., Millard, N., Fan, J., Slowikowski, K., Zhang, F., Wei, K., Baglaenko, Y., Brenner, M., Loh, P.-r., & Raychaudhuri, S. (2019). Fast, sensitive and accurate integration of single-cell data with Harmony. *Nature Methods*, *16*(12). https://doi.org/10.1038/s41592-019-0619-0

Kozlowska, A. K., Tseng, H. C., Kaur, K., Topchyan, P., Inagaki, A., Bui, V. T., Kasahara, N., Cacalano, N., & Jewett, A. (2016). Resistance to cytotoxicity and sustained release of interleukin-6 and interleukin-8 in the presence of decreased interferon-gamma after differentiation of glioblastoma by human natural killer cells. *Cancer Immunol Immunother*, *65*(9), 1085-1097. https://doi.org/10.1007/s00262-016-1866-x

Krämer, C., Kilian, M., Chih, Y.-C., Kourtesakis, A., Hoffmann, D. C., Boschert, T., Koopmann, P., Sanghvi, K., De Roia, A., Jung, S., Jähne, K., Day, B., Shultz, L. D., Ratliff, M., Harbottle, R., Green, E. W., Will, R., Wick, W., Platten, M., &

Bunse, L. (2024). NLGN4X TCR transgenic T cells to treat gliomas. *Neuro-oncology*, *26*(2). https://doi.org/10.1093/neuonc/noad172

Laaker, C., Baenen, C., Kovács, K. G., Sandor, M., & Fabry, Z. (2023). Immune cells as messengers from the CNS to the periphery: the role of the meningeal lymphatic system in immune cell migration from the CNS. *Frontiers in Immunology*, *14*. https://doi.org/10.3389/fimmu.2023.1233908

Lara-Velazquez, M., Shireman, J. M., Lehrer, E. J., Bowman, K. M., Ruiz-Garcia, H., Paukner, M. J., Chappell, R. J., & Dey, M. (2021). A Comparison Between Chemo-Radiotherapy Combined With Immunotherapy and Chemo-Radiotherapy Alone for the Treatment of Newly Diagnosed Glioblastoma: A Systematic Review and Meta-Analysis. *Frontiers in Oncology*, *11*. https://doi.org/10.3389/fonc.2021.662302

Latzer, P., Zelba, H., Battke, F., Reinhardt, A., Shao, B., Bartsch, O., Rabsteyn, A., Harter, J., Schulze, M., Okech, T., Golf, A., Kyzirakos-Feger, C., Kayser, S., Pieper, N., Feldhahn, M., Wünsche, J., Seitz, C., Hadaschik, D., Garbe, C., . . . Biskup, S. (2024). A real-world observation of patients with glioblastoma treated with a personalized peptide vaccine. *Nature Communications 2024 15:1*, *15*(1). https://doi.org/10.1038/s41467-024-51315-8

Lauber, K., Ernst, A., Orth, M., Herrmann, M., & Belka, C. (2012). Dying cell clearance and its impact on the outcome of tumor radiotherapy. *Frontiers in Oncology*, *2*. https://doi.org/10.3389/fonc.2012.00116

Leblond, M. M., Pérès, E. A., Helaine, C., Gérault, A. N., Moulin, D., Anfray, C., Divoux, D., Petit, E., Valable, M. B. S., Leblond, M. M., Pérès, E. A., Helaine, C., Gérault, A. N., Moulin, D., Anfray, C., Divoux, D., Petit, E., & Valable, M. B. S. (2017). M2 macrophages are more resistant than M1 macrophages following radiation therapy in the context of glioblastoma. *Oncotarget*, *8*(42). https://doi.org/10.18632/oncotarget.19994

Lehman, N. L. (2008). Central Nervous System Tumors With Ependymal Features: A Broadened Spectrum of Primarily Ependymal Differentiation? *Journal of Neuropathology & Experimental Neurology*, *67*(3). https://doi.org/10.1097/NEN.0b013e31816543a6

Lei, A., Yu, H., Lu, S., Lu, H., Ding, X., Tan, T., Zhang, H., Zhu, M., Tian, L., Wang, X., Su, S., Xue, D., Zhang, S., Zhao, W., Chen, Y., Xie, W., Zhang, L., Zhu, Y., Zhao, J., . . . Zhang, J. (2024). A second-generation M1-polarized CAR macrophage with antitumor efficacy. *Nature Immunology*, *25*(1), 102-116. https://doi.org/10.1038/s41590-023-01687-8

Li, Q., & Barres, B. A. (2018). Microglia and macrophages in brain homeostasis and disease. *Nat Rev Immunol*, *18*(4), 225-242. https://doi.org/10.1038/nri.2017.125

Li, Y. Q., Chen, P., Haimovitz-Friedman, A., Reilly, R. M., & Wong, C. S. (2003). Endothelial apoptosis initiates acute blood-brain barrier disruption after ionizing radiation. *Cancer Research*, *63*(18), 5950-5956. https://www.ncbi.nlm.nih.gov/pubmed/14522921

Liang, H., Deng, L., Hou, Y., Meng, X., Huang, X., Rao, E., Zheng, W., Mauceri, H., Mack, M., Xu, M., Fu, Y.-X., & Weichselbaum, R. R. (2017). Host STING-dependent MDSC mobilization drives extrinsic radiation resistance. *Nature Communications*, *8*(1). https://doi.org/10.1038/s41467-017-01566-5

Lickefett, B., Chu, L., Ortiz-Maldonado, V., Warmuth, L., Barba, P., Doglio, M., Henderson, D., Hudecek, M., Kremer, A., Markman, J., Nauerth, M., Negre, H., Sanges, C., Staber, P. B., Tanzi, R., Delgado, J., Busch, D. H., Kuball, J., Luu, M., & Jager, U. (2023). Lymphodepletion - an essential but undervalued part of the chimeric antigen receptor T-cell therapy cycle. *Front Immunol*, *14*, 1303935. https://doi.org/10.3389/fimmu.2023.1303935

Liljedahl, E., Konradsson, E., Gustafsson, E., Jonsson, K. F., Olofsson, J. K., Ceberg, C., & Redebrandt, H. N. (2022). Long-term anti-tumor effects following both conventional radiotherapy and FLASH in fully immunocompetent animals with

glioblastoma. *Scientific Reports*, *12*(1). https://doi.org/10.1038/s41598-022-16612-6

Lim, M., Weller, M., Idbaih, A., Steinbach, J., Finocchiaro, G., Raval, R. R., Ansstas, G., Baehring, J., Taylor, J. W., Honnorat, J., Petrecca, K., De Vos, F., Wick, A., Sumrall, A., Sahebjam, S., Mellinghoff, I. K., Kinoshita, M., Roberts, M., Slepetis, R., . . . Omuro, A. (2022). Phase III trial of chemoradiotherapy with temozolomide plus nivolumab or placebo for newly diagnosed glioblastoma with methylated MGMT promoter. *Neuro-oncology*, *24*(11). https://doi.org/10.1093/neuonc/noac116

Lin, H., Liu, C., Hu, A., Zhang, D., Yang, H., & Mao, Y. (2024). Understanding the immunosuppressive microenvironment of glioma: mechanistic insights and clinical perspectives. *Journal of Hematology & Oncology*, *17*(1). https://doi.org/10.1186/s13045-024-01544-7

Liu, C., Sage, Jonathan C., Miller, Michael R., Verhaak, Roel G. W., Hippenmeyer, S., Vogel, H., Foreman, O., Bronson, Roderick T., Nishiyama, A., Luo, L., & Zong, H. (2011). Mosaic Analysis with Double Markers Reveals Tumor Cell of Origin in Glioma. *Cell*, *146*(2). https://doi.org/10.1016/j.cell.2011.06.014

Liu, S. D., Tomassian, T., Bruhn, K. W., Miller, J. F., Poirier, F., & Miceli, M. C. (2009). Galectin-1 tunes TCR binding and signal transduction to regulate CD8 burst size. *J Immunol*, *182*(9), 5283-5295. https://doi.org/10.4049/jimmunol.0803811

Liu, T., Pei, P., Shen, W., Hu, L., & Yang, K. (2023). Radiation-Induced Immunogenic Cell Death for Cancer Radioimmunotherapy. *Small Methods*, *7*(5). https://doi.org/10.1002/smtd.202201401

Lok, E., Chung, A. S., Swanson, K. D., & Wong, E. T. (2014). Melanoma brain metastasis globally reconfigures chemokine and cytokine profiles in patient cerebrospinal fluid. *Melanoma Res*, *24*(2), 120-130. https://doi.org/10.1097/CMR.0000000000000045

Lomax, M. E., Folkes, L. K., & O'Neill, P. (2013). Biological consequences of radiation-induced DNA damage: relevance to radiotherapy. *Clinical Oncology*, *25*(10), 578-585. https://doi.org/10.1016/j.clon.2013.06.007

Louis, D. N., Perry, A., Wesseling, P., Brat, D. J., Cree, I. A., Figarella-Branger, D., Hawkins, C., Ng, H. K., Pfister, S. M., Reifenberger, G., Soffietti, R., von Deimling, A., & Ellison, D. W. (2021). The 2021 WHO Classification of Tumors of the Central Nervous System: a summary. *Neuro-oncology*, *23*(8). https://doi.org/10.1093/neuonc/noab106

Luce, A., Abate, M., Scognamiglio, G., Montella, M., Iervolino, D., Campione, S., Di Mauro, A., Sepe, O., Gigantino, V., Tathode, M. S., Ferrara, G., Monaco, R., De Dominicis, G., Misso, G., Gentile, V., Franco, R., Zappavigna, S., & Caraglia, M. (2024). Immune cell infiltration and inflammatory landscape in primary brain tumours. *J Transl Med*, *22*(1), 521. https://doi.org/10.1186/s12967-024-05309-1

Lugade, A. A., Moran, J. P., Gerber, S. A., Rose, R. C., Frelinger, J. G., & Lord, E. M. (2005). Local radiation therapy of B16 melanoma tumors increases the generation of tumor antigen-specific effector cells that traffic to the tumor. *J Immunol*, *174*(12), 7516-7523. https://doi.org/10.4049/jimmunol.174.12.7516

Luksik, A. S., Yazigi, E., Shah, P., & Jackson, C. M. (2023). CAR T Cell Therapy in Glioblastoma: Overcoming Challenges Related to Antigen Expression. *Cancers*, *15*(5). https://doi.org/10.3390/cancers15051414

Ma, Q., Ineichen, B. V., Detmar, M., & Proulx, S. T. (2017). Outflow of cerebrospinal fluid is predominantly through lymphatic vessels and is reduced in aged mice. *Nat Commun*, *8*(1), 1434. https://doi.org/10.1038/s41467-017-01484-6

Majzner, R. G., Ramakrishna, S., Yeom, K. W., Patel, S., Chinnasamy, H., Schultz, L. M., Richards, R. M., Jiang, L., Barsan, V., Mancusi, R., Geraghty, A. C., Good, Z., Mochizuki, A. Y., Gillespie, S. M., Toland, A. M. S., Mahdi, J., Reschke, A., Nie, E. H., Chau, I. J., . . . Monje, M. (2022). GD2-CAR T cell therapy for H3K27M-

mutated diffuse midline gliomas. *Nature*, *603*(7903). https://doi.org/10.1038/s41586-022-04489-4

Makuch, E., Jasyk, I., Kula, A., Lipinski, T., & Siednienko, J. (2022). IFNbeta-Induced CXCL10 Chemokine Expression Is Regulated by Pellino3 Ligase in Monocytes and Macrophages. *Int J Mol Sci*, *23*(23). https://doi.org/10.3390/ijms232314915

Marchetti, L., & Engelhardt, B. (2020). Immune cell trafficking across the blood-brain barrier in the absence and presence of neuroinflammation. *Vascular Biology*, *2*(1). https://doi.org/10.1530/VB-19-0033

Martinet, L., Guellec, S. L., Filleron, T., Lamant, L., Meyer, N., Rochaix, P., Garrido, I., & Girard, J.-P. (2012). High endothelial venules (HEVs) in human melanoma lesions: Major gateways for tumor-infiltrating lymphocytes. *OncoImmunology*, *1*(6). https://doi.org/10.4161/onci.20492

Mathios, D., Kim, J. E., Mangraviti, A., Phallen, J., Park, C.-K., Jackson, C. M., Garzon-Muvdi, T., Kim, E., Theodros, D., Polanczyk, M., Martin, A. M., Suk, I., Ye, X., Tyler, B., Bettegowda, C., Brem, H., Pardoll, D. M., & Lim, M. (2016). Anti–PD-1 antitumor immunity is enhanced by local and abrogated by systemic chemotherapy in GBM. *Science Translational Medicine*, *8*(370). https://doi.org/10.1126/scitranslmed.aag2942

Matuszak, N., Suchorska, W. M., Milecki, P., Kruszyna-Mochalska, M., Misiarz, A., Pracz, J., & Malicki, J. (2022). FLASH radiotherapy: an emerging approach in radiation therapy. *Rep Pract Oncol Radiother*, *27*(2), 344-351. https://doi.org/10.5603/RPOR.a2022.0038

McKelvey, K. J., Hudson, A. L., Donaghy, H., Stoner, S. P., Wheeler, H. R., Diakos, C. I., & Howell, V. M. (2022). Differential effects of radiation fractionation regimens on glioblastoma. *Radiation Oncology*, *17*(1). https://doi.org/10.1186/s13014-022-01990-y

Mellman, I., Chen, D. S., Powles, T., & Turley, S. J. (2023). The cancer-immunity cycle: Indication, genotype, and immunotype. *Immunity*, *56*(10), 2188-2205. https://doi.org/10.1016/j.immuni.2023.09.011

Meza Guzman, L. G., Keating, N., & Nicholson, S. E. (2020). Natural Killer Cells: Tumor Surveillance and Signaling. *Cancers (Basel)*, *12*(4). https://doi.org/10.3390/cancers12040952

Monje, M. L., Mizumatsu, S., Fike, J. R., & Palmer, T. D. (2002). Irradiation induces neural precursor-cell dysfunction. *Nature Medicine*, *8*(9). https://doi.org/10.1038/nm749

Montoya, M. L., Kasahara, N., & Okada, H. (2020). Introduction to immunotherapy for brain tumor patients: challenges and future perspectives. *Neuro-Oncology Practice*, *7*(5). https://doi.org/10.1093/nop/npaa007

Morantz, R. A., Wood, G. W., Foster, M., Clark, M., & Gollahon, K. (1979). Macrophages in experimental and human brain tumors. *Journal of Neurosurgery*, *50*(3). https://doi.org/10.3171/jns.1979.50.3.0305

Morganti, J. M., Jopson, T. D., Liu, S., Gupta, N., & Rosi, S. (2014). Cranial Irradiation Alters the Brain's Microenvironment and Permits CCR2+ Macrophage Infiltration. *PLOS ONE*, *9*(4). https://doi.org/10.1371/journal.pone.0093650

Murakami, T., Nakazawa, T., Natsume, A., Nishimura, F., Nakamura, M., Matsuda, R., Omoto, K., Tanaka, Y., Shida, Y., Park, Y. S., Motoyama, Y., Nakagawa, I., Yamada, S., Tamura, K., Takeshima, Y., Takamura, Y., Wakabayashi, T., & Nakase, H. (2018). Novel Human NK Cell Line Carrying CAR Targeting EGFRvIII Induces Antitumor Effects in Glioblastoma Cells. *Anticancer Res*, *38*(9), 5049-5056. https://doi.org/10.21873/anticanres.12824

Nakamura, Y., Ishii, J., & Kondo, A. (2013). Bright Fluorescence Monitoring System Utilizing Zoanthus sp. Green Fluorescent Protein (ZsGreen) for Human G-Protein-Coupled Receptor Signaling in Microbial Yeast Cells. *PLOS ONE*, *8*(12). https://doi.org/10.1371/journal.pone.0082237

Newcomb, E. W., Demaria, S., Lukyanov, Y., Shao, Y., Schnee, T., Kawashima, N., Lan, L., Dewyngaert, J. K., Zagzag, D., McBride, W. H., & Formenti, S. C. (2006). The Combination of Ionizing Radiation and Peripheral Vaccination Produces Long-term Survival of Mice Bearing Established Invasive GL261 Gliomas. *Clinical Cancer Research*, *12*(15). https://doi.org/10.1158/1078-0432.CCR-06-0593

Novitzky-Basso, I., & Rot, A. (2012). Duffy antigen receptor for chemokines and its involvement in patterning and control of inflammatory chemokines. *Frontiers in Immunology*, *3*. https://doi.org/10.3389/fimmu.2012.00266

Omuro, A., Brandes, A. A., Carpentier, A. F., Idbaih, A., Reardon, D. A., Cloughesy, T., Sumrall, A., Baehring, J., van den Bent, M., Bähr, O., Lombardi, G., Mulholland, P., Tabatabai, G., Lassen, U., Sepulveda, J. M., Khasraw, M., Vauleon, E., Muragaki, Y., Di Giacomo, A. M., . . . Weller, M. (2023). Radiotherapy combined with nivolumab or temozolomide for newly diagnosed glioblastoma with unmethylated MGMT promoter: An international randomized phase III trial. *Neuro-oncology*, *25*(1). https://doi.org/10.1093/neuonc/noac099

Ostrom, Q. T., Fahmideh, M. A., Cote, D. J., Muskens, I. S., Schraw, J. M., Scheurer, M. E., & Bondy, M. L. (2019). Risk factors for childhood and adult primary brain tumors. *Neuro-oncology*, *21*(11). https://doi.org/10.1093/neuonc/noz123

Ostrom, Q. T., Price, M., Neff, C., Cioffi, G., Waite, K. A., Kruchko, C., & Barnholtz-Sloan, J. S. (2023). CBTRUS Statistical Report: Primary Brain and Other Central Nervous System Tumors Diagnosed in the United States in 2016—2020. *Neuro-oncology*, *25*. https://doi.org/10.1093/neuonc/noad149

Padilla, O., Minns, H. E., Wei, H.-J., Fan, W., Webster-Carrion, A., Tazhibi, M., McQuillan, N. M., Zhang, X., Gallitto, M., Yeh, R., Zhang, Z., Hei, T. K., Szalontay, L., Pavisic, J., Tan, Y., Deoli, N., Garty, G., Garvin, J. H., Canoll, P. D., . . . Gartrell, R. D. (2024). Immune Response following FLASH and Conventional Radiation in Diffuse Midline Glioma. *International Journal of Radiation Oncology, Biology, Physics*, *119*(4). https://doi.org/10.1016/j.ijrobp.2024.01.219

Panaretakis, T., Kepp, O., Brockmeier, U., Tesniere, A., Bjorklund, A. C., Chapman, D. C., Durchschlag, M., Joza, N., Pierron, G., Endert, P. v., Yuan, J., Zitvogel, L., Madeo, F., Williams, D. B., & Kroemer, G. (2009). Mechanisms of pre-apoptotic calreticulin exposure in immunogenic cell death. *The EMBO Journal*, *28*(5). https://doi.org/10.1038/emboj.2009.1

Park, H. J., Griffin, R. J., Hui, S., Levitt, S. H., & Song, C. W. (2012). Radiation-induced vascular damage in tumors: implications of vascular damage in ablative hypofractionated radiotherapy (SBRT and SRS). *Radiat Res*, *177*(3), 311-327. https://doi.org/10.1667/rr2773.1

Pashenkov, M., Soderstrom, M., & Link, H. (2003). Secondary lymphoid organ chemokines are elevated in the cerebrospinal fluid during central nervous system inflammation. *J Neuroimmunol*, *135*(1-2), 154-160. https://doi.org/10.1016/s0165-5728(02)00441-1

Peeters, M. C. M., Dirven, L., Koekkoek, J. A. F., Gortmaker, E. G., Fritz, L., Vos, M. J., & Taphoorn, M. J. B. (2020). Prediagnostic symptoms and signs of adult glioma: the patients' view. *Journal of Neuro-Oncology*, *146*(2). https://doi.org/10.1007/s11060-019-03373-y

Pellerino, A., Caccese, M., Padovan, M., Cerretti, G., & Lombardi, G. (2022). Epidemiology, risk factors, and prognostic factors of gliomas. *Clinical and Translational Imaging*, *10*(5), 467-475. https://doi.org/10.1007/s40336-022-00489-6

Perillo, N. L., Pace, K. E., Seilhamer, J. J., & Baum, L. G. (1995). Apoptosis of T cells mediated by galectin-1. *Nature*, *378*(6558), 736-739. https://doi.org/10.1038/378736a0

Persa, E., Balogh, A., Safrany, G., & Lumniczky, K. (2015). The effect of ionizing radiation on regulatory T cells in health and disease. *Cancer Lett*, *368*(2), 252-261. https://doi.org/10.1016/j.canlet.2015.03.003

Platten, M., Bunse, L., Wick, A., Bunse, T., Le Cornet, L., Harting, I., Sahm, F., Sanghvi, K., Tan, C. L., Poschke, I., Green, E., Justesen, S., Behrens, G. A., Breckwoldt, M. O., Freitag, A., Rother, L.-M., Schmitt, A., Schnell, O., Hense, J., . . . Wick, W. (2021). A vaccine targeting mutant IDH1 in newly diagnosed glioma. *Nature*, *592*(7854). https://doi.org/10.1038/s41586-021-03363-z

Qu, Y., Jin, S., Zhang, A., Zhang, B., Shi, X., Wang, J., & Zhao, Y. (2010). Gamma-ray resistance of regulatory CD4+CD25+Foxp3+ T cells in mice. *Radiat Res*, *173*(2), 148-157. https://doi.org/10.1667/RR0978.1

Reardon, D. A., Brandes, A. A., Omuro, A., Mulholland, P., Lim, M., Wick, A., Baehring, J., Ahluwalia, M. S., Roth, P., Bähr, O., Phuphanich, S., Sepulveda, J. M., Souza, P. D., Sahebjam, S., Carleton, M., Tatsuoka, K., Taitt, C., Zwirtes, R., Sampson, J., & Weller, M. (2020). Nivolumab vs Bevacizumab in Patients With Recurrent Glioblastoma. *JAMA Oncology*, *6*(7). https://doi.org/10.1001/jamaoncol.2020.1024

Reardon, D. A., Gokhale, P. C., Klein, S. R., Ligon, K. L., Rodig, S. J., Ramkissoon, S. H., Jones, K. L., Conway, A. S., Liao, X., Zhou, J., Wen, P. Y., Van Den Abbeele, A. D., Hodi, F. S., Qin, L., Kohl, N. E., Sharpe, A. H., Dranoff, G., & Freeman, G. J. (2016). Glioblastoma Eradication Following Immune Checkpoint Blockade in an Orthotopic, Immunocompetent Model. *Cancer Immunology Research*, *4*(2). https://doi.org/10.1158/2326-6066.CIR-15-0151

Reardon, D. A., Omuro, A., Brandes, A. A., Rieger, J., Wick, A., Sepulveda, J., Phuphanich, S., de Souza, P., Ahluwalia, M. S., Lim, M., Vlahovic, G., & Sampson, J. (2017). OS10.3 Randomized Phase 3 Study Evaluating the Efficacy and Safety of Nivolumab vs Bevacizumab in Patients With Recurrent Glioblastoma: CheckMate 143. *Neuro-oncology*, *19*(suppl_3). https://doi.org/10.1093/neuonc/nox036.071

Renier, N., Wu, Z., Simon, D. J., Yang, J., Ariel, P., & Tessier-Lavigne, M. (2014). iDISCO: a simple, rapid method to immunolabel large tissue samples for volume imaging. *Cell*, *159*(4), 896-910. https://doi.org/10.1016/j.cell.2014.10.010

Rossi, M. L., Hughes, J. T., Esiri, M. M., Coakham, H. B., & Brownell, D. B. (1987). Immunohistological study of mononuclear cell infiltrate in malignant gliomas. *Acta Neuropathol*, *74*(3), 269-277. https://doi.org/10.1007/BF00688191

Rustenhoven, J., Drieu, A., Mamuladze, T., de Lima, K. A., Dykstra, T., Wall, M., Papadopoulos, Z., Kanamori, M., Salvador, A. F., Baker, W., Lemieux, M., Da Mesquita, S., Cugurra, A., Fitzpatrick, J., Sviben, S., Kossina, R., Bayguinov, P., Townsend, R. R., Zhang, Q., . . . Kipnis, J. (2021). Functional characterization of the dural sinuses as a neuroimmune interface. *Cell*, *184*(4), 1000-1016 e1027. https://doi.org/10.1016/j.cell.2020.12.040

Saeed, A. M., Bentzen, S. M., Ahmad, H., Pham, L., Woodworth, G. F., & Mishra, M. V. (2024). Systematic review and pooled analysis of the impact of treatment-induced lymphopenia on survival of glioblastoma patients (vol 19, 36, 2024). *Radiation Oncology*, *19*(1). https://doi.org/10.1186/s13014-024-02443-4

Sahm, K., Kessler, T., Eisele, P., Ratliff, M., Sperk, E., König, L., Breckwoldt, M. O., Seliger, C., Mildenberger, I., Schrimpf, D., Herold-Mende, C., Zeiner, P. S., Tabatabai, G., Meuth, S. G., Capper, D., Bendszus, M., von Deimling, A., Wick, W., Sahm, F., & Platten, M. (2023). Concurrent gliomas in patients with multiple sclerosis. *Communications Medicine*, *3*(1). https://doi.org/10.1038/s43856-023-00381-y

Sampson, J. H., Choi, B. D., Sanchez-Perez, L., Suryadevara, C. M., Snyder, D. J., Flores, C. T., Schmittling, R. J., Nair, S. K., Reap, E. A., Norberg, P. K., Herndon, J. E., Kuan, C.-T., Morgan, R. A., Rosenberg, S. A., & Johnson, L. A. (2014). EGFRvIII mCAR-Modified T-Cell Therapy Cures Mice with Established Intracerebral Glioma and Generates Host Immunity against Tumor-Antigen Loss. *Clinical Cancer Research*, *20*(4). https://doi.org/10.1158/1078-0432.CCR-13-0709

Sato, H., Jeggo, P. A., & Shibata, A. (2019). Regulation of programmed death-ligand 1 expression in response to DNA damage in cancer cells: Implications for precision medicine. *Cancer Science*, *110*(11). https://doi.org/10.1111/cas.14197

Sayour, E. J., McLendon, P., McLendon, R., De Leon, G., Reynolds, R., Kresak, J., Sampson, J. H., & Mitchell, D. A. (2015). Increased proportion of FoxP3+ regulatory T cells in tumor infiltrating lymphocytes is associated with tumor recurrence and reduced survival in patients with glioblastoma. *Cancer Immunol Immunother*, *64*(4), 419-427. https://doi.org/10.1007/s00262-014-1651-7

Schmidt, A., Oberle, N., & Krammer, P. H. (2012). Molecular mechanisms of treg-mediated T cell suppression. *Front Immunol*, *3*, 51. https://doi.org/10.3389/fimmu.2012.00051

Schumacher, T., Bunse, L., Pusch, S., Sahm, F., Wiestler, B., Quandt, J., Menn, O., Osswald, M., Oezen, I., Ott, M., Keil, M., Balß, J., Rauschenbach, K., Grabowska, A. K., Vogler, I., Diekmann, J., Trautwein, N., Eichmüller, S. B., Okun, J., . . . Platten, M. (2014). A vaccine targeting mutant IDH1 induces antitumour immunity. *Nature*, *512*(7514). https://doi.org/10.1038/nature13387

Seung, S. K., Curti, B. D., Crittenden, M., Walker, E., Coffey, T., Siebert, J. C., Miller, W., Payne, R., Glenn, L., Bageac, A., & Urba, W. J. (2012). Phase 1 Study of Stereotactic Body Radiotherapy and Interleukin-2—Tumor and Immunological Responses. *Science Translational Medicine*. https://doi.org/10.1126/scitranslmed.3003649

Sha, D., Jin, Z., Budzcies, J., Kluck, K., Stenzinger, A., & Sinicrope, F. A. (2020). Tumor Mutational Burden (TMB) as a Predictive Biomarker in Solid Tumors. *Cancer discovery*, *10*(12). https://doi.org/10.1158/2159-8290.CD-20-0522

Shapouri-Moghaddam, A., Mohammadian, S., Vazini, H., Taghadosi, M., Esmaeili, S.-A., Mardani, F., Seifi, B., Mohammadi, A., Afshari, J. T., & Sahebkar, A. (2018). Macrophage plasticity, polarization, and function in health and disease. *Journal of Cellular Physiology*, *233*(9). https://doi.org/10.1002/jcp.26429

Sharanek, A., Burban, A., Hernandez-Corchado, A., Madrigal, A., Fatakdawala, I., Najafabadi, H. S., Soleimani, V. D., & Jahani-Asl, A. (2021). Transcriptional control of brain tumor stem cells by a carbohydrate binding protein. *Cell Rep*, *36*(9), 109647. https://doi.org/10.1016/j.celrep.2021.109647

Sharma, P., Templin, T., & Grabham, P. (2013). Short term effects of gamma radiation on endothelial barrier function: uncoupling of PECAM-1. *Microvasc Res*, *86*, 11-20. https://doi.org/10.1016/j.mvr.2012.11.007

Singh, R., Lehrer, E. J., Wang, M., Perlow, H. K., Zaorsky, N. G., Trifiletti, D. M., Bovi, J., Navarria, P., Scoccianti, S., Gondi, V., Brown, P. D., & Palmer, J. D. (2021). Dose Escalated Radiation Therapy for Glioblastoma Multiforme: An International Systematic Review and Meta-Analysis of 22 Prospective Trials. *Int J Radiat Oncol Biol Phys*, *111*(2), 371-384. https://doi.org/10.1016/j.ijrobp.2021.05.001

Smolders, J., Fransen, N. L., Hsiao, C. C., Hamann, J., & Huitinga, I. (2020). Perivascular tissue resident memory T cells as therapeutic target in multiple sclerosis. *Expert Review of Neurotherapeutics*, *20*(8), 835-848. https://doi.org/10.1080/14737175.2020.1776609

Smyth, L. C. D., Xu, D., Okar, S. V., Dykstra, T., Rustenhoven, J., Papadopoulos, Z., Bhasiin, K., Kim, M. W., Drieu, A., Mamuladze, T., Blackburn, S., Gu, X., Gaitán, M. I., Nair, G., Storck, S. E., Du, S., White, M. A., Bayguinov, P., Smirnov, I., . . . Kipnis, J. (2024). Identification of direct connections between the dura and the brain. *Nature*, *627*(8002). https://doi.org/10.1038/s41586-023-06993-7

Snyder, H., Robinson, K., Shah, D., Brennan, R., & Handrigan, M. (1993). Signs and symptoms of patients with brain tumors presenting to the emergency department. *Journal of Emergency Medicine*, *11*(3). https://doi.org/10.1016/0736-4679(93)90042-6

Solar, P., Zamani, A., Kubickova, L., Dubovy, P., & Joukal, M. (2020). Choroid plexus and the blood-cerebrospinal fluid barrier in disease. *Fluids Barriers CNS*, *17*(1), 35. https://doi.org/10.1186/s12987-020-00196-2

Spies, T., Cerundolo, V., Colonna, M., Cresswell, P., Townsend, A., & Demars, R. (1992). Presentation of Viral-Antigen by Mhc Class-I Molecules Is Dependent on a Putative Peptide Transporter Heterodimer. *Nature*, *355*(6361), 644-646. https://doi.org/DOI 10.1038/355644a0

Stoeckius, M., Zheng, S., Houck-Loomis, B., Hao, S., Yeung, B. Z., Mauck, W. M., 3rd, Smibert, P., & Satija, R. (2018). Cell Hashing with barcoded antibodies enables multiplexing and doublet detection for single cell genomics. *Genome Biol*, *19*(1), 224. https://doi.org/10.1186/s13059-018-1603-1

Strazielle, N., Creidy, R., Malcus, C., Boucraut, J., & Ghersi-Egea, J.-F. (2016). T-Lymphocytes Traffic into the Brain across the Blood-CSF Barrier: Evidence Using a Reconstituted Choroid Plexus Epithelium. *PLOS ONE*, *11*(3). https://doi.org/10.1371/journal.pone.0150945

Stuart, T., Butler, A., Hoffman, P., Hafemeister, C., Papalexi, E., Mauck, W. M., 3rd, Hao, Y., Stoeckius, M., Smibert, P., & Satija, R. (2019). Comprehensive Integration of Single-Cell Data. *Cell*, *177*(7), 1888-1902 e1821. https://doi.org/10.1016/j.cell.2019.05.031

Stupp, R., Mason, W. P., van den Bent, M. J., Weller, M., Fisher, B., Taphoorn, M. J. B., Belanger, K., Brandes, A. A., Marosi, C., Bogdahn, U., Curschmann, J., Janzer, R. C., Ludwin, S. K., Gorlia, T., Allgeier, A., Lacombe, D., Cairncross, J. G., Eisenhauer, E., & Mirimanoff, R. O. (2005). Radiotherapy plus Concomitant and Adjuvant Temozolomide for Glioblastoma. *New England Journal of Medicine*, *352*(10). https://doi.org/10.1056/NEJMoa043330

Sun, L., Kienzler, J. C., Reynoso, J. G., Lee, A., Shiuan, E., Li, S., Kim, J., Ding, L., Monteleone, A. J., Owens, G. C., Phillips, J. J., Everson, R. G., Nathanson, D., Cloughesy, T. F., Li, G., Liau, L. M., Hugo, W., Kim, W., & Prins, R. M. (2023). Immune checkpoint blockade induces distinct alterations in the microenvironments of primary and metastatic brain tumors. *Journal of Clinical Investigation*, *133*(17). https://doi.org/10.1172/JCI169314

Suryadevara, C. M., Desai, R., Abel, M. L., Riccione, K. A., Batich, K. A., Shen, S. H., Chongsathidkiet, P., Gedeon, P. C., Elsamadicy, A. A., Snyder, D. J., Herndon, J. E., 2nd, Healy, P., Archer, G. E., Choi, B. D., Fecci, P. E., Sampson, J. H., & Sanchez-Perez, L. (2018). Temozolomide lymphodepletion enhances CAR abundance and correlates with antitumor efficacy against established glioblastoma. *OncoImmunology*, *7*(6), e1434464. https://doi.org/10.1080/2162402X.2018.1434464

Sutherland, B. M., Bennett, P. V., Sidorkina, O., & Laval, J. (2000). Clustered DNA damages induced in isolated DNA and in human cells by low doses of ionizing radiation. *Proc Natl Acad Sci U S A*, *97*(1), 103-108. https://doi.org/10.1073/pnas.97.1.103

Sutherland, B. M., Bennett, P. V., Sutherland, J. C., & Laval, J. (2002). Clustered DNA damages induced by x rays in human cells. *Radiat Res*, *157*(6), 611-616. https://doi.org/10.1667/0033-7587(2002)157[0611:cddibx]2.0.co;2

Tan, C. L., Lindner, K., Boschert, T., Meng, Z., Rodriguez Ehrenfried, A., De Roia, A., Haltenhof, G., Faenza, A., Imperatore, F., Bunse, L., Lindner, J. M., Harbottle, R. P., Ratliff, M., Offringa, R., Poschke, I., Platten, M., & Green, E. W. (2024). Prediction of tumor-reactive T cell receptors from scRNA-seq data for personalized T cell therapy. *Nature Biotechnology*. https://doi.org/10.1038/s41587-024-02161-y

Thiriot, A., Perdomo, C., Cheng, G., Novitzky-Basso, I., McArdle, S., Kishimoto, J. K., Barreiro, O., Mazo, I., Triboulet, R., Ley, K., Rot, A., & von Andrian, U. H. (2017). Differential DARC/ACKR1 expression distinguishes venular from non-venular

endothelial cells in murine tissues. *BMC Biol*, *15*(1), 45. https://doi.org/10.1186/s12915-017-0381-7

Tran, T.-A.-T., Kim, Y.-H., Duong, T.-H.-O., Jung, S., Kim, I.-Y., Moon, K.-S., Jang, W.-Y., Lee, H.-J., Lee, J.-J., & Jung, T.-Y. (2020). Peptide Vaccine Combined Adjuvants Modulate Anti-tumor Effects of Radiation in Glioblastoma Mouse Model. *Frontiers in Immunology*, *11*. https://doi.org/10.3389/fimmu.2020.01165

Trapnell, C., Cacchiarelli, D., Grimsby, J., Pokharel, P., Li, S., Morse, M., Lennon, N. J., Livak, K. J., Mikkelsen, T. S., Rinn, J. L., Trapnell, C., Cacchiarelli, D., Grimsby, J., Pokharel, P., Li, S., Morse, M., Lennon, N. J., Livak, K. J., Mikkelsen, T. S., & Rinn, J. L. (2014). The dynamics and regulators of cell fate decisions are revealed by pseudotemporal ordering of single cells. *Nature Biotechnology 2014 32:4*, *32*(4). https://doi.org/10.1038/nbt.2859

Tsai, C. S., Chen, F. H., Wang, C. C., Huang, H. L., Jung, S. M., Wu, C. J., Lee, C. C., McBride, W. H., Chiang, C. S., & Hong, J. H. (2007). Macrophages from irradiated tumors express higher levels of iNOS, arginase-I and COX-2, and promote tumor growth. *Int J Radiat Oncol Biol Phys*, *68*(2), 499-507. https://doi.org/10.1016/j.ijrobp.2007.01.041

Turco, V., Pfleiderer, K., Hunger, J., Horvat, N. K., Karimian-Jazi, K., Schregel, K., Fischer, M., Brugnara, G., Jähne, K., Sturm, V., Streibel, Y., Nguyen, D., Altamura, S., Agardy, D. A., Soni, S. S., Alsasa, A., Bunse, T., Schlesner, M., Muckenthaler, M. U., . . . Platten, M. (2023). T cell-independent eradication of experimental glioma by intravenous TLR7/8-agonist-loaded nanoparticles. *Nature Communications*, *14*(1). https://doi.org/10.1038/s41467-023-36321-6

van de Walle, T., Vaccaro, A., Ramachandran, M., Pietilä, I., Essand, M., & Dimberg, A. (2021). Tertiary Lymphoid Structures in the Central Nervous System: Implications for Glioblastoma. *Frontiers in Immunology*, *12*. https://doi.org/10.3389/fimmu.2021.724739

van Hooren, L., Vaccaro, A., Ramachandran, M., Vazaios, K., Libard, S., van de Walle, T., Georganaki, M., Huang, H., Pietila, I., Lau, J., Ulvmar, M. H., Karlsson, M. C. I., Zetterling, M., Mangsbo, S. M., Jakola, A. S., Olsson Bontell, T., Smits, A., Essand, M., & Dimberg, A. (2021). Agonistic CD40 therapy induces tertiary lymphoid structures but impairs responses to checkpoint blockade in glioma. *Nature Communications*, *12*(1), 4127. https://doi.org/10.1038/s41467-021-24347-7

van Hooren, L., Vaccaro, A., Ramachandran, M., Vazaios, K., Libard, S., van de Walle, T., Georganaki, M., Huang, H., Pietilä, I., Lau, J., Ulvmar, M. H., Karlsson, M. C. I., Zetterling, M., Mangsbo, S. M., Jakola, A. S., Olsson Bontell, T., Smits, A., Essand, M., Dimberg, A., . . . Dimberg, A. (2021). Agonistic CD40 therapy induces tertiary lymphoid structures but impairs responses to checkpoint blockade in glioma. *Nature Communications 2021 12:1*, *12*(1). https://doi.org/10.1038/s41467-021-24347-7

Vanpouille-Box, C., Alard, A., Aryankalayil, M. J., Sarfraz, Y., Diamond, J. M., Schneider, R. J., Inghirami, G., Coleman, C. N., Formenti, S. C., & Demaria, S. (2017). DNA exonuclease Trex1 regulates radiotherapy-induced tumour immunogenicity. *Nature Communications*, *8*(1). https://doi.org/10.1038/ncomms15618

Venkatesulu, B. P., Mallick, S., Lin, S. H., & Krishnan, S. (2018). A systematic review of the influence of radiation-induced lymphopenia on survival outcomes in solid tumors. *Crit Rev Oncol Hematol*, *123*, 42-51. https://doi.org/10.1016/j.critrevonc.2018.01.003

Verschuere, T., Toelen, J., Maes, W., Poirier, F., Boon, L., Tousseyn, T., Mathivet, T., Gerhardt, H., Mathieu, V., Kiss, R., Lefranc, F., Van Gool, S. W., & De Vleeschouwer, S. (2014). Glioma-derived galectin-1 regulates innate and adaptive antitumor immunity. *Int J Cancer*, *134*(4), 873-884. https://doi.org/10.1002/ijc.28426

Vespa, G. N., Lewis, L. A., Kozak, K. R., Moran, M., Nguyen, J. T., Baum, L. G., & Miceli, M. C. (1999). Galectin-1 specifically modulates TCR signals to enhance TCR apoptosis but inhibit IL-2 production and proliferation. *J Immunol*, *162*(2), 799-806. https://www.ncbi.nlm.nih.gov/pubmed/9916701

Voshart, D. C., Klaver, M., Jiang, Y., Weering, H. R. J. v., Buuren-Broek, F. v., Linden, G. P. v. d., Cinat, D., Kiewiet, H. H., Malimban, J., Vazquez-Matias, D. A., Nazario, L. R., Scholma, A. C., Sewdihal, J., Goethem, M.-J. v., Luijk, P. v., Coppes, R. P., & Barazzuol, L. (2024). Proton therapy induces a local microglial neuroimmune response. *Radiotherapy and Oncology*, *193*. https://doi.org/10.1016/j.radonc.2024.110117

Voshart, D. C., Oshima, T., Jiang, Y., van der Linden, G. P., Ainslie, A. P., Reali Nazario, L., van Buuren-Broek, F., Scholma, A. C., van Weering, H. R. J., Brouwer, N., Sewdihal, J., Brouwer, U., Coppes, R. P., Holtman, I. R., Eggen, B. J. L., Kooistra, S. M., & Barazzuol, L. (2024). Radiotherapy induces persistent innate immune reprogramming of microglia into a primed state. *Cell Rep*, *43*(2), 113764. https://doi.org/10.1016/j.celrep.2024.113764

Walle, T., Kraske, J. A., Liao, B., Lenoir, B., Timke, C., Halbach, E. v. B. u., Tran, F., Griebel, P., Albrecht, D., Ahmed, A., Suarez-Carmona, M., Jiménez-Sánchez, A., Beikert, T., Tietz-Dahlfuß, A., Menevse, A. N., Schmidt, G., Brom, M., Pahl, J. H. W., Antonopoulos, W., . . . Huber, P. E. (2022). Radiotherapy orchestrates natural killer cell dependent antitumor immune responses through CXCL8. *Science Advances*, *8*(12). https://doi.org/10.1126/sciadv.abh4050

Wang, G.-M., Cioffi, G., Patil, N., Waite, K. A., Lanese, R., Ostrom, Q. T., Kruchko, C., Berens, M. E., Connor, J. R., Lathia, J. D., Rubin, J. B., & Barnholtz-Sloan, J. S. (2022). Importance of the intersection of age and sex to understand variation in incidence and survival for primary malignant gliomas. *Neuro-oncology*, *24*(2). https://doi.org/10.1093/neuonc/noab199

Wang, N. H., Lei, Z., Yang, H. N., Tang, Z., Yang, M. Q., Wang, Y., Sui, J. D., & Wu, Y. Z. (2022). Radiation-induced PD-L1 expression in tumor and its microenvironment facilitates cancer-immune escape: a narrative review. *Ann Transl Med*, *10*(24), 1406. https://doi.org/10.21037/atm-22-6049

Weiss, T., Schneider, H., Silginer, M., Steinle, A., Pruschy, M., Polić, B., Weller, M., & Roth, P. (2018). NKG2D-Dependent Antitumor Effects of Chemotherapy and Radiotherapy against Glioblastoma. *Clinical Cancer Research*, *24*(4). https://doi.org/10.1158/1078-0432.CCR-17-1766

Weiss, T., Weller, M., Guckenberger, M., Sentman, C. L., & Roth, P. (2018). NKG2D-Based CAR T Cells and Radiotherapy Exert Synergistic Efficacy in Glioblastoma. *Cancer Research*, *78*(4). https://doi.org/10.1158/0008-5472.CAN-17-1788

Weller, M., van den Bent, M., Preusser, M., Le Rhun, E., Tonn, J. C., Minniti, G., Bendszus, M., Balana, C., Chinot, O., Dirven, L., French, P., Hegi, M. E., Jakola, A. S., Platten, M., Roth, P., Rudà, R., Short, S., Smits, M., Taphoorn, M. J. B., . . . Wick, W. (2020). EANO guidelines on the diagnosis and treatment of diffuse gliomas of adulthood. *Nature Reviews Clinical Oncology*, *18*(3). https://doi.org/10.1038/s41571-020-00447-z

Weller, M., Wen, P. Y., Chang, S. M., Dirven, L., Lim, M., Monje, M., & Reifenberger, G. (2024). Glioma. *Nature Reviews Disease Primers*, *10*(1). https://doi.org/10.1038/s41572-024-00516-y

Wichmann, T. O., Damkier, H. H., & Pedersen, M. (2022). A Brief Overview of the Cerebrospinal Fluid System and Its Implications for Brain and Spinal Cord Diseases. *Frontiers in Human Neuroscience*, *15*. https://doi.org/10.3389/fnhum.2021.737217

Wijerathne, H., Langston, J. C., Yang, Q., Sun, S., Miyamoto, C., Kilpatrick, L. E., & Kiani, M. F. (2021). Mechanisms of radiation-induced endothelium damage: Emerging models and technologies. *Radiotherapy and oncology : journal of the European*

Society for Therapeutic Radiology and Oncology, *158*. https://doi.org/10.1016/j.radonc.2021.02.007

Xiao, Z., Todd, L., Huang, L., Noguera-Ortega, E., Lu, Z., Huang, L., Kopp, M., Li, Y., Pattada, N., Zhong, W., Guo, W., Scholler, J., Liousia, M., Assenmacher, C. A., June, C. H., Albelda, S. M., & Pure, E. (2023). Desmoplastic stroma restricts T cell extravasation and mediates immune exclusion and immunosuppression in solid tumors. *Nat Commun*, *14*(1), 5110. https://doi.org/10.1038/s41467-023-40850-5

Xiong, Z., Raphael, I., Olin, M., Okada, H., Li, X., & Kohanbash, G. (2024). Glioblastoma vaccines: past, present, and opportunities. *eBioMedicine*, *100*. https://doi.org/10.1016/j.ebiom.2023.104963

Xu, H., Lotfy, P., Gelb, S., Pragana, A., Hehnly, C., Byer, L. I. J., Shipley, F. B., Zawadzki, M. E., Cui, J., Deng, L., Taylor, M., Webb, M., Lidov, H. G. W., Andermann, M. L., Chiu, I. M., Ordovas-Montanes, J., & Lehtinen, M. K. (2024). The choroid plexus synergizes with immune cells during neuroinflammation. *Cell*, *187*(18), 4946-4963 e4917. https://doi.org/10.1016/j.cell.2024.07.002

Yabo, Y. A., Moreno-Sanchez, P. M., Pires-Afonso, Y., Kaoma, T., Nosirov, B., Scafidi, A., Ermini, L., Lipsa, A., Oudin, A., Kyriakis, D., Grzyb, K., Poovathingal, S. K., Poli, A., Muller, A., Toth, R., Klink, B., Berchem, G., Berthold, C., Hertel, F., . . . Golebiewska, A. (2024). Glioblastoma-instructed microglia transition to heterogeneous phenotypic states with phagocytic and dendritic cell-like features in patient tumors and patient-derived orthotopic xenografts. *Genome Med*, *16*(1), 51. https://doi.org/10.1186/s13073-024-01321-8

Yamazaki, T., Hannani, D., Poirier-Colame, V., Ladoire, S., Locher, C., Sistigu, A., Prada, N., Adjemian, S., Catani, J. P., Freudenberg, M., Galanos, C., Andre, F., Kroemer, G., & Zitvogel, L. (2014). Defective immunogenic cell death of HMGB1-deficient tumors: compensatory therapy with TLR4 agonists. *Cell Death Differ*, *21*(1), 69-78. https://doi.org/10.1038/cdd.2013.72

Yi, R., Chen, E., Roberts, E. W., Krummel, M. F., & Serwas, N. K. (2022). Impact of protein identity on tumor-associated antigen uptake into infiltrating immune cells: A comparison of different fluorescent proteins as model antigens. *PLOS ONE*, *17*(8). https://doi.org/10.1371/journal.pone.0272857

Yovino, S., & Grossman, S. A. (2012). Severity, etiology and possible consequences of treatment-related lymphopenia in patients with newly diagnosed high-grade gliomas. *CNS Oncology*, *1*(2). https://doi.org/10.2217/cns.12.14

Yu, R., Zhu, B., & Chen, D. (2022). Type I interferon-mediated tumor immunity and its role in immunotherapy. *Cell Mol Life Sci*, *79*(3), 191. https://doi.org/10.1007/s00018-022-04219-z

Yu, X., Qian, J., Ding, L., Yin, S., Zhou, L., & Zheng, S. (2023). Galectin-1: A Traditionally Immunosuppressive Protein Displays Context-Dependent Capacities. *Int J Mol Sci*, *24*(7). https://doi.org/10.3390/ijms24076501

Zarodniuk, M., Steele, A., Lu, X., Li, J., & Datta, M. (2023). CNS tumor stroma transcriptomics identify perivascular fibroblasts as predictors of immunotherapy resistance in glioblastoma patients. *NPJ Genom Med*, *8*(1), 35. https://doi.org/10.1038/s41525-023-00381-w

Zeng, J., See, A. P., Phallen, J., Jackson, C. M., Belcaid, Z., Ruzevick, J., Durham, N., Meyer, C., Harris, T. J., Albesiano, E., Pradilla, G., Ford, E., Wong, J., Hammers, H. J., Mathios, D., Tyler, B., Brem, H., Tran, P. T., Pardoll, D., . . . Lim, M. (2013). Anti-PD-1 blockade and stereotactic radiation produce long-term survival in mice with intracranial gliomas. *Int J Radiat Oncol Biol Phys*, *86*(2), 343-349. https://doi.org/10.1016/j.ijrobp.2012.12.025

Zhai, L., Bell, A., Ladomersky, E., Lauing, K. L., Bollu, L., Nguyen, B., Genet, M., Kim, M., Chen, P., Mi, X., Wu, J. D., Schipma, M. J., Wray, B., Griffiths, J., Unwin, R. D., Clark, S. J., Acharya, R., Bao, R., Horbinski, C., . . . Wainwright, D. A. (2021). Tumor Cell IDO Enhances Immune Suppression and Decreases Survival

Independent of Tryptophan Metabolism in Glioblastoma. *Clinical Cancer Research*, *27*(23). https://doi.org/10.1158/1078-0432.CCR-21-1392

Zhang, I., Alizadeh, D., Liang, J., Zhang, L., Gao, H., Song, Y., Ren, H., Ouyang, M., Wu, X., D'Apuzzo, M., & Badie, B. (2016). Characterization of Arginase Expression in Glioma-Associated Microglia and Macrophages. *PLOS ONE*, *11*(12). https://doi.org/10.1371/journal.pone.0165118

6 Supplementary data

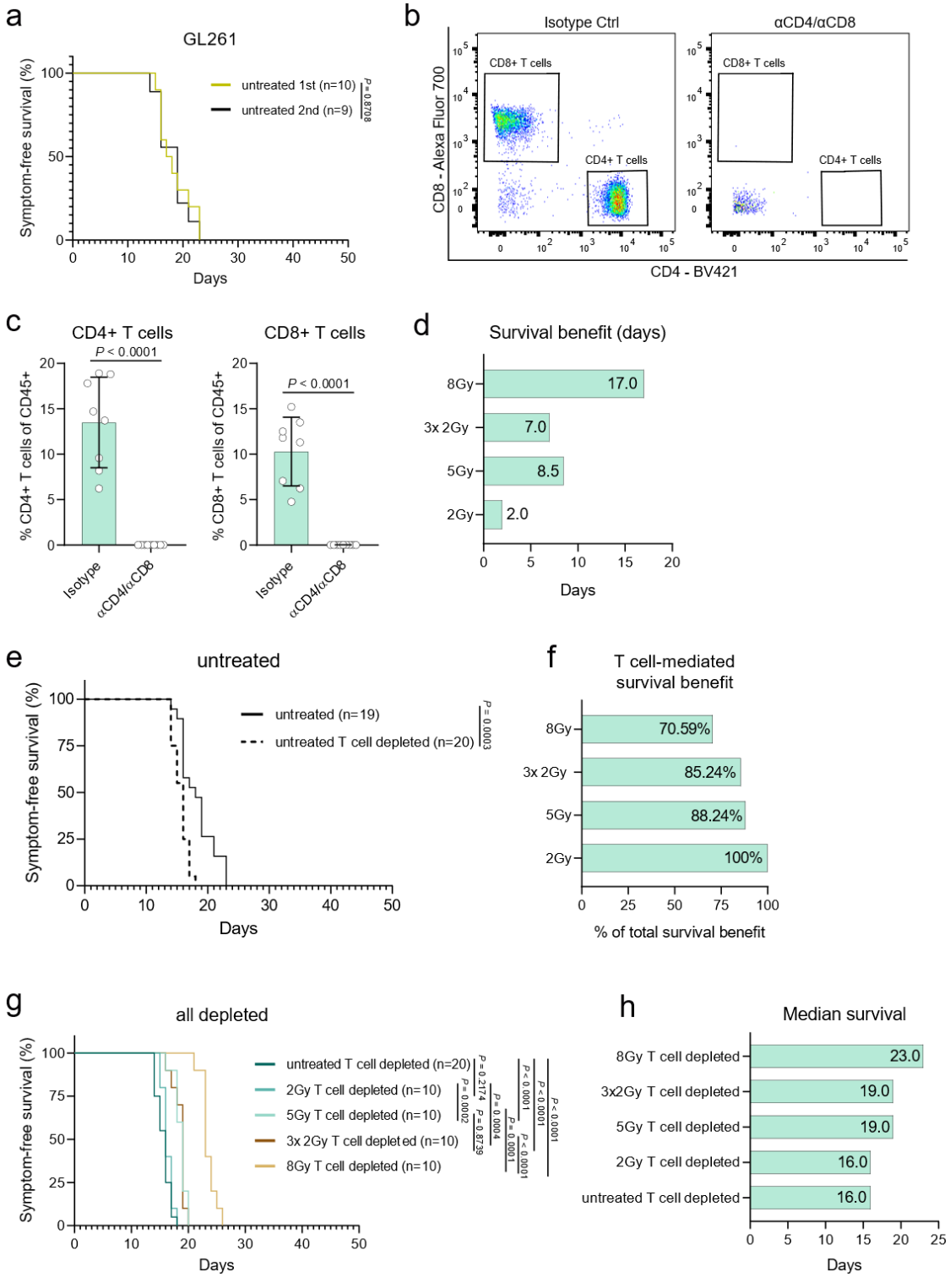

Supplementary Figure 1: Symptom-free survival after radiotherapy.

(a) Kaplan-Meier curve of symptom-free survival in mice from two individual experiments to test the reproducibility and comparability of performed experiments. (b) Flow cytometry analysis of blood samples from isotype of anti-CD4/anti-CD8 treated mice to check for successful T cell depletion. (c) Quantification of flow cytometry analysis. Statistical test performed by unpaired t-test. (d) Survival benefit in days of mice treated with 2, 3x 2, 5, or 8 Gy irradiation. (e) Kaplan-

Meier curve of symptom-free survival in untreated mice with or without T cell depletion to demonstrate the endogenous T cell response. (f) T cell-mediated survival benefit (in %) of the total survival benefit. (g) Kaplan-Meier curve of symptom-free survival and (h) median survival in all T cell-depleted groups. Statistical analysis on all symptom-free survival was performed by Log-rank (Mantel-Cox) test.

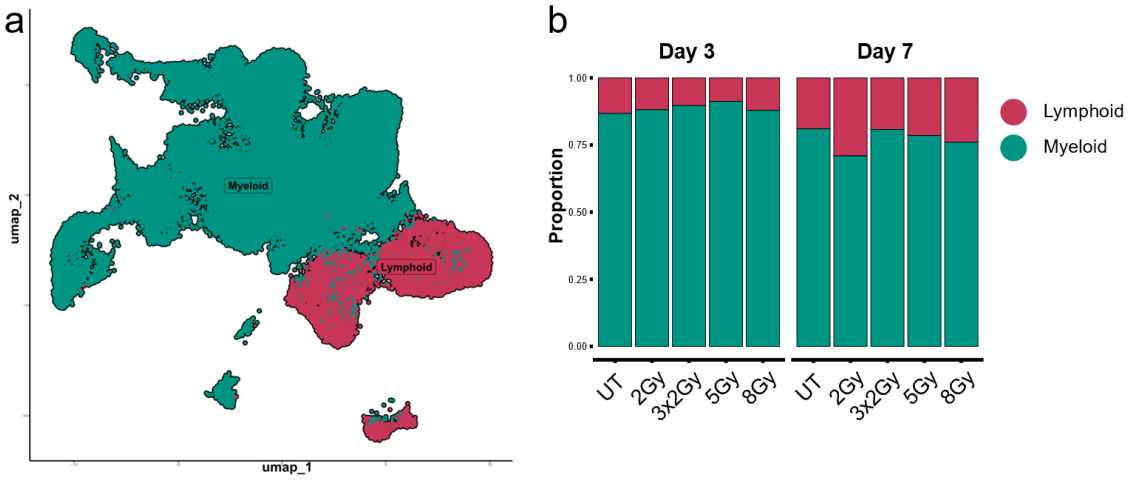

Supplementary Figure 2: Overview of the lymphoid and myeloid populations.

(a) UMAP of all cells divided in lymphoid and myeloid cells. (b) Proportion (in %) of the lymphoid and myeloid population among all cells at day 3 and day 7 within the different treatment groups. Bioinformatic processing by Clara Tejido Dierssen.

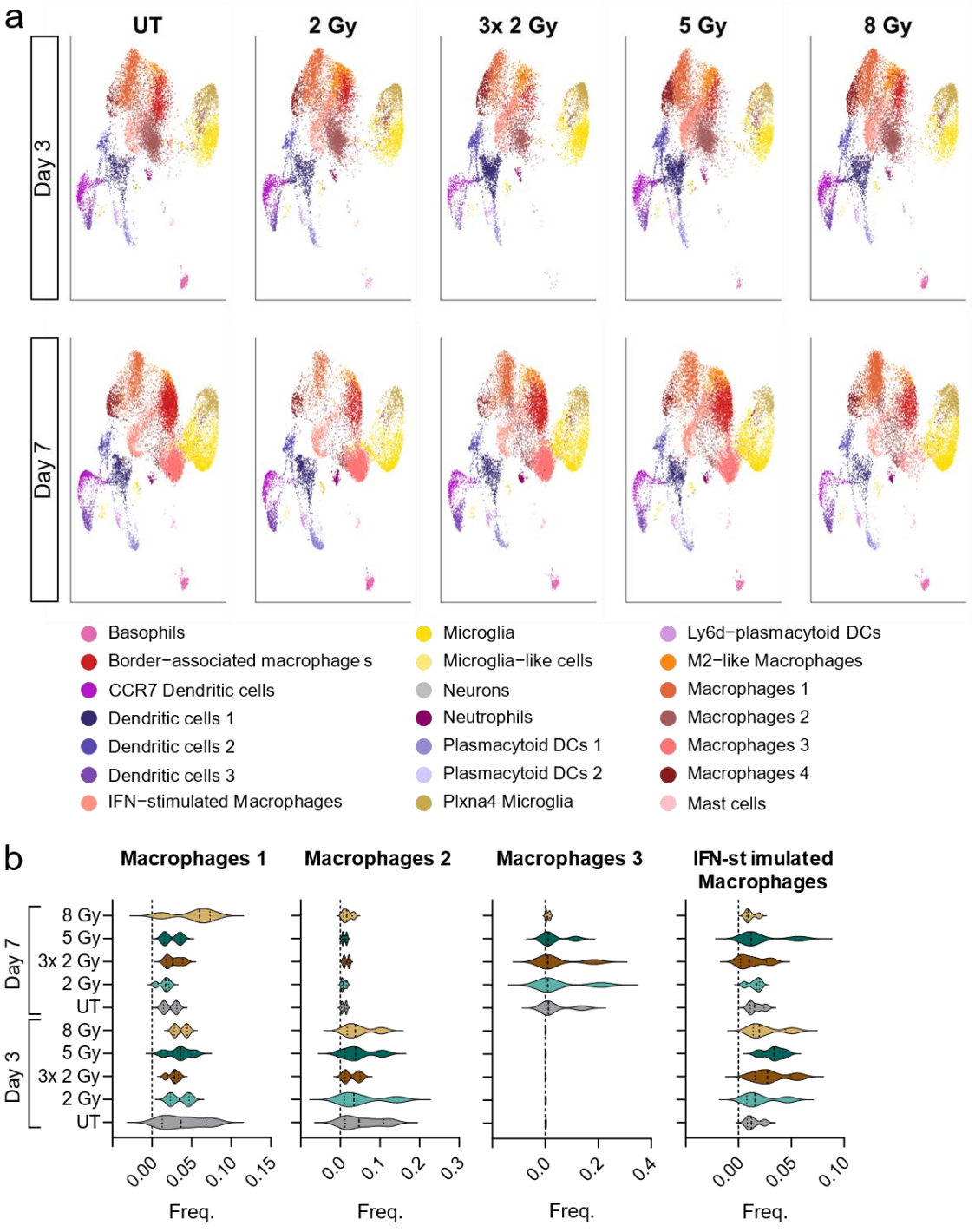

Supplementary Figure 3: Overview and abundancies of myeloid cell clusters.

(a) UMAP of all treatment groups at day 3 and 7. (b) Frequency (Freq.) of selected myeloid cell clusters at day 3 and 7 in the different treatment groups. Bioinformatic processing by Clara Tejido Dierssen.

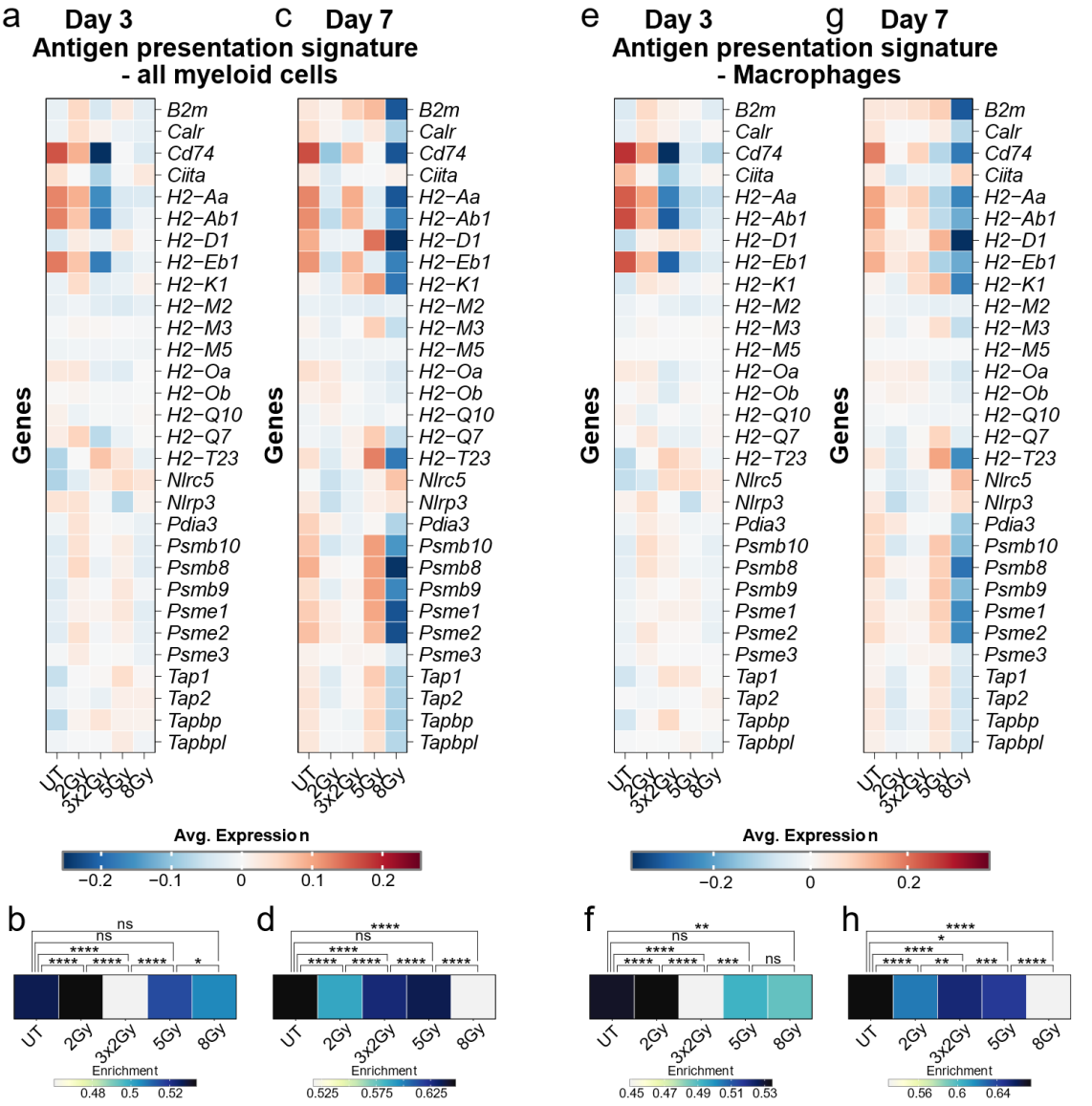

Supplementary Figure 4: Antigen presentation signature in all myeloid cells and macrophages.

(a) Heatmap of the antigen presentation signature and the average expression of genes in all myeloid cells at day 3. (b) Enrichment of the type antigen presentation signature in all myeloid cells at day 3. (c) Heatmap of the antigen presentation signature and the average expression of genes in myeloid cells at day 7. (d) Enrichment of the antigen presentation signature in all myeloid cells at day 7. (e) Heatmap of the antigen presentation signature and the average expression of genes in all macrophages at day 3. (f) Enrichment of antigen presentation signature in all macrophages at day 3. (g) Heatmap of the antigen presentation signature and the average expression of genes in all macrophages at day 7. (h) Enrichment of the antigen presentation signature in all macrophages at day 7. Statistical analysis was performed with one-way ANOVA and subsequent Tukey test. Significance was defined as P-value ≤ 0.05. Significance is displayed as * = P-value ≤ 0.05; ** = P-value ≤ 0.005; *** = P-value ≤ 0.0005; **** = P-value ≤ 0.0001; ns = not significant. Bioinformatic processing by Clara Tejido Dierssen.

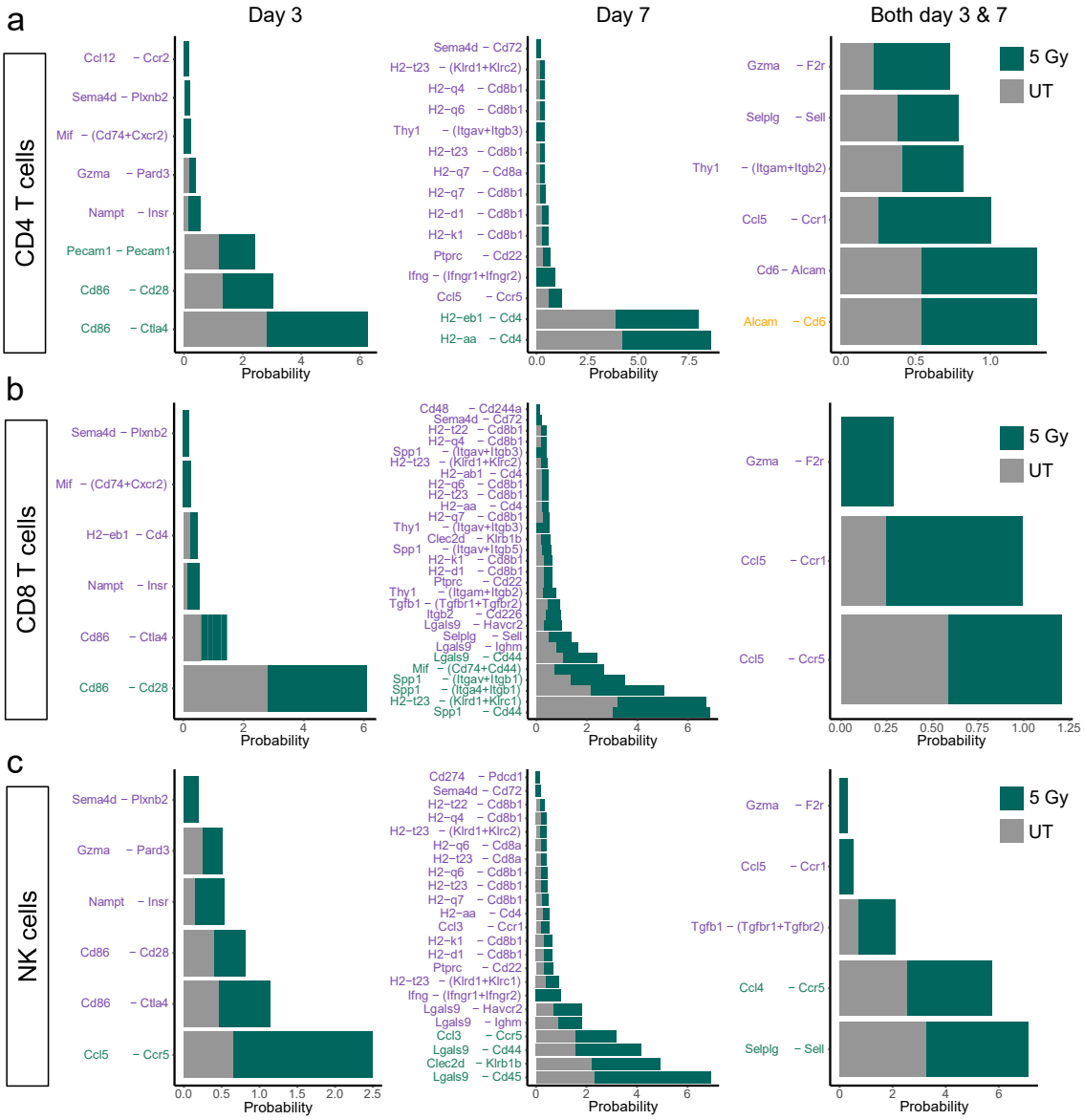

Supplementary Figure 5: The irradiation-specific interactome in T and NK cells.

Receptor-ligand pairs and their probability of interaction, which are exclusively only in the 5 Gy treated group or significantly upregulated compared to the untreated group at day 3, day 7 or on both timepoints in (a) CD4 T cells, (b) CD8 T cells and (c) NK cells. Only statistically significant (P-value ≤ 0.05) interactions were included. Statistical testing was performed by one-sided permutation test. Bioinformatic processing by Clara Tejido Dierssen.

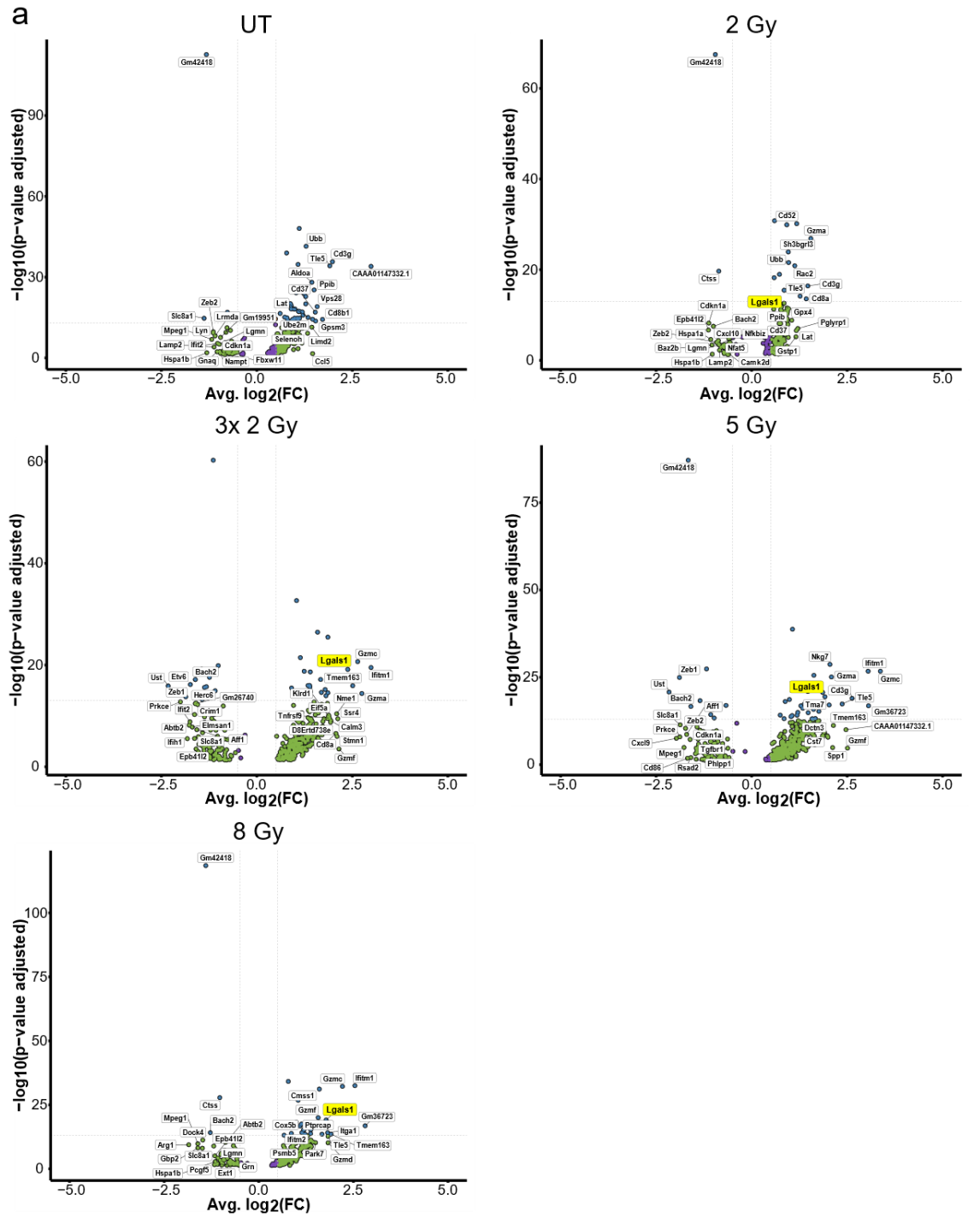

Supplementary Figure 6: Differential gene expression in CD8+ T cells over time.

(a) Volcano plots of differentially expressed genes in CD8+ T cells between on day 7 compared to day 3 in all treatment groups. Annotated are the top 15 up- and downregulated genes. Green dots genes over the threshold of >0.5 avg. log2 fold change (FC).

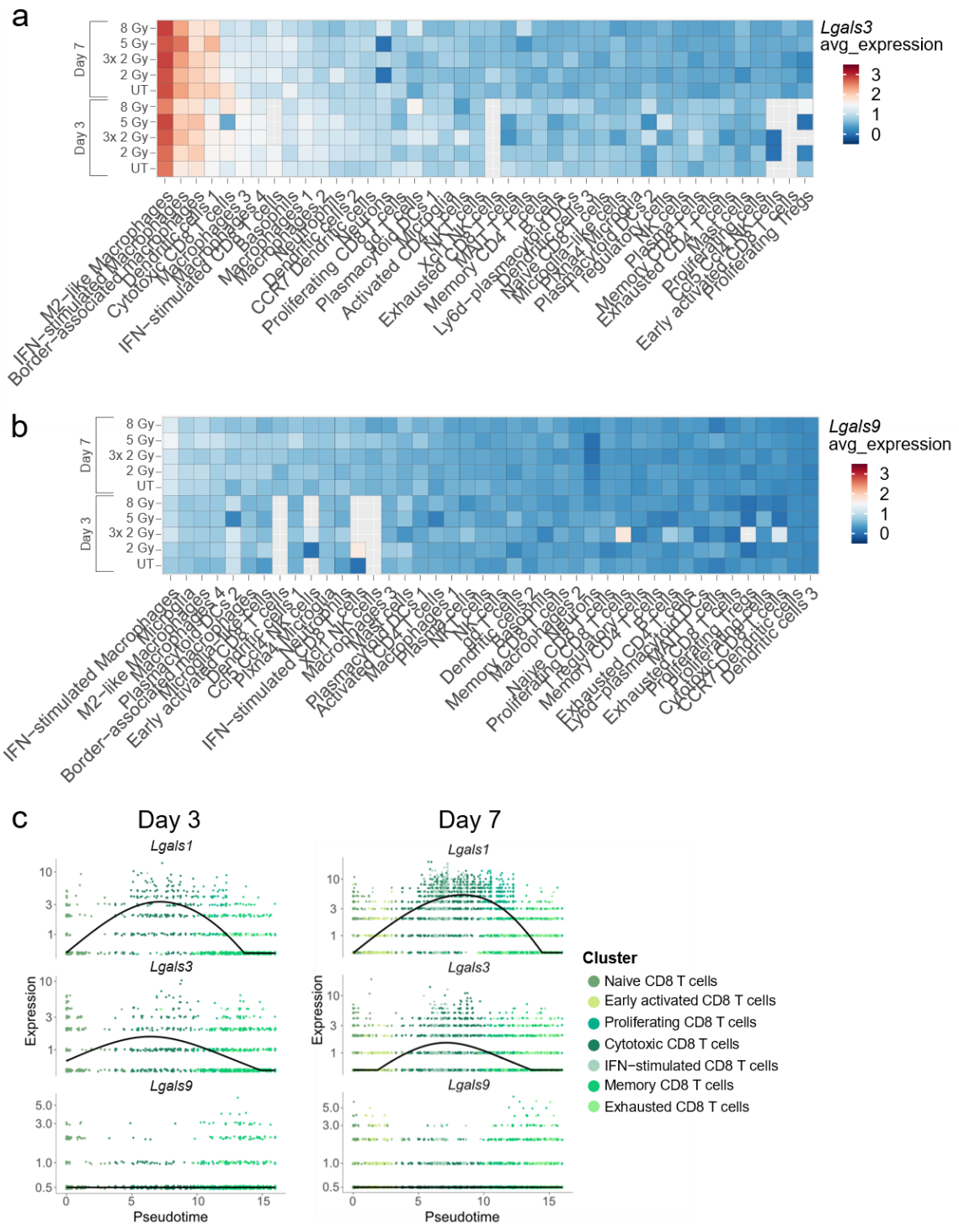

Supplementary Figure 7: Overview of *Lgals3* and *Lgals9* expression.

Average expression of (a) *Lgals3* and (b) *Lgals9* in all cell types in the different treatment groups at day 3 and day 7. (c) Expression level of Lgals1, Lgals3 and Lgals9 in CD8 T cell clusters along their pseudotime trajectory. Bioinformatic processing by Clara Tejido Dierssen.

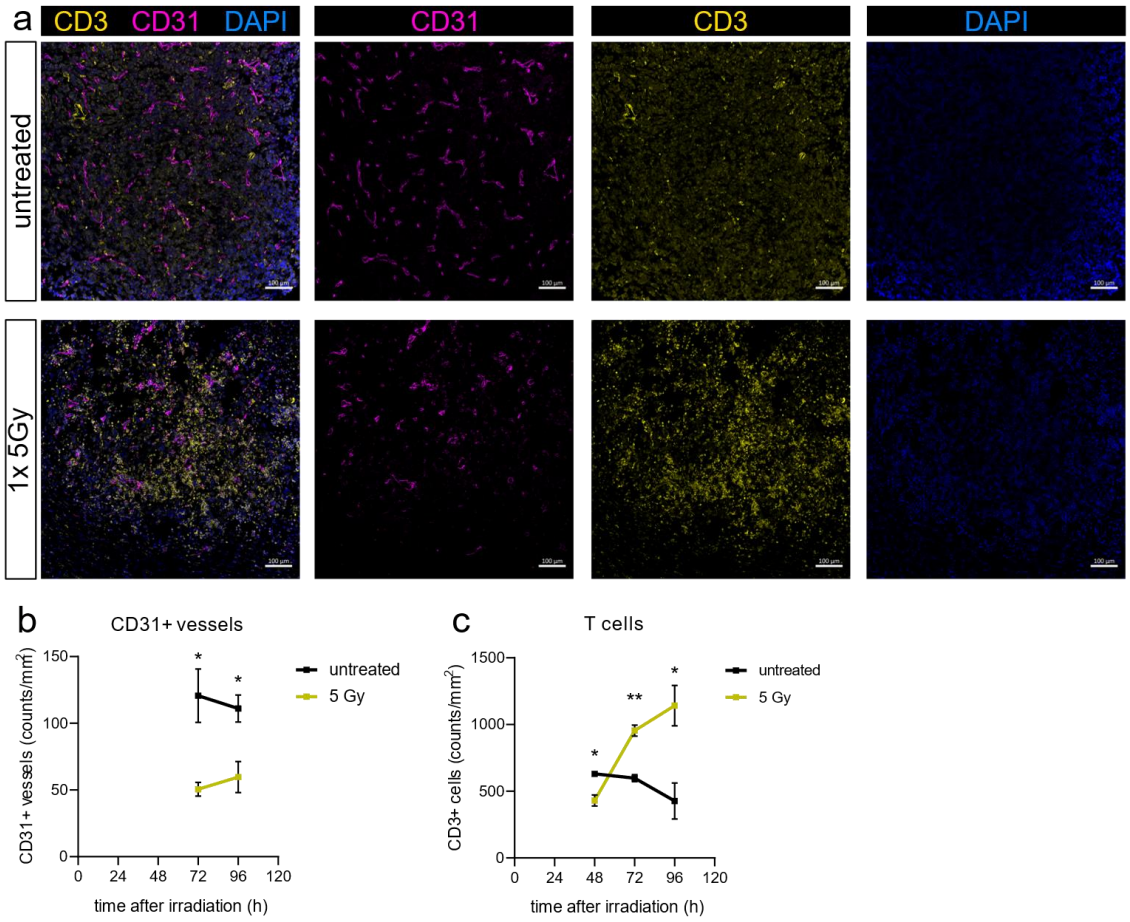

Supplementary Figure 8: CD31+ vessels and T cells in untreated and irradiated tumors.

(a) Immunofluorescence staining and confocal laser scanning microscopy of CD3+ T cells (yellow), CD31+ ECs (magenta) and DAPI (blue) in untreated (top) and 1x 5 Gy irradiated tumors (bottom) 72h after treatment. Scale bars 100 µm. (b) Quantification of CD31+ vessels (counts/mm2). (c) Quantification of CD3+ T cells (counts/mm2). Statistical analysis performed by unpaired t-test and each timepoint.

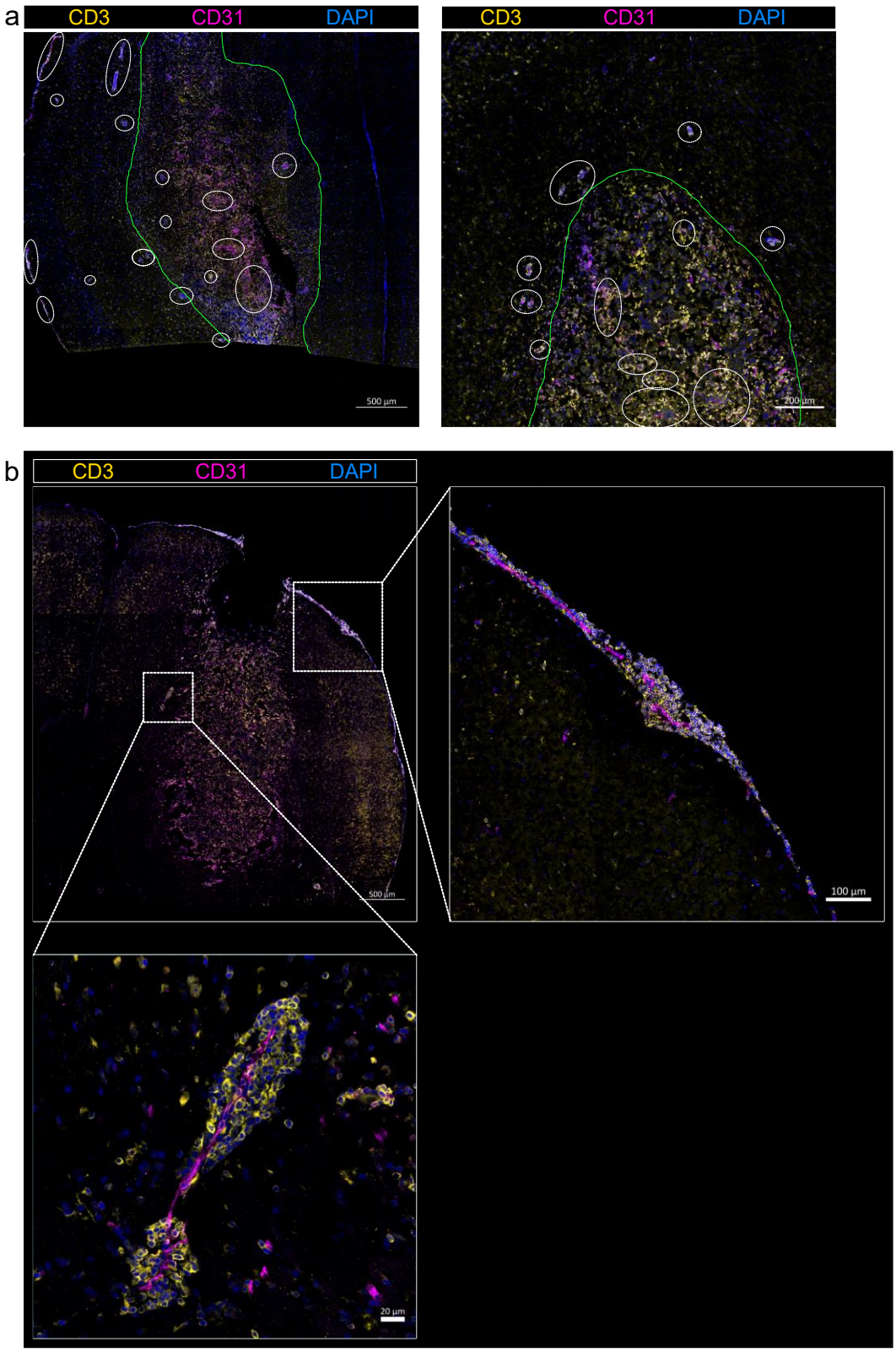

Supplementary Figure 9: Overview of PVTN localization tumor-bearing hemispheres.

(a) Exemplary tile-scans of GL261 tumor-bearing brain hemispheres. PVTNs are circled with white dotted lines and are located intratumoral, extratumoral and extratumoral at the meninges. The approximate outline of the tumor mass is marked by the green dotted line. (b) Exemplary images and close-ups of PVTNs next to the tumor (bottom) and at the meninges (right). All images

were taken of samples excised on day 13 after tumor cell injection. All images were taken using a 20x magnification on a confocal laser scanning microscope.

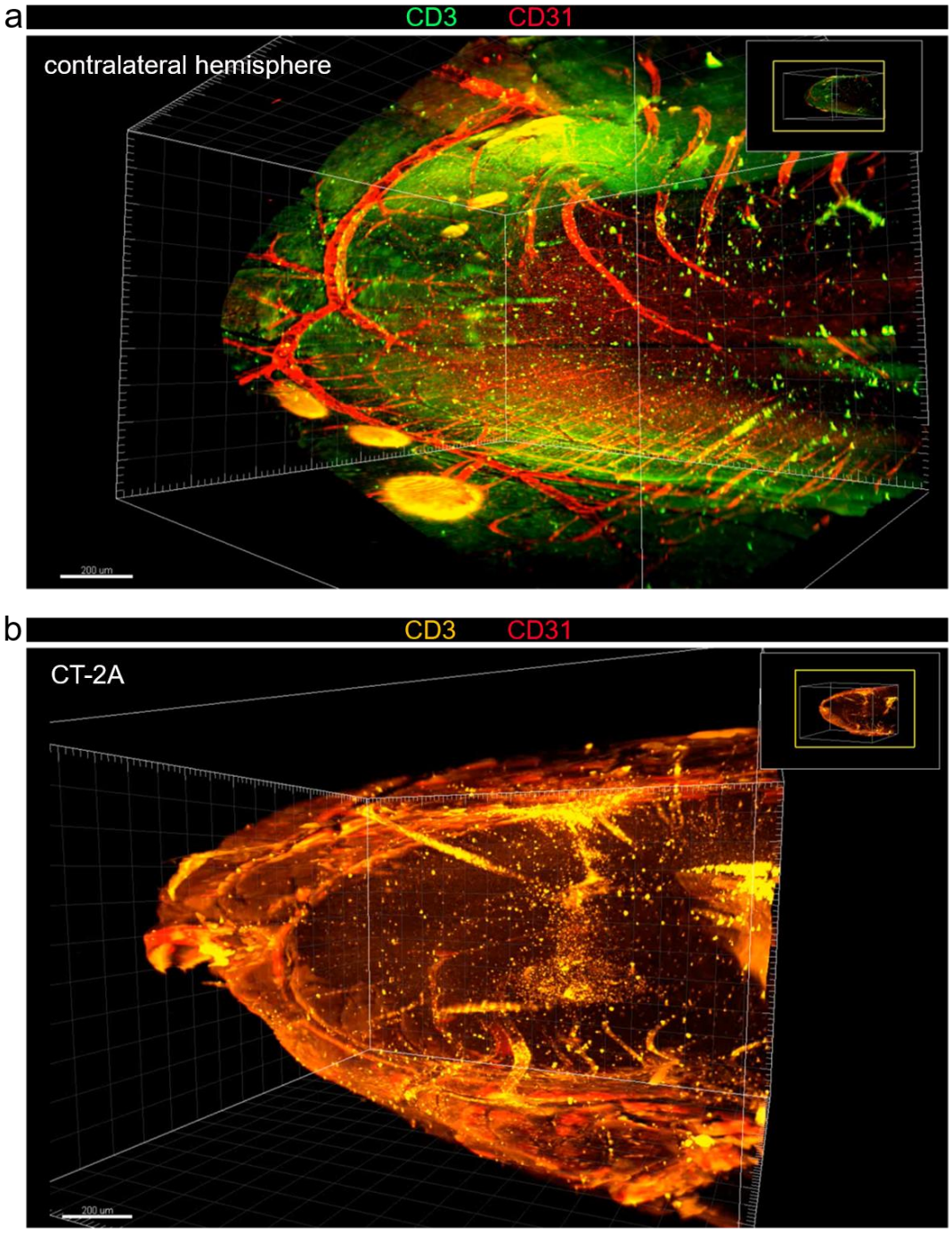

Supplementary Figure 10: 3D structure of PVTNs in the contralateral hemisphere and in CT-2A tumors.

(a) 3D reconstruction of images taken by light sheet fluorescence microscopy of cleared brains (a) showing the contralateral non-tumor-bearing hemisphere of an untreated mice bearing a GL261 tumor. CD3+ T cells (green) and CD31+ vessels (red). (b) showing the tumor-bearing hemisphere of an untreated mouse injected with the glioma model CT-2A. CD3+ T cells (yellow) and CD31+ vessels (red). Both brains were excised on day 13 after tumor injection. Scale bars 200 µm.

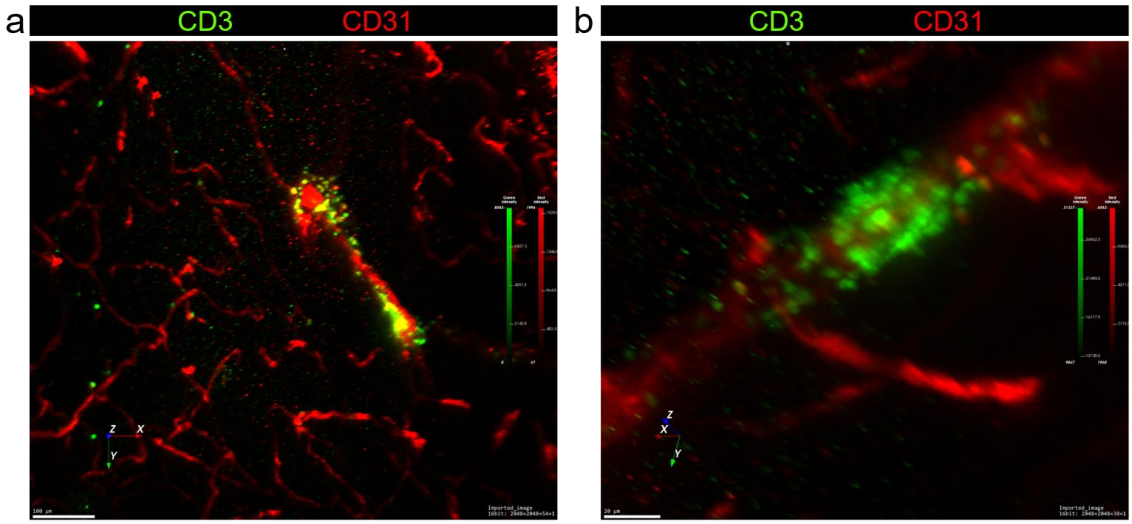

Supplementary Figure 11: 3D structure of PVTNs in human glioma patients.

(a-b) 3D reconstruction of images taken by light sheet fluorescence microscopy of cleared human tumor samples from glioma patients. Localization within the brain or tumor/healthy tissue are unknown. CD3+ T cells (green) and CD31+ vessels (red). Scale bars bottom left 100 µm (a) and 20 µm (b).